On sea turtle-associated Craspedostauros (Bacillariophyta), with description of three novel species

On sea turtle-associated Craspedostauros (Bacillariophyta), with description of three novel species

Journal:	*Journal of Phycology*
Manuscript ID	JPY-20-017-ART.R1
Manuscript Type:	Regular Article
Date Submitted by the Author:	n/a
Complete List of Authors:	Majewska, Roksana; North-West University, Unit for Environmental Sciences and Management; South African Institute for Aquatic Biodiversity (SAIAB), Ashworth, Matt; University of Texas, Austin, Integrative Biology Bosak, Suncica; University of Zagreb, Faculty of Science, Department of Biology Goosen, William; Nelson Mandela University, Centre for High Resolution Transmission Electron Microscopy Nolte, Christopher; Nelson Mandela University Filek, Klara; University of Zagreb Van de Vijver, Bart; Botanic Garden Meise Taylor, Jonathan; North-West University Manning, Schonna; University of Texas at Austin College of Natural Sciences, Molecular Biosciences Nel, Ronel; Nelson Mandela Metropolitan University
Keywords:	biogeography, diatom, microalgae, molecular, morphology, phylogeny, symbiosis, taxonomy, ultrastructure
Alternate Keywords:	Craspedostauros, barnacle, Chelonibia, epizoic diatom, leatherback, loggerhead, phylogeny, Platylepas, sea turtle

Potchefstroom, 29.01.2020

COVER LETTER

We declare that our paper „**On sea turtle-associated *Craspedostauros* (Bacillariophyta), with description of three novel species**" has not been published previously, that it is not under consideration for publication elsewhere, that its publication is approved by all authors and by the responsible authorities where the work was carried out, and that, if accepted, it will not be published elsewhere in the same form, in English or in any other language, including electronically without the written consent of the copyright-holder. We believe that the presented manuscript is a valuable addition to the scientific literature as it describes three novel sea turtle-associated diatom species and provides some additional information about the epizoic diatom diversity and ecology.

We confirm that there are no known conflicts of interest associated with this publication and there has been no significant financial support for this work that could have influenced its outcome.

We confirm that the manuscript has been read and approved by all named authors and that there are no other persons who satisfied the criteria for authorship but are not listed. We further confirm that all of us have approved the order of authors listed in the manuscript.

We understand that the Corresponding Author is the sole contact for the Editorial process (including Editorial Manager and direct communications with the office). She is responsible for communicating with the other authors about progress, submissions of revisions and final approval of proofs. We confirm that we have provided a current, correct email address, which is accessible by the Corresponding Author.

Corresponding author's contact details:
Mailing address: Unit for Environmental Sciences and Management, School of Biological Sciences, North-West University, Private Bag X6001, Potchefstroom 2520, South Africa
Mobile: +27 (0)725034563
E-mail address: roksana.majewska@nwu.ac.za; proximina@o2.pl

Yours faithfully, Roksana Majewska, on behalf of all the co-authors

Roksana Majewska

On sea turtle-associated *Craspedostauros* (Bacillariophyta), with description of three novel species

*Roksana Majewska**

Unit for Environmental Sciences and Management, School of Biological Sciences, North-West University, Potchefstroom 2520, South Africa

South African Institute for Aquatic Biodiversity (SAIAB), Grahamstown 6140, South Africa

*author for correspondence: roksana.majewska@nwu.ac.za

ORCID: https://orcid.org/0000-0003-2681-4304

Matt P. Ashworth

Department of Molecular Biosciences, The University of Texas at Austin, Austin, TX. 78712, USA

ORCID: https://orcid.org/0000-0002-4162-2004

Sunčica Bosak

Department of Biology, Faculty of Science, University of Zagreb, 10000 Zagreb, Croatia

ORCID: https://orcid.org/0000-0002-4604-2324

William E. Goosen

Centre for High Resolution Transmission Electron Microscopy, Faculty of Science, Nelson Mandela University, 6031 Port Elizabeth, South Africa

ORCID: https://orcid.org/0000-0002-8877-6086

Christopher Nolte

Department of Zoology, Institute for Coastal and Marine Research, Nelson Mandela University, 6031 Port Elizabeth, South Africa

ORCID: https://orcid.org/0000-0002-1429-587X

Klara Filek

Department of Biology, Faculty of Science, University of Zagreb, 10000 Zagreb, Croatia

ORCID: https://orcid.org/0000-0003-2518-4494

Bart Van de Vijver

Research Department, Botanic Garden Meise, B-1860 Meise, Belgium

Department of Biology, University of Antwerp, ECOBE, 2020 Antwerpen, Belgium

ORCID: https://orcid.org/0000-0002-6244-1886

Jonathan C. Taylor

Unit for Environmental Sciences and Management, School of Biological Sciences, North-West University, Potchefstroom 2520, South Africa

South African Institute for Aquatic Biodiversity (SAIAB), Grahamstown 6140, South Africa

ORCID: https://orcid.org/0000-0003-2717-3246

Schonna R. Manning

Department of Molecular Biosciences, The University of Texas at Austin, Austin, TX. 78712, USA

ORCID: https://orcid.org/0000-0002-7705-2111

and Ronel Nel

Department of Zoology, Institute for Coastal and Marine Research, Nelson Mandela University, 6031 Port Elizabeth, South Africa

ORCID: https://orcid.org/0000-0003-2551-6428

Running title: Sea turtle-associated *Craspedostauros*

ABSTRACT

Despite recent advances in the research on sea turtle-associated diatoms, some of the key aspects of the diatom-sea turtle relationship, including compositional and functional features of the epizoic diatom community, remain understudied and poorly understood. The current paper focuses on four species belonging to the primarily marine diatom genus *Craspedostauros* that were observed growing attached to numerous sea turtles and sea turtle-associated barnacles from Croatia and South Africa. Three of the examined taxa, *C. danayanus* sp. nov., *C. legouvelloanus* sp. nov., and *C. macewanii* sp. nov. represent novel species and are described based on morphological and, whenever possible, molecular characteristics. The new taxa exhibit characters not yet observed in other members of the genus, such as the presence of more than two rows of cribrate areolae on the girdle bands, shallow perforated septa, and a complete reduction of the stauros. In addition, *C. alatus*, recently described from museum sea turtle specimens, is reported for the first time from loggerheads rescued in Europe. A 3-gene phylogenetic analysis including DNA sequence data for three sea turtle-associated *Craspedostauros* species and other marine and epizoic diatom taxa indicated that *Craspedostauros* is monophyletic and sister to *Achnanthes*. This study, being based on a large number of samples and animal specimens analysed and using different preservation and processing methods, provides some new insights into the genus ecology and biogeography, and sheds more light on the level of intimacy and permanency in the host-epibiont interaction within the epizoic *Craspedostauros* species.

Key index words: *Craspedostauros*, barnacle, *Chelonibia*, epizoic diatom, leatherback, loggerhead, phylogeny, *Platylepas*, sea turtle

Abbreviations: BS, bootstrap support; CRW, Comparative RNA Web; LM, light microscopy; ML, maximum likelihood; SEM, scanning electron microscopy; SSU, small subunit

INTRODUCTION

~~The increased interest in epizoic, and more specifically, sea turtle-associated diatoms has in recent years brought about some significant advances in our understanding of the complex relationships between diatoms and their animal hosts.~~ As indicated by s~~S~~everal studies, ~~indicated that~~ diatom communities inhabiting both the skin and the carapace of marine turtles are composed largely of species not observed on other biotic or abiotic substrata (Frankovich et al. 2015, 2016, Majewska et al. 2015a, 2015b, 2017a, 2017b, Robinson et al. 2016, Azari et al. 2020). These observations further suggest a certain level of host-specific evolutionary adaptations used by diatoms. Although intimate relationships between animals and microbes are common and extensively studied, reports of truly epizoic microalgae are generally rare (Ezenwa et al. 2012, Redford et al. 2012, Apprill 2017). Perhaps due to the fact that ubiquitous photosynthetic organisms, such as diatoms, are not immediately perceived as an essential element of any vertebrate microbiome, these new findings are particularly noteworthy. Based on their high frequency of occurrence and high relative abundances recorded from various sea turtle species and geographical regions, as well as lack of records from other types of substrata, several of the newly described sea turtle-associated diatom taxa are currently believed to be strictly epizoic or even sea turtle-specific. While this may be true, many other diatoms present in the sea turtle samples are likely opportunistic species that attached to biofilm in the later stages of its development ~~While several of the newly described sea turtle-associated diatom taxa are currently believed to be strictly epizoic or even sea turtle-specific based on their high frequency of occurrence and high relative abundances recorded from various sea turtle species and geographical regions, as well as lack of records from other types of substrata, many other diatoms present in the sea turtle samples are likely opportunistic species that attached to biofilm in the later stages of its development~~ (Majewska et al. 2015b, 2017b, 2019a,b). Although opportunistic taxa ~~the latter group~~ often dominate~~s~~ specific epizoic habitats in terms of the species

number, they ~~opportunistic taxa~~ rarely reach high relative abundance, which may suggest their lack of some key functional adaptations to the epizoic lifestyle.

~~As it has already been proposed, studies on sea turtle-associated diatoms may shed more light on the mechanistic processes of divergence and adaptive evolution of diatoms. Furthermore, provided the close relationship between epizoic diatoms and sea turtles holds up under the scrutiny of increased data sampling, new diatom-based tools may be designed to assess the overall well-being of the host in the future (Robinson et al. 2016). Currently, however, the role of diatoms in the sea turtle microbiome functioning remains unknown. Thus, there is no evidence in the existing data for a relationship between the presence or absence of certain diatom groups and the etiopathology of various sea turtle illnesses and disorders. In addition, the interplay between the host and non-host factors influencing the epizoic diatom communities is poorly understood. Therefore, before this endeavour can be accomplished, baseline compositional and ecological data on sea turtle-associated diatom flora must be collected.~~

The present study focuses on the sea turtle-associated species belonging to the diatom genus *Craspedostauros* E.J.Cox. At present, the genus comprises ten validly described species including one, *C. alatus* Majewska et Ashworth, described from museum specimens of sea turtles (Cox 1999, Sabbe et al. 2003, Van de Vijver et al. 2012, Ashworth et al. 2017, Majewska et al. 2018). *Craspedostauros* is a predominantly marine genus, although *C. laevissimus* (W. et G.S. West) Sabbe is described as "a widespread endemic species restricted to the Antarctic Continent" and may be of brackish or freshwater origin (Sabbe et al. 2003, Van de Vijver et al. 2012). Most of the *Craspedostauros* members share the typical of the genus morphological characters such as cribrate areolae, numerous doubly-perforated girdle bands, two fore and aft chloroplasts, and a usually narrow stauros. Nevertheless, the latter is reduced or strongly reduced in two species: *C. alyoubii* J.Sabir et Ashworth and *C. paradoxus** Ashworth et Lobban. Molecular phylogenetic analysis indicated that the genus is closely related to *Achnanthes* Bory and *Staurotropis* Paddock (Ashworth

et al. 2017). Both taxa, as well as another marine genus *Druehlago* Lobban et Ashworth, which has yet to be characterized molecularly, share several morphological similarities with *Craspedostauros* (Cox 1999, Ashworth et al. 2017). For example, all the above-mentioned taxa possess valves and girdle bands perforated by cribrate areolae. Moreover, *Craspedostauros* and *Druehlago* share the general frustule morphology, including frustules with central constriction (Ashworth et al. 2017), whereas the fore and aft arrangement of chloroplasts, typical of *Craspedostauros,* can be observed in several *Achnanthes* species (Cox 1999).

Three novel species, *C. danayanus* Majewska et Ashworth sp. nov., *C. legouvelloanus* Majewska et Bosak sp. nov., and *C. macewanii* Majewska et Ashworth sp. nov., were found in the course of the ongoing survey on sea turtle-associated diatoms and are described in the current paper. Moreover, a small population of *C. alatus* is for the first time reported from Europe. A large number of samples analysed and different preservation and processing techniques applied allowed us to document the ultrastructure of the frustule and, whenever possible, the morphology of the plastids as well as the colony type and attachment mode of the cells. These observations were supplemented by a 3-gene phylogenetic analysis including DNA sequence data for three sea turtle-associated *Craspedostauros* species and other marine and epizoic diatom taxa.

* the specific epithet in *Craspedostauros paradoxa* should be changed to '*paradoxus*' following the recommendations of the International Code of Nomenclature for algae, fungi, and plants (Articles 23.5 & 62; Turland et al. 2018).

MATERIALS AND METHODS

Material collection and preservation

Diatom samples were collected from captive and wild sea turtles from Croatia and South Africa. All biofilm samples from carapace and skin were taken using single-use sterile toothbrushes according to the sampling protocols suitable for diatom culturing and standard morphology-based diatom analysis proposed by Pinou et al. (2019). In Croatia, 76 (skin and carapace) samples were collected from 38 loggerhead sea turtles *Caretta caretta* L. rescued and rehabilitated at the Marine Turtle Rescue Centre in Aquarium Pula between 2016 and 2019, on the day of or shortly after their arrival at the facility. In South Africa, 196 (skin and carapace) biofilm samples were collected from 78 loggerheads and 20 leatherbacks *Dermochelys coriacea* Vandelli nesting in Kosi Bay (Indian Ocean) over two nesting seasons, in 2017/2018 and 2018/2019. In addition, 6-mm skin biopsy punches were taken from either front or rear flippers of 30 loggerheads and six leatherbacks and preserved in 4 % formaldehyde solution in seawater immediately after collection. Samples of sea turtle-associated barnacles *Chelonibia testudinaria* L. from 100+ loggerheads and *Platylepas coriacea* Monroe et Limpus from 15 leatherbacks were taken using a plastic paint scraper or a blunt knife during four nesting seasons, in 2015/2016, 2016/2017, 2017/2018, and 2018/2019. Barnacle samples comprised of more than one specimen, were divided into two parts and either frozen (-20°C) or fixed with 4 % formaldehyde solution in seawater. Single-specimen barnacle samples were frozen (-20°C). Furthermore, skin and carapace samples were collected from seven sea turtles (three loggerheads, three green turtles *Chelonia mydas* L., and one hawksbill *Eretmochelys imbricata* L.) resident at the uShaka Sea World in Durban on 28 June 2019.

Material collection was performed by, or under close supervision of, qualified field researchers, and the applied techniques and procedures respected ethical principles of the Declaration of Helsinki (World Medical Association 2013) as well as all applicable national laws.

Material processing and microscopy

Diatoms were detached from the frozen barnacles using a Transsonic T310 (Elma, Singen, Germany) ultrasound bath as described in Majewska et al. (2019b). Diatom biofilm from the sea turtle skin, carapace, and barnacles was cleaned from organic matter using either a rapid digestion with a mixture of concentrated HNO_3 and H_2SO_4 (at a ratio of 2:1) according to the method proposed by von Stosch (South African and Croatian samples; Hasle and Syvertsen 1997) or heated 37% H_2O_2 with addition of $KMnO_4$ (Croatian culture strain; van der Werff 1953~~5~~). Cleaned material was mounted on slides using Naphrax (Brunel Microscopes Ltd, Chippenham, UK; Croatian samples) and Pleurax ~~(~~prepared according to the method proposed by von Stosch (1974; South African samples). The slides were~~and~~ examined using a Nikon Eclipse 80i light microscope with Differential Interference Contrast (DIC) and a Nikon DS-Fi1 5MP digital camera (Nikon Instruments Inc., Melville, NY; South African samples) as well as a Zeiss Axio I~~i~~mager A2 with DIC and an Axiocam 305 digital camera (Carl Zeiss, Jena, Germany; Croatian samples). In addition, fresh material containing living diatoms attached to the sea turtle scutes and skin flakes was stained with blue writing ink (Scheaffer ®) to reveal the colonies of the diatom-associated bacteria.

For scanning electron microscopy (SEM), the oxidized suspension was filtered through 1-µm or 1.2-µm Isopore™ (Merck Millipore, Darmstadt, Germany) or 3-µm Nucleopore (Nucleopore, Pleasanton, CA, USA) polycarbonate membrane filters. Formalin-preserved skin and barnacle samples were dehydrated in an alcohol series (30%, 50%, 60%, 70%, 80%, 90%, 95%, 99.9%) followed by critical point-drying in an E3100 Critical Point Dryer (Microscience Division, Watford, UK). Subsequently, the samples were mounted on aluminium stubs with carbon tape and sputter-coated with either gold-palladium using Cressington 108Auto and Cressington 208HR sputter-coaters (Cressington Scientific Instruments Ltd., Watford, UK), palladium using a Precision Etching and Coating System, PECS II (Gatan Inc., CA, USA), or iridium using Emitech K575X (Emitech Ltd., Ashford, Kent, UK) and Cressington 208 Bench Top sputter-coaters. Diatom specimens were analysed with JEOL JSM-7800F, JEOL JSM-7001F (JEOL, Tokyo, Japan), FEI

Quanta Feg 250 (FEI Corporate, Hillsboro, OR, USA), Zeiss Ultra Plus (Carl Zeiss, Oberkochen, Germany), and Zeiss SUPRA 40 VP (Carl Zeiss Microscopy, Thornwood, NY, USA) scanning electron microscopes at 3−10 kV. To determine the relative abundance of the new species, 400 diatom valves were counted and identified in each sample along arbitrarily chosen transects using SEM. The morphology and frustule ultrastructure of the new taxa was compared with those of all known *Craspedostauros* species worldwide (Cox 1999, Sabbe et al. 2003, Van de Vijver et al. 2012, Ashworth et al. 2017, Majewska et al. 2018).

Culturing

Living diatoms from the fresh material (unpreserved samples containing sea turtle biofilm and filtered seawater; Pinou et al. 2019) were isolated using a glass pipette with a tip pulled and thinned over a flame into 16x100 mm glass culture tubes (South African strains) or plastic culture flasks (Croatian strains) filled with 34 PSU (South African strains) or 38 PSU (Croatian strains) f/2 growth medium (Guillard 1975). Strains were lit by natural light from a south-facing window (South African strains) or white fluorescent light with a photoperiod of 12h (Croatian strains) and maintained at a temperature of 20–24°C. The well-growing cultures were divided into two parts, one of which was used for DNA extraction. The remaining part was cleaned with a mixture of 30% H_2O_2 and 70% HNO_3 and rinsed with distilled water until the near-neutral pH of the fluid phase was reached. Croatian strain (PMFTB0003) was cleaned using saturated $KMnO_4$ solution and ca. 30% HCl following a slightly modified protocol proposed by Simonsen (1974). Permanent microscopy slides and SEM stubs were prepared as described above.

DNA preparation and phylogenetic analysis

The cultures were harvested as cell pellets using an Eppendorf 5415C centrifuge (Eppendorf North America, Hauppauge, NY, USA) for 10 minutes at 8-000 rpm. The QIAGEN DNeasy Plant Mini Kit (QIAGEN Sciences, Valencia, California, USA) was used for DNA extraction following the manufacturer's protocol, with the addition of an initial cell disruption by 1.0 mm glass beads in a Mini-Beadbeater (Biospec Products, Inc, Bartlesville, OK, USA) for 45 sec. PCR-based DNA amplification and di-deoxy Sanger sequencing of small-subunit nuclear rRNA and the chloroplast-encoded rbcL and psbC markers followed Theriot et al. (2010).

Phylogenetic analysis of the DNA sequence data was conducted using a three-gene dataset: nuclear-encoded small subunit (SSU) rRNA, and plastid-encoded *rbc*L and *psb*C. Alignment of the SSU sequences, accounting for secondary structure, was done using the SSUalign program (Nawrocki et al. 2009), with the covariance model based on the 10 diatoms included with the program download, plus 23 additional diatoms from the CRW website (Cannone et al. 2002). Post alignment, SSU sequences were concatenated to the chloroplast sequences into a single matrix (Supplementary Table S1). Eight separate partitions were created for the data (SSU paired and unpaired sites, plus the first, second and third codon positions of each of *rbc*L and *psb*C). This dataset and partitioning scheme were run under maximum likelihood (ML) using RAxML ver. 8.2.7 (Stamatakis 2014) compiled as the pthread-AVX version on an Intel i7 based processor, using the GTR+G model. Twenty-five replicates, each with 500 rapid BS replicates, were run with ML optimizations. Bootstrap support was assessed using the BS replicates from the run with the optimal ML score.

RESULTS

Morphological observations

***Craspedostauros danayanus* Majewska & Ashworth sp. nov. (Figs 2–24)**

Cells with two fore and aft H-shaped chloroplasts (Figs 2–5). Frustules extremely delicate and very lightly silicified (Figs 6–16). In girdle view, frustules rectangular, moderately constricted at the centre (Figs 5, 7 & 11). Valves narrow, linear, very slightly constricted in the valve middle, with bluntly rounded apices (Figs 4, 12–16).

Light microscopy (Figs 12–16):

Valve dimensions (n = 30): length 28–61 µm, width 2–2.5 µm, length/width ratio: 14–30.5. In cleaned (acid-digested) material, partially dissolved valve margins barely noticeable (Figs 14 & 15, arrows), intact frustules absent. Striae indiscernible (Figs 12–16). Raphe-sternum thickened, clearly visible (Figs 12–16). ~~Raphe straight (Figs 12–16).~~ Thickenings at both central and terminal raphe endings (Figs 12–16).

Scanning electron microscopy (Figs 17–24):

Externally: In cleaned material, valve face appearing flat, with very shallow mantle and straight margin (Figs 17 & 18). Striae uniseriate, 49–51 in 10 µm, parallel, becoming radiate towards the apices, alternate or opposite, composed of up to eight areolae (Figs 17 & 18). Areolae largely similar in size, becoming somewhat smaller around the central area, squarish to roundish, externally occluded by~~covered with~~ cribra (Figs 17–19). Each cribrum perforated by 2–8 pores (Fig.~~s~~ 17~~–19~~). Axial area narrow (Figs 17 & 18). Raphe-sternum not raised (Figs 17–19). Raphe branches straight (Fig. 18). Central area large, symmetrical, amygdaliform~~fusiform~~ (Figs 18 & 19). Central raphe endings straight, elongated, slightly expanded (Figs 18 & 19). Terminal raphe endings disappearing under somewhat triangular silica flaps extending from the raphe-sternum, giving the impression of unilaterally bent terminal raphe fissures (Figs 17 & 18). A large, irregular depression present at the apical flap fold (Figs 17 & 18, arrowheads). Shortened striae composed of cribrate areolae radiating

around the apices beyond the apical silica flaps (Fig. 17). Asymmetrical pore-free~~hyaline~~ area present beyond the terminal raphe endings in the immediate vicinity of the apical flap fold (Fig. 17).

Internally~~:,~~ R~~r~~aphe slit opening laterally onto the more or less uniformly thickened and distinctly raised raphe-sternum (Fig. 20). Stauros absent (Figs 20 & 21). Central area mirroring the external structure in size and shape (Figs 20 & 21). Central raphe endings elongated, very slightly unilaterally bent, terminating onto weakly constricted rectelevatum (Figs 20 & 21). Terminal raphe endings positioned somewhat laterally on a large and rounded apical part of the raphe-sternum, terminating in ~~prominent~~ helictoglossae (Figs 20 & 23). Asymmetrical thickening extending from the apical part of the raphe-sternum towards the valve margin, corresponding to the external apical silica flaps (Fig. 23, arrowheads). Areolae externally occluded with cribra~~, appearing sunken~~ (Figs 21–23).

Cingulum composed of numerous (14+) open copulae, bearing two rows of typically squarish, roundish or elongated areolae, ca. 50–60 in 10 µm (Figs 18, 23 & 24). Areolae occluded~~covered~~ externally by cribra (Figs 23 & 24).

Taxonomic remarks

Craspedostauros danayanus is most similar to *C. paradoxus*, sharing the general valve outline and lacking the stauros. However, *C. danayanus* differs from the latter in being distinctly smaller (28–61 µm vs 80–85 µm)~~ µm~~ and more slender (2–2.5 µm vs 6.5–9 µm), possessing a higher stria density (~~36–40 vs~~ 49–51 vs 36–40), and lacking the lip-like silica flaps (externally) and the central knob (internally) present in *C. paradoxus* (Table 1).

HOLOTYPE: Permanent slide SANDC-ST012 ~~and unmounted material~~ (prepared from sample ZA0019A/ZA1824E) deposited in the South African Diatom Collection housed by North-West University, Potchefstroom, South Africa.

TYPE LOCALITY: Mabibi Beach, Elephant Coast, South Africa (27° 21′ 30″ S, 32° 44′ 20″ E). Collected from the barnacle *Platylepas coriacea* growing on the egg-lying leatherback sea turtle (tag numbers: ZA0019A, ZA1824E) by R. Majewska, 7 December 2018.

ETYMOLOGY: The epithet honours Danay A. Stoppel (North-West University, Potchefstroom, South Africa), who made the first observations of the new taxon, in recognition of her contribution to the sea turtle diatom project in South Africa.

ECOLOGY: Epizoic on carapaces of adult leatherback sea turtles and on leatherback-associated barnacles *Platylepas coriacea* growing on adult leatherbacks from Kosi Bay (South Africa). Attaching to the animal surface through one end of the valve, motile in culture.

The taxon was found in twelve leatherback skin samples (out of 20 examined) and in all *P. coriacea* samples examined (n = 15) reaching relative abundances of 35% (skin samples) and 79% (barnacle samples). It was found in neither loggerhead nor loggerhead-associated barnacle samples from the same location (Kosi Bay, South Africa). Leatherback skin samples containing *C. danayanus* were dominated by *Navicula* spp., *Tursiocola* sp., and *Poulinea* spp. The new taxon was dominant in most of the *P. coriacea* samples along with *Cylindrotheca* sp. Both taxa colonised various anatomical parts of the barnacle showing preference for rough surfaces and cavities. The extremely lightly silicified frustules may be an adaptation to the pelagic lifestyle of the host, as the open ocean waters contain significantly lower concentrations of dissolved silica than coastal habitats (Tréguer et al. 1995).

Craspedostauros legouvelloanus **Majewska & Bosak sp. nov. (Figs 25–47)**

Light microscopy (Figs 25–30):

Intact frustules lying almost always in girdle view (due to large cell depth/valve width ratio), slightly constricted in the middle (Figs 25, 26, 28–30), ~~broad~~ with several girdle bands (Figs 26, 28 & 30). Valve margin expanded at the centre (Figs 25, 28 & 30). Frustules lightly silicified and delicate. Valves narrow, linear to linear-lanceolate, slightly constricted at the central area, with bluntly rounded apices (Fig. 27). Valve dimensions (n = 30): length 18–34 µm, width 3–5 µm, length/width ratio: 5.6–9.4. Striae indiscernible (Figs 25–30). Stauros narrow (Figs 25, 27–30), widening towards the biarcuate valve margins (Fig. 30, arrows). Raphe-sternum clearly visible (Figs 25–30). Raphe straight, biarcuate in girdle view (Figs 25, 26, 28 & 30).

Scanning electron microscopy (Figs 31~~8~~–40~~17~~):

Externally: Valves somewhat convex, with no clear valve face-mantle junction (Figs 31–33~~6~~). Valve margin clearly expanded at the centre beyond the stauros (Fig. 33). Striae uniseriate, 46–49 in 10 µm, parallel throughout the valve centre, becoming convergent near the apices, alternate or opposite, composed of up to 13 areolae (Figs 31, 32 & 38). Areolae similar in size throughout the entire valve, squarish, externally occluded by~~covered with~~ cribra (Figs 31–33 & 38). Each cribrum perforated by 4 pores (Figs 31–33 & 38). Axial area very narrow (Figs 31 & ~~–~~32~~3~~). Raphe-sternum very slightly raised (Figs 31–33). Raphe branches more or less straight (Fig. 31). Central area forming a narrow rectangular fascia (Figs 31 & 38). Central raphe endings covered entirely by rimmed lip-like silica flaps extending from one side of the axial area (Figs 31 & 38). At the apices, axial area expanding into somewhat triangular silica flaps covering the terminal raphe endings giving the impression of unilaterally bent terminal raphe fissures (Figs 31–33). An oval or irregular depression present at the apical flap fold (Fig. 31, arrows). Shortened stria composed of regular areolae and simple puncta radiating around the apices beyond the terminal raphe endings (Figs 31–33).

Internally:, Rraphe slit opening laterally onto the uniformly thick and clearly raised raphe-sternum (Figs 35 & 36). Stauros raised, very narrow, broadening abruptly at the mantle expansion and merging with the pore-freehyaline area at the valve margin (Figs 36 & 39), slightly more expanded and somewhat thicker on the side corresponding to the external lip-like silica flaps (Figs 36, arrowheads, 39 & 40). Central raphe endings straight or slightly unilaterally bent, elongated, terminating onto a weakly developed, elongated and rectelevatum flattened helictoglossae (Figs 35, 36, 39 & 40)., Abearing a blunt cylindrical knob with a small central cavity present between the raphe endings (Figs 35, 36, 39 & 40). Areolae externally occluded bycovered with cribra, appearing sunken, especially close to the stauros (Figs 39 & 40). Stauros-adjacent virgae appearing hollow, suggesting a more complex valve structure in that area (Fig. 39, arrowheads). Terminal raphe endings positioned somewhat laterally on the raphe-sternum, terminating onto prominent helictoglossae. At the apices, within an expanded raphe-sternum expanded laterally towards the valve margin, merged with pore-freehyaline area corresponding to the external apical silica flaps (Figs 36 & 37).

Cingulum composed of numerous (12+) open copulae, bearing two rows of typically squarish or elongated areolae, ca. 50–60 in 10 μm (Figs 32–35). Areolae occludedcovered externally by cribra with 4–12 pores per cribrum (Figs 32–35). Valvocopula curved, distinctly narrower and pore-freehyaline besideat the stauros (Fig. 33, arrowheads). An internal ridgethickening perforated by puncta, resembling a reduced septum, present in each copula except for valvocopula (Figs 33–35, arrowheads).

Adriatic population (Figs 41–47)

Specimens resembling *C. leguovelloanus* were found on the carapace of six loggerhead sea turtles sampled on the Croatian coast of the Adriatic Sea. Most of the morphological features observed in the Adriatic population (Figs 41–47) agreed well with those found in *C. legouvelloanus* (Figs 41–

47). The cells possessed two fore and aft H-shaped chloroplasts (Fig. 41, arrows) observed previously in other *Craspedostauros* species (Cox 1999, Ashworth et al. 2017, Majewska et al. 2018). The specimens were slightly longer (23–39 µm) and wider (3.5–6 µm, length/width ratio: 5.2–7.8, n = 25) than those from the South African population and their stria density was lower (40–44 in 10 µm vs. 46–49 in 10 µm; Table 1). In general, the frustules showed a relatively high degree of irregularity in the areolae structure and the size and shape of stauros, axial area, and facia (Figs 42–45).

Taxonomic remarks

Currently, *C. legouvelloanus* is the only *Craspedostauros* species with septate girdle bands. ValvesFrustules of this speciestaxon differ from those of all known stauros-bearing *Craspedostauros* species in possessing a very high stria density (above 40 in 10 µm). Although a similarly high or higher stria density was observed in *C. alyoubii* (~40 in 10 µm) and *C. danayanus* (49–51 in 10 µm), the two species are larger (83–105 µm and 28–61 µm) than *C. legouvelloanus* (18–34 [39] µm) and their general morphology differs remarkably from that of the new taxon in, for example, possessing a reduced or strongly reduced stauros (Table 1). Several of the characters of *C. legouvelloanus*, such as largely uniform valve areolae with four pores per cribrum and internal central knob, agree with the description of *C. australis* E.J.Cox (Cox 1999). However, the new species can be easily distinguished from the latter by its clearly centrally expanded valve margin and well-developed lip-like silica flaps externally covering the central raphe endings absent in *C. australis* (Table 1).

Although wild specimens belonging to the Adriatic population of *C. legouvelloanus* exhibited numerous irregularities in the shape and size of taxonomically important characters such as areolae, striae, stauros, and central area, we were unable to indicate and unambiguously describe features that would distinguish them from the type population. High morphological plasticity and

polymorphy in diatoms have been reported from both epizoic and non-epizoic habitats (Cox 2011, De Martino et al. 2011, Urbánková et al. 2016, Riaux-Gobin et al. 2014, 2017, Edlund and Burge 2019), and it is conceivable that the morphological differences observed between the two populations could be induced by environmental triggers, such as differences in salinity or nutrient concentrations (Schultz 1971, Czarnecki 1987, 1994, De Martino et al. 2011). Unfortunately, the Croatian strain PMFTB0003 (Figs 41, 43, 45 & 46) isolated from the sample TB13 did not survive and the DNA material could not be obtained at the time of this study. Therefore, in the light of the current lack of any additional information about the phylogenetic relationships between the two populations, they should be considered conspecific until otherwise proven.

HOLOTYPE: Permanent slide SANDC-ST003 and unmounted material (prepared from sample ZA0762D/ZA0763D) deposited in the South African Diatom Collection housed by North-West University, Potchefstroom, South Africa.

PARATYPE: Permanent slide HRNDC000150 and unmounted material (TB13) deposited in the Croatian National Diatom Collection housed by Faculty of Science, University of Zagreb, Croatia.

ISOTYPES: Permanent slides BR-XXXX and BR-XXXX deposited in the BR-collection housed by Meise Botanic Garden, Meise, Belgium.

TYPE LOCALITY: Kosi Bay, South Africa (26° 59′ 39″ S, 32° 51′ 60″ E). Collected from the carapace of the egg-lying loggerhead sea turtle (tag numbers: ZA0762D, ZA0763D) by R. Majewska, 15 December 2017 (holotype).

Marine Turtle Rescue Centre, Pula, Croatia (44°50′ 07″ N, 13°49 ′ 58″ E). Collected from a semi-adult female loggerhead *Caretta caretta* named ‘Mimi’ by K. Gobić Medica, 28 May 2019 (paratype).

ETYMOLOGY: The epithet honours Dr Diane Z. M. Le Gouvello du Timat (Nelson Mandela University, Port Elizabeth, South Africa), who assisted during the type material collection, in recognition of her invaluable help and on-going support to the sea turtle diatom project and sea turtle research in South Africa.

ECOLOGY: Epizoic on carapaces and skin of adult loggerhead sea turtles and on loggerhead-associated barnacles *Chelonibia testudinaria* growing on adult loggerheads from Kosi Bay (South Africa) and the Adriatic Sea (Croatia). Attaching to the animal surface through one end of the valve, motile in culture.

Although the taxon was present in numerous samples, its relative abundance rarely exceeded 4% of the total diatom number. Samples with *C. legouvelloanus* from both locations were each time dominated by *Poulinea* spp., *Berkeleya* spp., *Halamphora* spp., and *Nitzschia* spp., with addition of *Achnanthes elongata* Majewska et Van de Vijver, *Cyclophora tenuis* Castracane, *Proschkinia* spp., *Navicula* spp., *Licmophora* spp., and *Haslea* spp.

***Craspedostauros macewanii* Majewska & Ashworth sp. nov. (Figs 48–62)**

Light microscopy (Figs 48–54):

Cells with two fore and aft H-shaped chloroplasts (Figs 48 & 51). Frustules delicate and lightly silicified (Figs 48–54). In girdle view, frustules rectangular, moderately to strongly constricted at the centre (Figs 48–50). Cingulum composed of several girdle bands (Figs 498–50). Valves narrow, linear to linear-lanceolate, slightly constricted at the central area, with bluntly rounded apices (Figs 51–54). Valve margin straight (Fig. 49, arrow). Valve dimensions (n = 20): length 26–51 µm (up to ~~–~~65 µm in culture) ~~µm~~, width 4.5–5.5 µm (up to ~~–~~6 µm in culture) ~~µm~~, length/width ratio: 5.4–11.3. Valve face-mantle junction visible on each side of the raphe (Figs 52–54, arrows). Striae barely discernible, 28–31 in 10 µm (Figs 52–54). Central area narrow, bow tie-shaped (Figs 52–54).

Raphe-sternum thickened (Figs 52–54). Raphe straight (Fig. 54) with thickenings at the terminal raphe endings (Figs 52–54).

Scanning electron microscopy (Figs 55–62):

Externally: Valves slightly concave at the centre, with distinct valve face-mantle junction marked by a narrow pore-free~~hyaline~~ area (Figs 55 & 57). Valve face flat (Fig. 55). Mantle very deep (Fig. 55). Valve margin straight, with narrow pore-free~~hyaline~~ area at the mantle edge (Figs~~.~~ 56 & 57~~5~~). Striae uniseriate, parallel through most of the valve, becoming convergent near the apices, alternate or opposite, composed of up to 21 areolae (2–8 on the valve face and up to 13 on the mantle; Figs 55–58). Areolae similar in size, squarish, externally occluded~~covered~~ by~~with~~ cribra (Figs 56–58). Areolae bordering the narrow axial area usually only slightly larger and somewhat irregular in shape (Figs 56–58). Each cribrum perforated by highly variable number of pores (up to 13+; Figs 56–58). Raphe branches more or less straight (Fig. 55). Central area in the form of a narrow bow tie-shaped fascia (Figs 55 & 57). Central raphe endings covered by small lip-like silica flaps extending from one side of the axial area (Figs 55 & 57). Apices pore-free~~hyaline~~ (Figs 55, 56 & 58). Terminal raphe endings covered by triangular silica flaps giving the impression of unilaterally bent terminal raphe fissures (Figs 55, 56 & 58). An oval or irregular depression (Figs 55, arrowhead, 56 & 58) with several small areolae (Figs 56 & 58, arrowheads) present at the apical flap fold. Shortened striae composed of a single areola (occasionally with additional puncta) radiating around the apices beyond the terminal raphe endings (Figs 56 & 58).

Internally:~~,~~ R~~r~~aphe slit opening more or less centrally onto the uniformly thick raphe-sternum (59–61). Stauros raised, narrow, tapering towards the valve face-mantle junction and widening significantly on the valve mantle towards the mantle edge (Figs 59 & 61). Central raphe endings straight, elongated, terminating onto weakly developed, elongated and flattened helictoglossae ~~flattened rectelevatum~~ (Figs 59 & 61). A flatly ended cylindrical knob present at the central nodule

(Figs 59 & 61). Areolae externally occluded by~~covered with~~ cribra, appearing sunken, especially close to the raphe-sternum (Figs 60 & 61). Terminal raphe endings terminating onto prominent helictoglossae within an expanded and thickened pore-free~~hyaline~~ area corresponding to the curvature of the external silica flaps (Fig. 60). Several small areolae present at the end of the curved thickening (Fig. 60, arrowheads).

Cingulum composed of numerous open copulae bearing up to five rows of cribrate squarish or elongated areolae, ca. 38–45 in 10 µm (Figs 55, 59 & 62). Advalvar part of valvocopula pore-free~~hyaline~~ beside~~at~~ the stauros (Fig. 59).

Taxonomic remarks

The morphological character pattern in *Craspedostauros macewanii* is most similar to *C. australis* and *C. capensis* Cox. The three species share several features such as the presence of a bow tie-shaped fascia, rudimentary lip-like silica flaps extending from the raphe-sternum and partially covering the external central raphe endings, valve margin straight at the centre, and internally, a single knob at the central nodule (Table 1). Moreover, valve dimensions of *C. macewanii* (26–51 µm long, 4.5–5.5 µm wide) overlap with those reported for *C. australis* (35–78 µm long, 4–6 µm wide) and *C. capensis* (25–35 µm long, 4.5–5.5 µm wide). In *C. macewanii*, however, the stria density (28–31 in 10 µm) is significantly higher than in *C. capensis* (~19 in 10 µm) and lower than in *C. australis* (35 in 10 µm). In addition, *C. macewanii* can be distinguished from both *C. australis* and *C. capensis* by the presence of a distinct valve face-mantle junction running as a narrow, though clearly visible, pore-free~~hyaline~~ ridge from apex to apex. *Craspedostauros macewanii* differs further from *C. capensis* in possessing areolae of a similar size throughout the entire valve (variable in *C. capensis*), and from *C. australis* in having convergent stria at the apices (parallel in *C. australis*) and extended apical hyaline zone (Cox 1999). The new taxon is also the only

Craspedostauros species with girdle bands perforated by up to five rows of squarish areolae instead of two rows of usually transapically elongated areolae observed in other species.

HOLOTYPE: Permanent slide SANDC-ST242 ~~and unmounted material~~ (prepared from sample ST242) deposited in the South African Diatom Collection housed by North-West University, Potchefstroom, South Africa.

TYPE LOCALITY: uShaka Sea World, Durban, South Africa (29° 52′ 02.79″ S, 31° 02′ 45.29″ E). Collected from the carapace of a captive juvenile loggerhead named "Bubbles" by R. Majewska, 28 June 2019.

ETYMOLOGY: The epithet honours Tony McEwan, the uShaka Sea World director, whose scientific enthusiasm and support to the sea turtle diatom project are highly appreciated and acknowledged.

ECOLOGY: Epizoic on skin and carapaces of captive loggerheads and green turtles. Attaching to the animal surface through one end of the valve, motile in culture.

The taxon was found on two captive loggerheads (a juvenile named "Bubbles" and an adult female named "DJ") and two captive green turtles (a subadult named "Calypso" and an adult male named "Napoleon") each time reaching relative abundance of 0.5–1%. All carapace samples containing *C. macewanii* were dominated by the so-called "marine gomphonemoids": *Poulinea* spp. and *Chelonicola* spp., accompanied by *Amphora* spp., *Nitzschia* spp., *Achnanthes elongata* and *A. squaliformis* Majewska et Van de Vijver, whereas the most abundant taxa in the four skin samples were *Tursiocola* spp., *Medlinella* sp., and the two previously mentioned *Achnanthes* species.

***Craspedostauros alatus* Majewska & Ashworth (Figs 63–74)**

503 *Craspedostauros alatus* was found on the carapaces of several loggerhead sea turtles sampled at the
504 Marine Turtle Rescue Centre in Pula, Croatia. The taxon co-occurred with *C. legouvelloanus*. As in
505 the case of the latter, relative abundance of *C. alatus* was low (ca. 1–3% of the total diatom
506 number). The observed morphological features of the Adriatic population agreed with the original
507 description of the species (Majewska et al. 2018; Figs 63–74, Table 1). The examined specimens
508 were 26–34 µm long and 3–5 µm wide (length/width ratio: 6.3–8.8), with stria density 24–27 in 10
509 µm (n = 20), and possessed all species-specific features, including a very distinct valve face-mantle
510 junction and deep mantle (Figs 68, arrows, 69–71), wing-like silica flaps at the apices (Fig. 70), and
511 rectelevatum with central cavity (Figs 73 & 74).

512

513 *DNA-based phylogeny*

514 The genus *Craspedostauros* is monophyletic based on DNA sequence data generated from cultured
515 material thus far (Fig. 75), though not with strong bootstrap support (bs < 50%). Regarding the taxa
516 described here, *Craspedostauros macewanii* is sister to the rest of the clade (except *C.*
517 *amphoroides*) with high support (bs = 96%), while *C. danayanus* is sister to *C. alyoubii* and *C.*
518 *paradoxus* (bs = 71%).

519 Consistent with other molecular phylogenetic studies which include the genus (Ashworth et al.
520 2017), the position of the *Craspedostauros* clade can be found in a poorly supported (bs < 50%)
521 assemblage containing the *Staurotropis* clade and a clade of marine *Achnanthes* species. This
522 assemblage can be found within a clade with the Bacillariales (Supplementary Figure S1), though
523 the relationship between the *Staurotropis*+*Achnanthes*+*Craspedostauros* clade and the three
524 Bacillariales clades is poorly resolved. For taxa, strain voucher ID and GenBank accession numbers
525 for strains used in the analysis see Supplementary Table S1.

526

DISCUSSION

The three new species described in the current study share most of the morphological characters typical of the genus *Craspedostauros*, such as squarish or rectangular areolae occluded by cribra on the valve and girdle bands, multiple copulae with at least two rows of perforations, and two fore and aft chloroplasts. Their linear or linear-lanceolate valve outline and the central constriction of the cell seen in girdle view resemble previously described species. Interestingly, two of the novel species, *C. macewanii* and *C. legouvelloanus*, present features not yet observed in any other member of the genus. The former possesses more than two rows of cribrate areolae on the girdle bands, whereas the latter shows shallow perforated septa. Moreover, the leatherback-associated *C. danayanus* presents a complete reduction of the stauros being the second, after *C. paradoxus*, *Craspedostauros* species lacking this character.

It is interesting to note that as the number of character states, such as the reduction/loss of the stauros (*C. paradoxus* and *C. danayanus*) or addition of septate copulae (C. *legouvelloanus*), within *Craspedostauros* changes, the molecular data remain constant in their support (however tenuous) of monophyly for the genus. Cox (1999) ascribed the constricted girdle view to the presence of stauros. Yet the frustules of the two species lacking the latter, still show the central constriction, which may indicate that the lack of stauros is a secondary loss. One of the morphological features of the genus which has been maintained, regardless of newly described diversity, has been the cribrate areolar covering. While the degree of cribrum poration might change among species, the overall gestalt ultrastructure remains unchanged. Even more interesting is that this cribrum ultrastructure is also seen in *Staurotropis* and the *Achnanthes* species, which are commonly found (again, somewhat tenuously) sister to the *Craspedostauros* clade in molecular phylogenies. While there are other morphological similarities between the three genera, such as the stauros (though missing in some species of *Craspedostauros* and *Achnanthes*) and the fore and aft H-shaped or plate-like chloroplasts (missing in *Staurotropis* and some species of *Achnanthes*), so far it is the cribrate

552 areolae ultrastructure that remains constant. In this context, the phylogenetic position of the genus
553 *Druehlago*, which shares the same cribrum ultrastructure and the same chloroplast morphology of
554 *Staurotropis* and *Achnanthes longipes* Agardh, but thus far lacks a stauros-bearing taxon, is all the
555 more intriguing.

556 Microscopical analyses of the fresh and critical-point-dried sea turtle skin pieces and barnacles
557 revealed the mode of attachment and growth form of *C. danayanus* that attaches to the animal
558 substratum through one pole of the cell. A similar mode of attachment to the natural substratum was
559 observed in several members of the genus (R.Majewska, pers. observ.) suggesting that these taxa
560 can either develop as firmly attached, sessile colonies or remain motile in less favourable conditions
561 (e.g. in culture tubes).

562 In the course of the on-going surveys on sea turtle-associated diatoms, a recently described taxon,
563 *C. alatus*, was observed growing on the carapaces of several loggerhead sea turtles rescued in
564 Croatia. *Craspedostauros alatus* was originally described from museum specimens of juvenile
565 Kemp's ridleys (*Lepidochelys kempii* Garman) and a juvenile green turtle found cold-stunned and
566 beyond recovery on the New York (USA) beaches during various seasons between 2012 and 2014
567 (Majewska et al. 2018). Although the relative abundance of *C. alatus* did not exceed 5.5% (current
568 study, Majewska et al. 2018), observations of this taxon on a sea turtle from the Adriatic Sea may
569 indicate that a) *C. alatus* is not an uncommon element of the sea turtle diatom flora; b) being
570 associated with highly migratory animals such as sea turtles its geographical range is likely linked
571 to that of its hosts.

572 A similar conclusion can be drawn based on the records of *C. legouvelloanus*. The species occurred
573 on several of the Adriatic loggerheads as well as on dozens of sea turtles belonging to the same
574 species and their associated barnacles sampled on the eastern coast of South Africa. Even though
575 the taxon was found in two different ocean basins, it cannot be excluded that the sea turtles acted as
576 vectors that facilitated its dispersal among the various seas and oceans. There is a strong

observational and molecular evidence that the Indian Ocean loggerheads interact and mate with the Atlantic members of the species (Bowen et al. 1994, Bowen and Karl 2007, Le Gouvello du Timat et al., in prep.). Thus, it is conceivable that any diatom able to endure the changing conditions during the migrations of their hosts and survive in competition with native flora would inoculate all appropriate and available media and substrata encountered. With the exception of *C. danayanus*, the sea turtle-associated *Craspedostauros* species, although common on the sea turtle carapaces, were never among the dominant taxa, and it is still unclear whether the animal body surface is their preferred or alternative habitat. It is possible that the occurrence of these species in the sea turtle biofilm samples is linked to the presence of some other sea turtle epibionts (e.g. barnacles, sponges, bryozoans). *Craspedostauros danayanus* dominated most of the leatherback skin and barnacle samples that were analysed, and it is likely that this taxon is highly adapted to the conditions provided by the smooth body of the largest among the sea turtles, and, being associated with both the skin and the leatherback-specific barnacle species, *Platylepas coriacea*, its relationship with the host may be obligatory. Leatherbacks, contrary to other extant sea turtles, show the fully oceanic developmental pattern spending most of their lives in highly homogenous open-water environment devoid of refugia (Bolten 2003). They are unique among modern reptiles in being endothermal (Frair et al. 1972). This ability allows them to survive in both tropical and near-freezing waters (James et al. 2006). They are also significantly faster swimmers and deeper divers than other sea turtles (Eckert 2002, Doyle et al. 2008). Therefore, microhabitats provided by these animals, and thus their microbiomes, would differ substantially from those present on other sea turtles. Under such unique conditions, far from the diverse, species-rich shallow-water ecosystems, specific eco-physiological adaptations may be required to survive, and fewer diatom species would manage to thrive on the demanding substratum. An analogous phenomenon is known from marine cetaceans that seem to be colonised by only a few, highly specialized diatom taxa (e.g. Nemoto 1956, Holmes et al. 1993, Ferrario et al. 2018).

ACKNOWLEDGEMENTS

We thank Diane Z. M. Le Gouvello du Timat (Nelson Mandela University, South Africa), Franco De Ridder (North-West University, South Africa), and Karin Gobić Medica and Milena Mičić (Aquarium Pula, Croatia) for their help during the material collection. Danay A. Stoppel and Carla Swanepoel (North-West University, South Africa) processed some of the diatom samples collected in South Africa. Tony McEwan, Leanna Botha, and the rest of the uShaka Sea World staff and members of the South African Association for Marine Biological Research (SAAMBR) are acknowledged for their help in the sea turtle biofilm collection at the uShaka Sea World as well as their great enthusiasm, interest and support to this project. We are further grateful to Jan Neethling and the staff from the Centre for High Resolution Transmission Electron Microscopy, Nelson Mandela University (Port Elizabeth, South Africa) for their generous help during the SEM analyses.

All sampling activities performed in the iSimangaliso Wetland Park (South Africa) were carried out under research permits issued by the South African Department of Environmental Affairs (RES2016/67, RES2017/73, RES 2018/68, and RES 2019/05).

This work was done with partial financial support from The Systematics Association (UK) through the Systematics Research Fund Award granted to R. Majewska (2017) and the Croatian Science~~National~~ Foundation under the project UIP-2017-05-5635 (TurtleBIOME).

References

Apprill, A. 2017. Marine animal microbiomes: toward understanding host–microbiome interactions in a changing ocean. *Front. Mar. Sci.* 4:222. doi: 10.3389/fmars.2017.00222.

Ashworth, M. P., Lobban, C. S., Witkowski, A., Theriot, E. C., Sabir, M. J., Baeshen, M. N., Hajarah, N. H., Baeshen, N. A., Sabir J. S. & Jansen, R. K. 2017. Molecular and morphological investigations of the stauros-bearing, raphid pennate diatoms (Bacillariophyceae): *Craspedostauros* E.J. Cox, and *Staurotropis* T.B.B. Paddock, and their relationship to the rest of the Mastogloiales. *Protist* 168:48–70.

Azari, M., Farjad, Y., Nasrolahi, A., De Stefano, M., Ehsanpour, M., Dobretsov, S., Majewska, R. 2020. Diatoms on sea turtles and floating debris in the Persian Gulf (Western Asia). *Phycologia,* DOI: 10.1080/00318884.2020.1752533.

Bolten, A. B. 2003. Variation in Sea Turtle Life History Patterns: Neritic vs. Oceanic Developmental Stages. *In* Lutz, P. L., Musick, J. A. & Wyneken, J. [Eds.] *The Biology of Sea Turtles*, vol. 2. CRC Press, Boca Raton, USA, pp. 234–58.

Bowen, B. W., Kamezaki, N., Limpus, C. J., Hughes, G. H., Meylan, A. B. & Avise, J. C. 1994. Global phylogeography of the loggerhead turtle (*Caretta caretta*) as indicated by mitochondrial DNA haplotypes. *Evolution* 48:1820–8.

Bowen, B. W. & Karl, S. A. 2007. Population genetics and phylogeography of sea turtles. *Mol. Ecol.* 16:4886–907.

Cannone, J.J., Subramanian, S., Schnare, M.N., Collett, J.R., D'Souza, L.M., Du, Y., Feng, B., Lin, N., Madabusi, L.V., Müller, K.M., Pande, N., Shang, Z., Yu, N. & Gutell, R.R. 2002. The Comparative RNA Web (CRW) Site: an online database of comparative sequence and structure information for ribosomal, intron, and other RNAs. *BMC Bioinformatics* 3:2.

644 Cox, E. J. 1999. *Craspedostauros* gen. nov., a new diatom genus for some unusual marine raphid
645 species previously placed in *Stauroneis* Ehrenberg and *Stauronella* Mereschkowsky. *Eur. J. Phycol.*
646 34:131–47.

647 Cox E.J. 2011. Morphology, cell wall, cytology, ultrastructure and morphogenetic studies. *In*
648 Seckbach, J. & Kociolek, J. P. [Eds.] *The Diatom World*. Dordrecht, Springer, pp. 21–45.

649 Czarnecki, D. B. 1987. Mastogloia revisited: Laboratory confirmation of Stoermer's observation. *IX*
650 *North American Diatom Symposium, Abstracts No. 7*, Treehaven Field Station, Tomahawk,
651 Wisconsin.

652 Czarnecki, D. B. 1994. The freshwater diatom culture collection at Loras College, Dubuque, Iowa.
653 *In* Kociolek J.P. [Ed.] *Proc. Eleventh Int. Diatom Symp., Mem. Calif. Acad. Sci., Nr. 17*. San
654 Francisco, California Academy of Sciences, pp. 155–73.

655 De Martino, A., Bartual, A., Willis, A., Meichenin, A., Villazán, B., Maheswari, U. & Bowler, C.
656 2011. Physiological and molecular evidence that environmental changes elicit morphological
657 interconversion in the model diatom *Phaeodactylum tricornutum*. *Protist* 162:462–81.

658 Doyle, T. K., Houghton, J. D. R., O'Súilleabháin, P. F., Hobson, V. J., Marnell, F., Davenport, J. &
659 Hays, G. C. 2008. Leatherback turtles satellite-tagged in European waters. Endanger. *Species Res.*
660 4:23–31.

661 Eckert, S. A. 2002. Swim speed and movement patterns of gravid leatherback sea turtles
662 (*Dermochelys coriacea*) at St Croix, US Virgin Islands. *J. Exp. Biol.* 205:3689–97.

663 Edlund, M. B. & Burge, D. R. L. 2019. Polymorphism in *Mastogloia* (Bacillariophyceae) revisited.
664 *Plant Ecol. Evol.* 152:351–7.

665 Ezenwa, V. O., Gerardo, N. M., Inouye, D. W., Medina, M. & Xavier, J. B. 2012. Animal behavior
666 and the microbiome. *Science* 338:198–9.

667 Ferrario, M. E., Cefarelli, A. O., Fazio, A., Bordino, P. & Romero, O. E. 2018. *Bennettella ceticola*
668 (Nelson ex Bennett) Holmes on the skin of Franciscana dolphin (*Pontoporia blainvillei*) of the
669 Argentinean Sea: an emendation of the generic description. *Diatom Res.* 33:485–97.

670 Frair, W., Ackman, R. G. & Mrosovsky, N. 1972. Body temperatures of *Dermochelys coriacea*:
671 warm turtle from cold water. *Science* 177:791–3.

672 Frankovich, T. A., Sullivan, M. J. & Stacy, N. I. 2015. *Tursiocola denysii* sp. nov. (Bacillariophyta)
673 from the neck skin of Loggerhead sea turtles (*Caretta caretta*). *Phytotaxa* 234:227–36.

674 Frankovich, T. A., Ashworth, M. P., Sullivan, M. J., Vesela, J. & Stacy, N. I. 2016. *Medlinella*
675 *amphoroidea* gen. et sp. nov. (Bacillariophyta) from the neck skin of loggerhead sea turtles (*Caretta*
676 *caretta*). *Phytotaxa* 272:101–14.

677 Guillard, R.R.L. 1975. Culture of phytoplankton for feeding marine invertebrates. *In* Smith, W. L.
678 & Chanley, M. H. [Eds.] *Culture of Marine Invertebrate Animals*. Springer, Boston, MA. pp. 26–
679 60.

680 Hasle, G. R. & Syvertsen, E. E. 1997. Marine diatoms. *In* Tomas, C. R. [Ed.]. *Identifying marine*
681 *phytoplankton*. Academic Press, San Diego, pp. 5–385.

682 Holmes, R.W., Nagasawa, S. & Takano, H. 1993. The morphology and geographic distribution of
683 epidermal diatoms of the Dall's porpoise (*Phocoenoides dalli* True) in the Northern Pacific Ocean.
684 *Bull. Nat. Sci. Mus. Tokyo, Ser. B, Bot.* 19:1–18.

685 James, M. C., Davenport, J. & Hays, G. C. 2006. Expanded thermal niche for a diving vertebrate: a
686 leatherback turtle diving into near-freezing water. *J. Exp. Mar. Biol. Ecol.* 335:221–6.

687 Majewska, R., Kociolek, J.P., Thomas, E.W., De Stefano, M., Santoro, M., Bolanos, F. & Van De
688 Vijver, B. 2015a. *Chelonicola* and *Poulinea*, two new gomphonemoid diatom genera
689 (Bacillariophyta) living on marine turtles from Costa Rica. *Phytotaxa* 233:236–50.

690 Majewska, R., Santoro, M., Bolanos, F., Chaves, G. & De Stefano, M. 2015b. Diatoms and other
691 epibionts associated with olive ridley (*Lepidochelys olivacea*) sea turtles from the Pacific coast of
692 Costa Rica. *PLoS ONE*, 10:e0130351. doi: 10.1371/journal.pone.0130351.

693 Majewska, R., Van De Vijver, B., Nasrolahi, A., Ehsanpour, M., Afkhami, M., Bolañños, F.,
694 Iamunno, F., Santoro, M. & De Stefano, M. 2017a. Shared epizoic taxa and differences in diatom
695 community structure between green turtles (*Chelonia mydas*) from distant habitats. *Microb. Ecol*.
696 74:969–78.

697 Majewska, R., De Stefano, M., Ector, L., Bolañños, F., Frankovich, T. A., Sullivan, M. J.,
698 Ashworth, M. P. & Van De Vijver, B. 2017b. Two new epizoic *Achnanthes* species
699 (Bacillariophyta) living on marine turtles from Costa Rica. *Botanica Mar.* 60:303–18.

700 Majewska, R., Ashworth, M. P., Lazo-Wasem, E., Robinson, N. J., Rojas, L., Van de Vijver, B. &
701 Pinou, T. 2018. *Craspedostauros alatus* sp. nov., a new diatom (Bacillariophyta) species found on
702 museum sea turtle specimens. *Diatom Res.* 33:229–40.

703 Majewska, R., Bosak, S., Frankovich, T. A., Ashworth, M. P., Sullivan, M. J., Robinson, N. J.,
704 Lazo-Wasem, E. A., Pinou, T., Nel, R., Manning, S. R. & Van de Vijver, B. 2019a. Six new
705 epibiotic *Proschkinia* (Bacillariophyta) species and new insights into the genus phylogeny. *Eur. J.*
706 *Phycol.* 54:609–31.

707 Majewska, R., Robert, K., Van de Vijver, B. & Nel, R. 2019b. A new species of *Lucanicum*
708 (Cyclophorales, Bacillariophyta) associated with loggerhead sea turtles from South Africa. *Bot.*
709 *Letters.* DOI: https://doi.org/10.1080/23818107.2019.1691648

710 Nawrocki, E.P., Kolbe, D.L. & Eddy, S.R. 2009. Infernal 1.0: inference of RNA alignments.
711 *Bioinformatics* 25:1335–1337.

712 Nemoto, T. 1956. On the diatoms of the skin film of whales in the Northern Pacific. *Sci. Rep.*
713 *Whales Res. Inst., Tokyo* 11:99–132.

714 Pinou, T., Domenech, F., Lazo-Wasem, E. A., Majewska, R., Pfaller, J. B., Zardus, J. D. &
715 Robinson, N. J. 2019. Standardizing sea turtle epibiont sampling: outcomes of the epibiont
716 workshop at the 37th International Sea Turtle Symposium. *Mar. Turtle Newsl.* 157:22–32.

717 Redford, K. H., Segre, J. A., Salafsky, N., Martinez del Rio, C. & McAloose, D. 2012.
718 Conservation and the microbiome. *Conserv. Biol.* 26:195–7.

719 Riaux-Gobin, C., Coste, M., Jordan, R. W., Romero, O. E. & Le Cohu, R. 2014. *Xenococconeis*
720 *opunohusiensis* gen. et sp. nov. and *Xenococconeis neocaledonica* comb. nov. (Bacillariophyta)
721 from the tropical South Pacific. *Phycol. Res.* 62:153–69.

722 Riaux-Gobin, C., Witkowski, A., Kociolek, J. P., Ector, L., Chevallier, D. & Compèère, P. 2017.
723 New epizoic diatom (Bacillariophyta) species from sea turtles in the Eastern Caribbean and South
724 Pacific. *Diatom Res.* 32:109–25.

725 Robinson, N. J., Majewska, R., Lazo-Wasem, E., Nel, R., Paladino, F. V., Rojas, L., Zardus, J. D. &
726 Pinou, T. 2016. Epibiotic diatoms are universally present on all sea turtle species. *PLoS ONE* 11:
727 e0157011. doi: 10.1371/journal.pone.0157011.

728 Sabbe, K., Verleyen, E., Hodgson, D. A., Vanhoutte, K. & Vyverman, W. 2003. Benthic diatom
729 flora of freshwater and saline lakes in the Larsemann Hills and Rauer Islands, East Antarctica. *Ant.*
730 *Sci.* 15:227–48.

731 Simonsen, R. 1974. The diatom plankton of the Indian Ocean Expedition of R/V" Meteor" 1964-
732 1965. *Meteor Forsch. Ergebnisse. Reihe D*. 19:1–107.

733 Schultz M. E. 1971. Salinity-related polymorphism in the brackish-water diatom *Cyclotella*
734 *cryptica*. *Can. J. Bot.* 49:1285–9.

735 Stamatakis, A. 20141406. RAxML version 8: A tool for phylogenetic analysis and post analysis of
736 large phylogenies. *Bioinformatics* 30:1312–3.

Theriot, E.C., Ashworth, M., Ruck, E., Nakov, T. & Jansen, R.K. 2010. A preliminary multigene phylogeny of the diatoms (Bacillariophyta): challenges for future research. *Plant Ecol. Evol.* 143:278–96.

Tréguer, P., Nelson, D. M., Van Bennekom, A. J., DeMaster, D. J., Leynaert, A. & Quéguiner, B. 1995. The silica balance in the world ocean: a reestimate. *Science* 268:375–9.

Turland, N. J., Wiersema, J. H., Barrie, F. R., Greuter, W., Hawksworth, D. L., Herendeen, P. S., Knapp, S., Kusber, W.-H., Li, D.-Z., Marhold, K., May, T. W., McNeill, J., Monro, A. M., Prado, J., Price, M. J. & Smith, G. F. 2018. *International Code of Nomenclature for algae, fungi, and plants (Shenzhen Code) adopted by the Nineteenth International Botanical Congress Shenzhen, China, July 2017*. Regnum Vegetabile 159. Glashütten: Koeltz Botanical Books.

Urbánková, P., Scharfen, V. & Kulichová, J. 2016. Molecular and automated identification of the diatom genus Frustulia in northern Europe. *Diatom Res.* 31:217–29.

van der Werff, A. 1953~~5~~. A new method of concentrating and cleaning diatoms and other organisms. *Int. Ver. Theor. Angew. Limnol. Verh.* 12:276–7.

Van De Vijver, B., Tavernier, I., Kellogg, T. B., Gibson, J. A., Verleyen, E., Vyverman, W. & Sabbe, K. 2012. Revision of type materials of Antarctic diatom species (Bacillariophyta) described by West &West (1911), with the description of two new species. *Fottea* 12:149–69.

von Stosch, H.A. (1974) Pleurax, seine Synthese und seine Verwendung zur Einbettung und Darstellung der Zellwände von Diatomeen, Peridineen und anderen Algen, sowie für eine neue Methode zur Elektivfärbung von Dinoflagellaten-Panzern. *Arch. Protistenk.* 116: 132–141.

World Medical Association. 2013. World Medical Association Declaration of Helsinki, Ethical principles for medical research involving human subjects. *J. Am. Med. Assoc.* 310:2191–4. doi:10.1001/jama.2013.281053

760 **Figures legends**

761 **Fig. 1**. Sampling locations where *Craspedostauros danayanus* (1), *C. legouvelloanus* (2), *C.*
762 *macewanii* (3), and *C. alatus* (4) were found.

763

764 **Figures 2–11.** *Craspedostauros danayanus*. **Fig. 2.** Living cells of *C. danayanus* and *Cylindrotheca*
765 sp. attached to the leatherback skin scutes (light microscopy). **Fig. 3.** Stained colony of *C.*
766 *danayanus* and associated bacteria on the leatherback skin scutes. **Fig. 4.** Valve view of a living cell
767 (cultured strain). **Fig. 5.** Girdle view of a living cell (cultured strain). **Figs 6–11.** Scanning electron
768 micrographs of *C. danayanus* attached to its original substratum. **Fig. 6.** Monospecific colony
769 growing among the flaking skin of leatherback (dorsal side of the hind flipper). **Fig. 7.** Extremely
770 delicate and fragile cells of *C. danayanus* attached to the leatherback skin (dorsal side of the hind
771 flipper). **Fig. 8.** An overview of the leatherback-associated barnacle, *Platylepas coriacea*, colonized
772 by *C. danayanus*. **Fig. 9.** A detail of the external part of the barnacle with a sheath of host sea turtle
773 tissue overgrown with *C. danayanus*. Arrows indicate some of the monospecific clumps of *C.*
774 *danayanus* colonies. **Fig. 10.** A detail of the moveable plates of the barnacle overgrown with *C.*
775 *danayanus*. **Fig. 11.** A single cell of *C. danayanus* among dense colony of *Cylindrotheca* sp.
776 attached to the folds in the moveable plates of *P. coriacea*. Scale bars: 10 µm = **Figs 3–5, 7, 11**; 50
777 µm = **Fig. 2**; 100 µm = **Figs 6, 9 & 10**; 1mm = **Fig. 8**

778

779 **Figures 12–24.** *Craspedostauros danayanus*. **Figs 12–16.** Valve view (light micrographs). Arrows
780 indicate the barely noticeable valve margins. **Figs 17–24.** Scanning electron micrographs. **Fig. 17.**
781 Detail of the apical part of the valve (external view). Arrowheads indicate the large irregular
782 depression at the fold of the apical silica flap. **Fig. 18.** Frustule with partially detached girdle bands
783 (external view). Arrowheads indicate the large irregular depression at the fold of the apical silica

784 flap. **Fig. 19.** Detail of the central part of the valve (external view). **Fig. 20.** Internal valve view.
785 **Fig. 21.** Detail of the central part of the valve (internal view). **Fig. 22.** Cribrate areolae (internal
786 view). **Fig. 23.** Detail of the apical part of the valve (internal view). Arrowheads indicate the
787 asymmetrical thickening extending from the apical part of the raphe-sternum towards the valve
788 margin. **Fig. 24.** Detail of the girdle bands. Scale bars: 10 µm = **Figs 12–16, 18, 20**; 1 µm = **Figs**
789 **17, 19, 21–24**

790

791 **Figures 25–40.** *Craspedostauros legouvelloanus*. **Figs 25–30.** Light micrographs. **Figs 25, 26, 28–**
792 **30.** Girdle view. **Fig.s 25.** Valve with two girdle bands attached., **Figs 28 & 29.** Frustules with
793 detached valves. **Figs 26 & 30.** Complete frustules. Arrows indicate the biarcuate valve margin.
794 **Fig. 27.** Valve view. **Figs 31–40.** Scanning electron micrographs. **Fig. 31.** External valve view.
795 Arrows indicate depressions at the apical flap fold. **Fig. 32.** Detail of the apical part of the frustule
796 (external view). **Fig. 33.** Valve with attached girdle bands (girdle view). **Fig. 34.** Detail of the girdle
797 bands (internal view). Arrowheads indicate the internal thickening (septum). **Fig. 35.** Valve with
798 partially detached girdle bands (internal view). **Fig. 36.** Internal valve view. Arrowheads indicate
799 the slight expansion of the stauros on the side corresponding to the external lip-like silica flaps. **Fig.**
800 **37.** Detail of the apical part of the valve (internal view). **Fig. 38.** Detail of the central part of the
801 valve (external view). **Figs 39 & 40.** Detail of the central part of the valve (internal view).
802 Arrowheads indicate the hollows in the stauros-adjacent virgae. Scale bars: 10 µm = **Figs 25–31,**
803 **33, 35 & 36**; 1 µm = **Figs 32, 34 & 37–39**; 500nm = **Fig. 40**

804

805 **Figures 41–47.** *Craspedostauros legouvelloanus*. **Fig. 41.** Living cells in culture (light
806 microscopy). Arrows indicate the H-shaped chloroplasts with one lobe pressed against each valve, a
807 feature characteristic of the genus. **Fig. 42.** External valve view (wild population). **Fig. 43.** External
808 valve view (cultured strain). **Fig. 44.** Internal valve view (wild population). **Fig. 45.** Internal valve

view (cultured strain). **Fig. 46.** Detail of a girdle band showing internal thickening (septum) with perforations. **Fig. 47.** A single girdle band (external and internal view). Scale bars: 10 µm = **Figs 41–45**; 1 µm = **Figs 46 & 47**

Figures 48–62. *Craspedostauros macewanii*. **Figs 48–54.** Light micrographs. **Figs 48–51.** Fresh (unpreserved) material. **Figs 48 & 51.** Living cells. **Fig. 48.** Girdle view. **Fig. 51.** Valve view. **Figs 49 & 50.** Damaged cells in girdle view with the cell content (including plastids) spilling beyond the cell wall. **Figs 49.** Arrow indicates the straight valve margin. **Figs 52–54.** Cleaned material. Detached valves in valve view. Arrows indicate the distinct valve face-mantle junction. **Figs 55–62.** Scanning electron micrographs. **Fig. 55.** External valve view. **Fig. 56.** Detail of the apical part (external valve view). **Fig. 57.** Detail of the central area (external valve view). **Fig. 58.** Detail of the apical part (external girdle view). **Fig. 59.** Internal valve view and partially detached valvocopula. **Fig. 60.** Detail of the apical part (internal valve view). Arrowheads indicate several small areolae present at the end of the curved thickening. **Fig. 61.** Detail of the central area (internal valve view). **Fig. 62.** Detail of the valvocopula (internal view).

Scale bars: 10 µm = **Figs 48–55 & 59**; 1 µm = **Figs 56–58 & 60–62**

Figures 63–74. *Craspedostauros alatus* (Adriatic population). **Figs 63–68.** Light micrographs. **Figs 63, 66 & 67.** Valve view. **Fig. 63.** Broken frustule with both valves lying in valve view. **Fig. 64.** Single valve with attached girdle bands. **Figs 65 & 68.** Girdle view. Arrows indicate the clear valve face-mantle junction. **Figs 69–74.** Scanning electron micrographs. **Fig. 69.** Frustule with partially detached girdles bands (external view). **Fig. 70.** Detail of the apical part of the frustule with the winged-liked silica flaps, a feature typical of the species (external view). **Fig. 71.** Frustule with partially detached girdles bands (external girdle view). **Fig. 72.** Internal valve view. **Figs 73 & 74.**

833 Detail of the central part of the valve (internal view). Scale bars: 10 μm = **Figs 63–69, 71 & 72**; 1
834 μm = **Figs 70 & 73**; 500 nm = **Fig. 74**

835

836 **Figure 75.** Maximum likelihood (ML) phylogram based on the 3-gene dataset (nuclear-encoded
837 ribosomal SSU, chloroplast encoded rbcL, psbC markers). For clarity, only the clade of raphid
838 diatoms containing *Staurotropis*, *Craspedostauros*, and *Achnanthes* is presented in the figure. The
839 ML tree presenting the complete taxon sampling can be viewed in the Supplementary Figure S1.

840

841 **Supplementary Figure S1**

842 Maximum likelihood tree based on the 3-gene dataset (nuclear-encoded ribosomal SSU,
843 chloroplast-encoded rbcL, psbC markers) with bootstrap values from 1000 pseudoreplicates over
844 the corresponding nodes. The araphid pennate taxon outgroup *Asterionellopsis socialis* was used as
845 the outgroup.

846

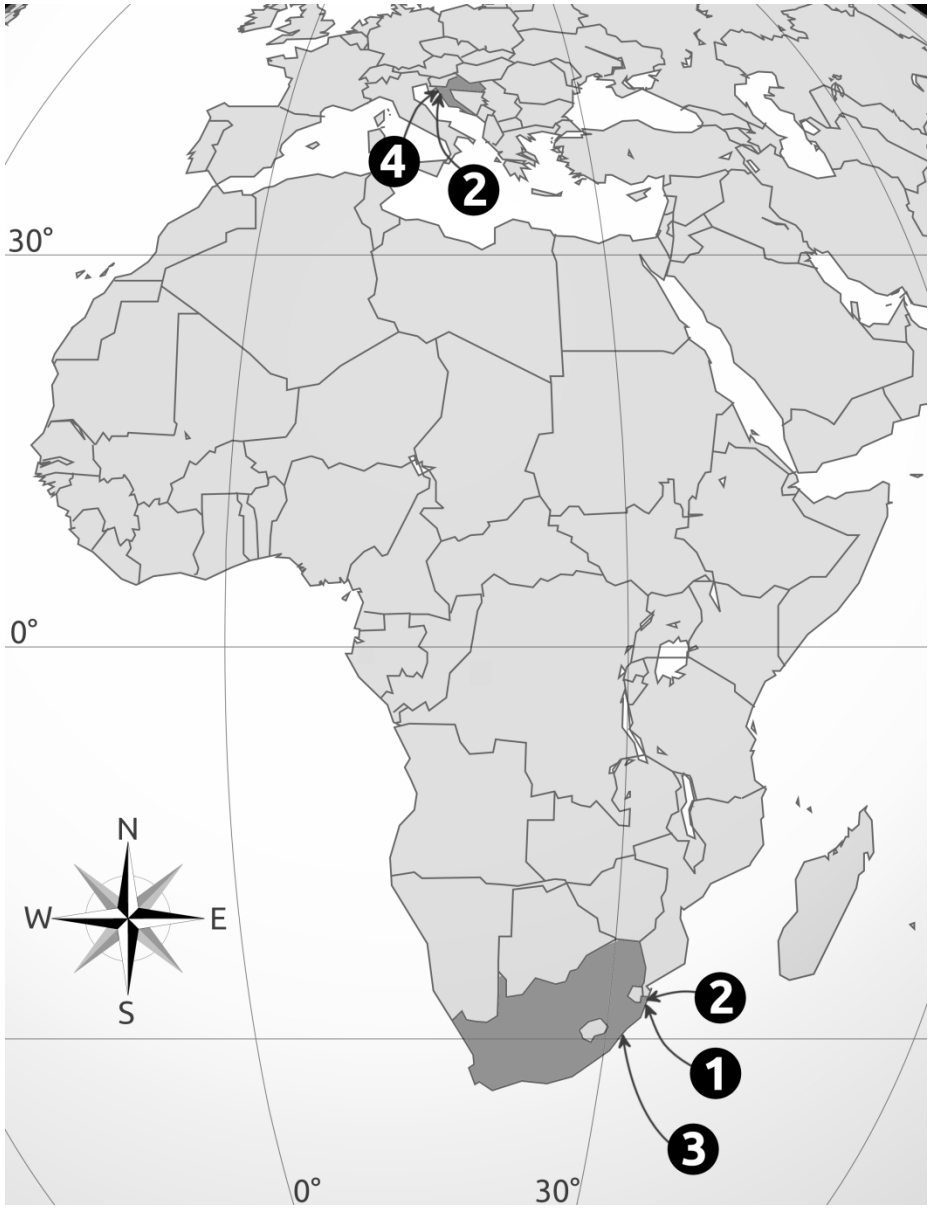

Sampling locations where Craspedostauros danayanus (1), C. legouvelloanus (2), C. macewanii (3), and C. alatus (4) were found.

123x160mm (600 x 600 DPI)

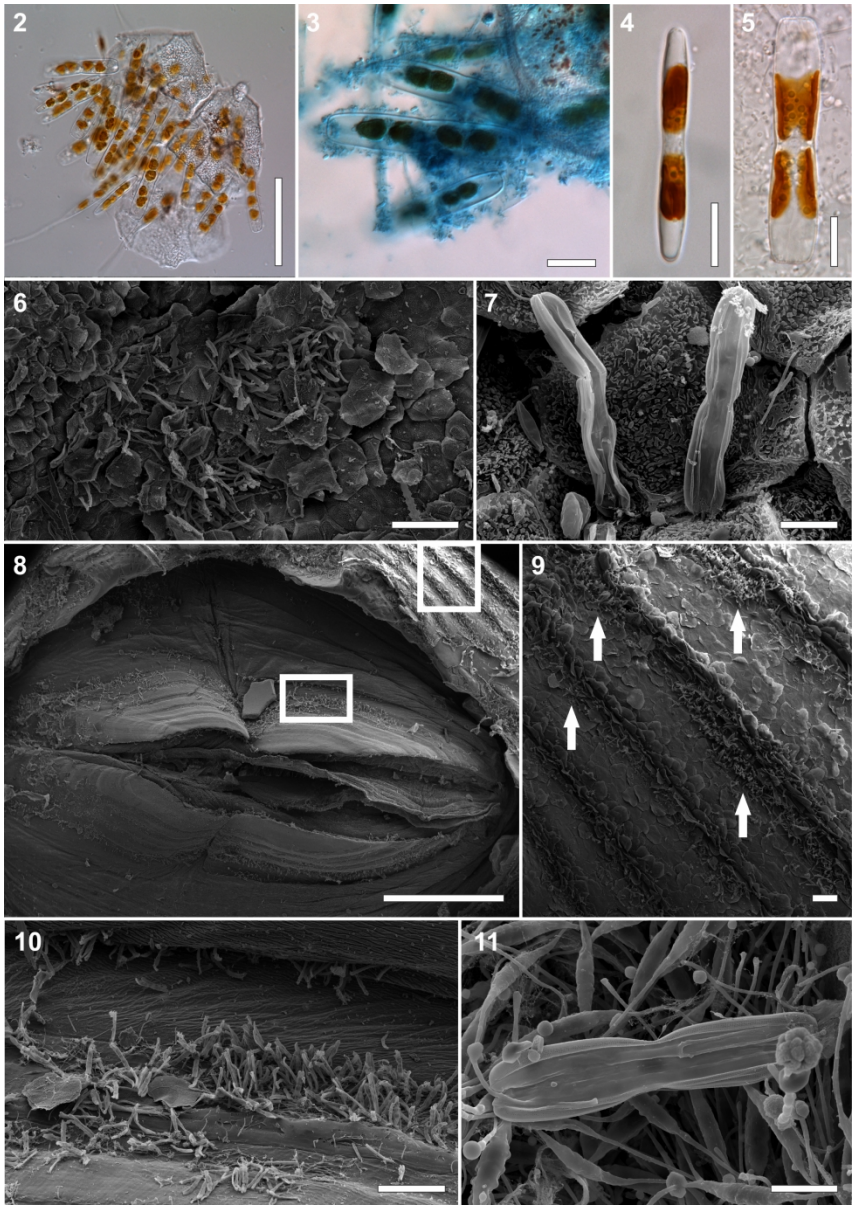

Craspedostauros danayanus. Fig. 2. Living cells of C. danayanus and Cylindrotheca sp. attached to the leatherback skin scutes (light microscopy). Fig. 3. Stained colony of C. danayanus and associated bacteria on the leatherback skin scutes. Fig. 4. Valve view of a living cell (cultured strain). Fig. 5. Girdle view of a living cell (cultured strain). Figs 6–11. Scanning electron micrographs of C. danayanus attached to its original substratum. Fig. 6. Monospecific colony growing among the flaking skin of leatherback (dorsal side of the hind flipper). Fig. 7. Extremely delicate and fragile cells of C. danayanus attached to the leatherback skin (dorsal side of the hind flipper). Fig. 8. An overview of the leatherback-associated barnacle, Platylepas coriacea, colonized by C. danayanus. Fig. 9. A detail of the external part of the barnacle with a sheath of host sea turtle tissue overgrown with C. danayanus. Arrows indicate some of the monospecific clumps of C. danayanus colonies. Fig. 10. A detail of the moveable plates of the barnacle overgrown with C. danayanus. Fig. 11. A single cell of C. danayanus among dense colony of Cylindrotheca sp. attached to the folds in the moveable plates of P. coriacea. Scale bars: 10 μm = Figs 3–5, 7, 11; 50 μm = Fig. 2; 100 μm = Figs 6, 9 & 10; 1mm = Fig. 8

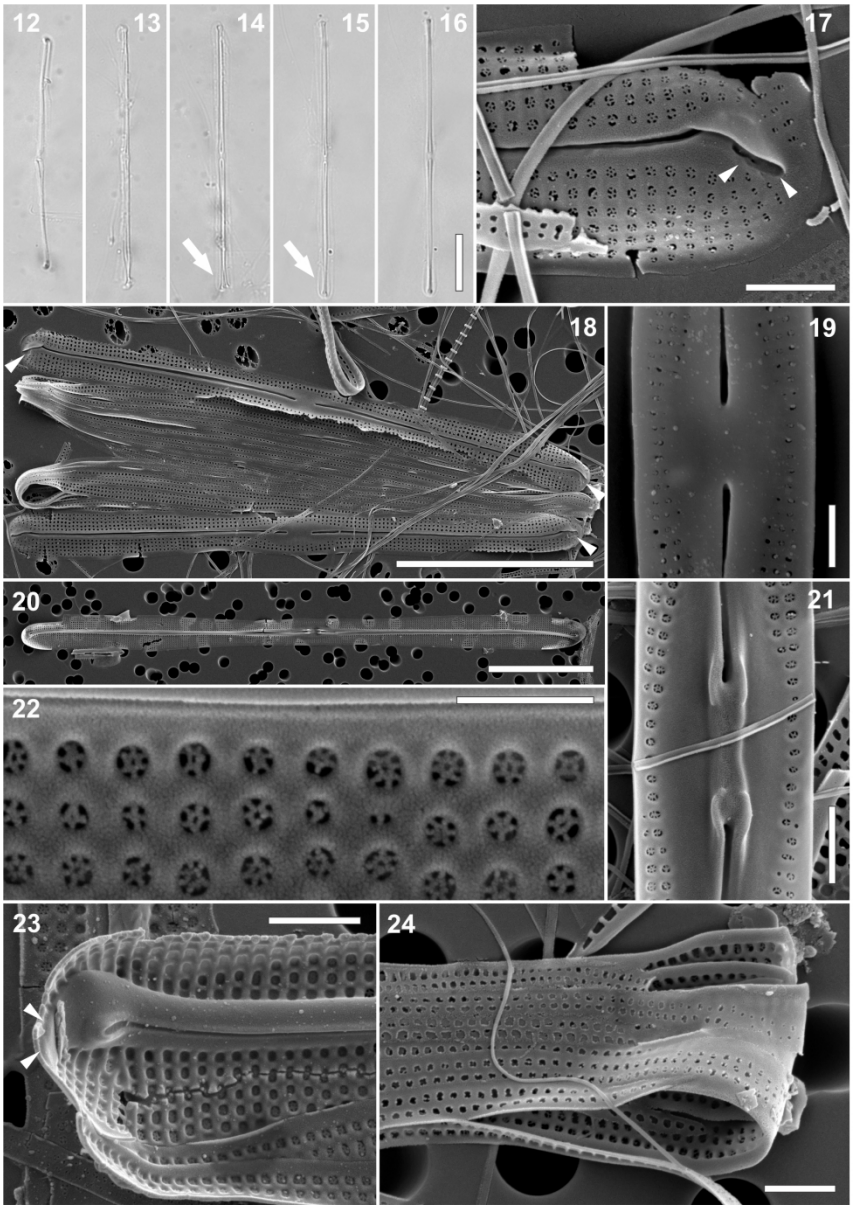

Craspedostauros danayanus. Figs 12–16. Valve view (light micrographs). Arrows indicate the barely noticeable valve margins. Figs 17–24. Scanning electron micrographs. Fig. 17. Detail of the apical part of the valve (external view). Arrowheads indicate the large irregular depression at the fold of the apical silica flap. Fig. 18. Frustule with partially detached girdle bands (external view). Arrowheads indicate the large irregular depression at the fold of the apical silica flap. Fig. 19. Detail of the central part of the valve (external view). Fig. 20. Internal valve view. Fig. 21. Detail of the central part of the valve (internal view). Fig. 22. Cribrate areolae (internal view). Fig. 23. Detail of the apical part of the valve (internal view). Arrowheads indicate the asymmetrical thickening extending from the apical part of the raphe-sternum towards the valve margin. Fig. 24. Detail of the girdle bands. Scale bars: 10 μm = Figs 12–16, 18, 20; 1 μm = Figs 17, 19, 21–24

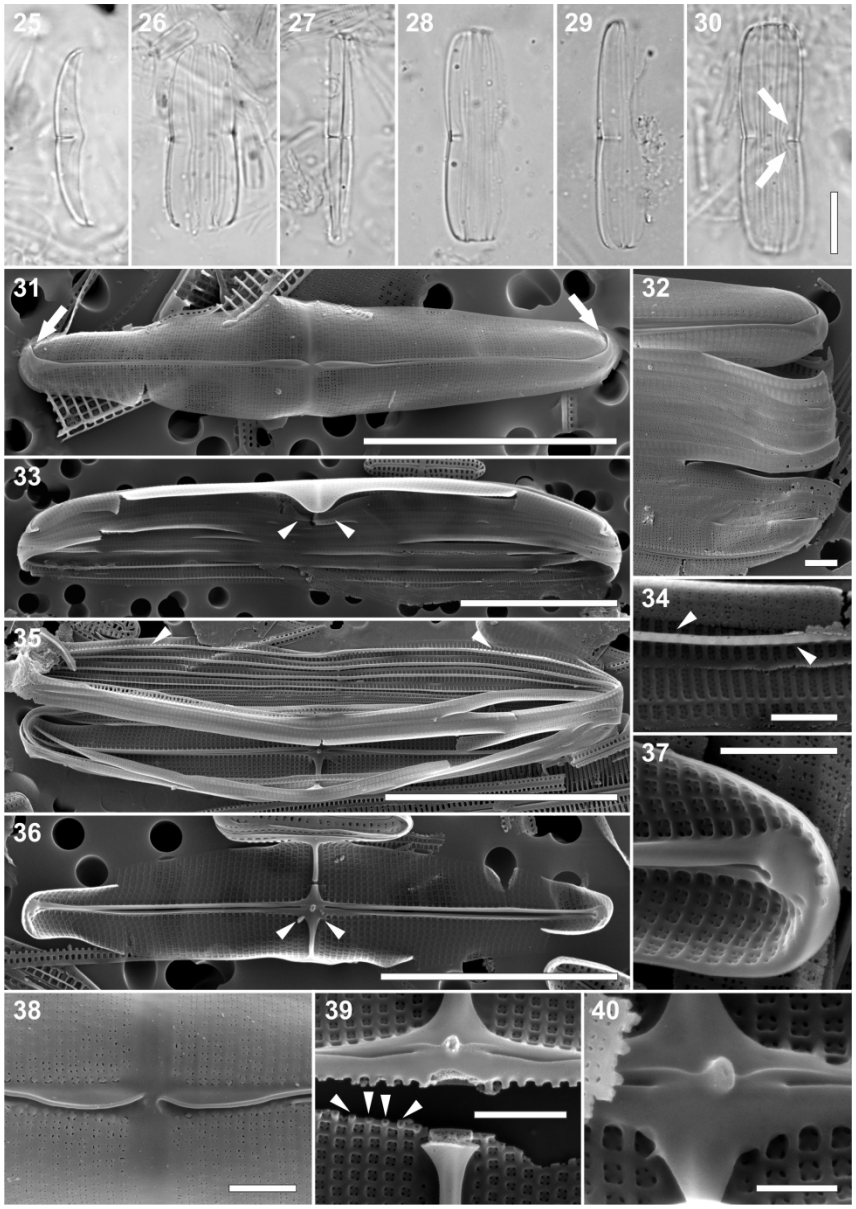

Craspedostauros legouvelloanus. Figs 25–30. Light micrographs. Figs 25, 26, 28–30. Girdle view. Fig. 25. Valve with two girdle bands attached. Figs 28 & 29. Frustules with detached valves. Figs 26 & 30. Complete frustules. Arrows indicate the biarcuate valve margin. Fig. 27. Valve view. Figs 31–40. Scanning electron micrographs. Fig. 31. External valve view. Arrows indicate depressions at the apical flap fold. Fig. 32. Detail of the apical part of the frustule (external view). Fig. 33. Valve with attached girdle bands (girdle view). Fig. 34. Detail of the girdle bands (internal view). Arrowheads indicate the internal thickening (septum). Fig. 35. Valve with partially detached girdle bands (internal view). Fig. 36. Internal valve view. Arrowheads indicate the slight expansion of the stauros on the side corresponding to the external lip-like silica flaps. Fig. 37. Detail of the apical part of the valve (internal view). Fig. 38. Detail of the central part of the valve (external view). Figs 39 & 40. Detail of the central part of the valve (internal view). Arrowheads indicate the hollows in the stauros-adjacent virgae. Scale bars: 10 µm = Figs 25–31, 33, 35 & 36; 1 µm = Figs 32, 34 & 37–39; 500nm = Fig. 40

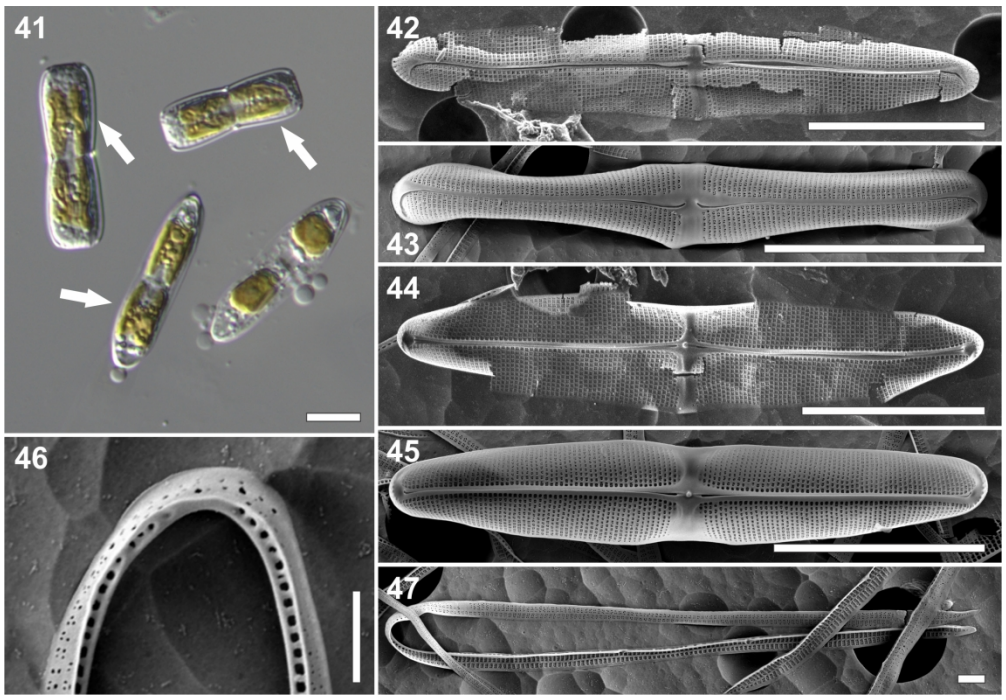

Craspedostauros legouvelloanus. Fig. 41. Living cells in culture (light microscopy). Arrows indicate the H-shaped chloroplasts with one lobe pressed against each valve, a feature characteristic of the genus. Fig. 42. External valve view (wild population). Fig. 43. External valve view (cultured strain). Fig. 44. Internal valve view (wild population). Fig. 45. Internal valve view (cultured strain). Fig. 46. Detail of a girdle band showing internal thickening (septum) with perforations. Fig. 47. A single girdle band (external and internal view). Scale bars: 10 µm = Figs 41–45; 1 µm = Figs 46 & 47

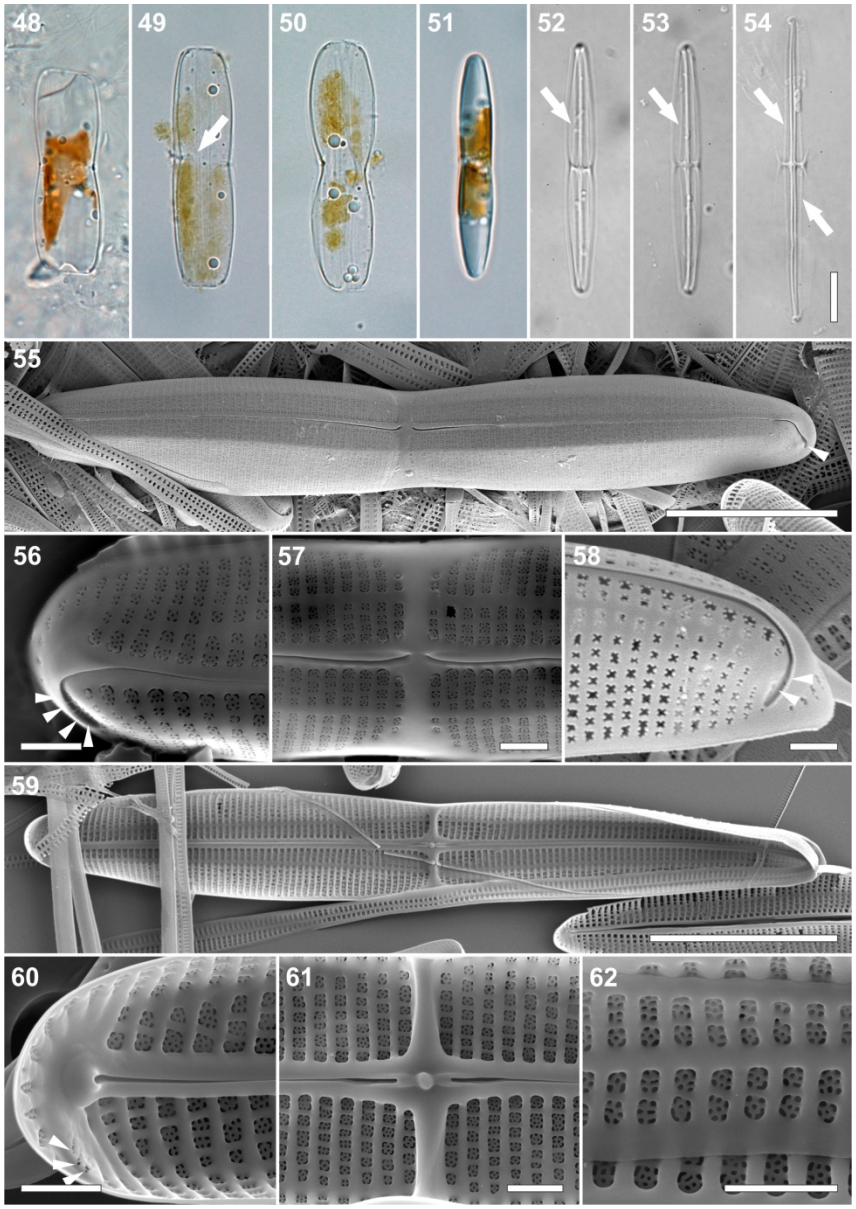

Craspedostauros macewanii. Figs 48–54. Light micrographs. Figs 48–51. Fresh (unpreserved) material. Figs 48 & 51. Living cells. Fig. 48. Girdle view. Fig. 51. Valve view. Figs 49 & 50. Damaged cells in girdle view with the cell content (including plastids) spilling beyond the cell wall. Figs 49. Arrow indicates the straight valve margin. Figs 52–54. Cleaned material. Detached valves in valve view. Arrows indicate the distinct valve face-mantle junction. Figs 55–62. Scanning electron micrographs. Fig. 55. External valve view. Fig. 56. Detail of the apical part (external valve view). Fig. 57. Detail of the central area (external valve view). Fig. 58. Detail of the apical part (external girdle view). Fig. 59. Internal valve view and partially detached valvocopula. Fig. 60. Detail of the apical part (internal valve view). Arrowheads indicate several small areolae present at the end of the curved thickening. Fig. 61. Detail of the central area (internal valve view). Fig. 62. Detail of the valvocopula (internal view).
Scale bars: 10 μm = Figs 48–55 & 59; 1 μm = Figs 56–58 & 60–62

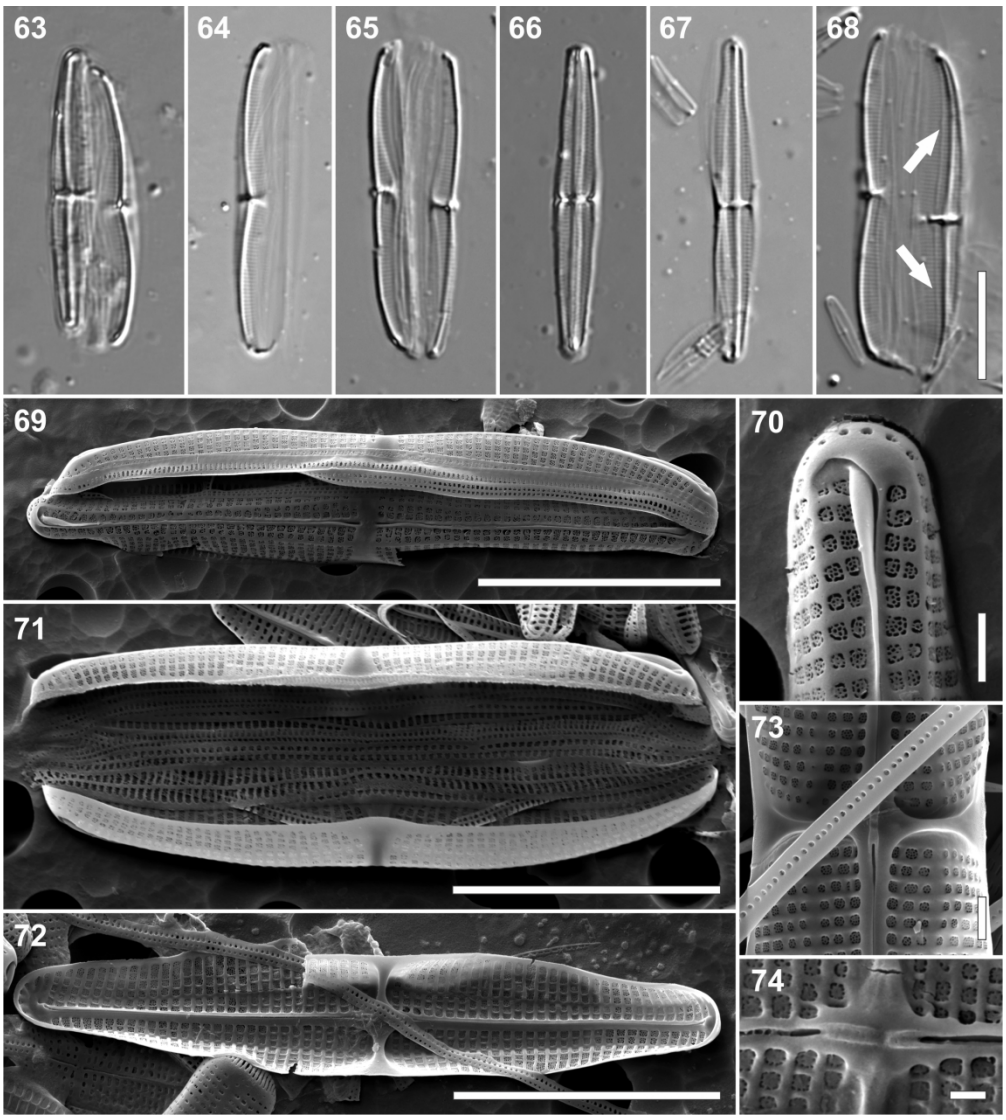

Craspedostauros alatus (Adriatic population). Figs 63–68. Light micrographs. Figs 63, 66 & 67. Valve view. Fig. 63. Broken frustule with both valves lying in valve view. Fig. 64. Single valve with attached girdle bands. Figs 65 & 68. Girdle view. Arrows indicate the clear valve face-mantle junction. Figs 69–74. Scanning electron micrographs. Fig. 69. Frustule with partially detached girdles bands (external view). Fig. 70. Detail of the apical part of the frustule with the winged-liked silica flaps, a feature typical of the species (external view). Fig. 71. Frustule with partially detached girdles bands (external girdle view). Fig. 72. Internal valve view. Figs 73 & 74. Detail of the central part of the valve (internal view). Scale bars: 10 µm = Figs 63–69, 71 & 72; 1 µm = Figs 70 & 73; 500 nm = Fig. 74

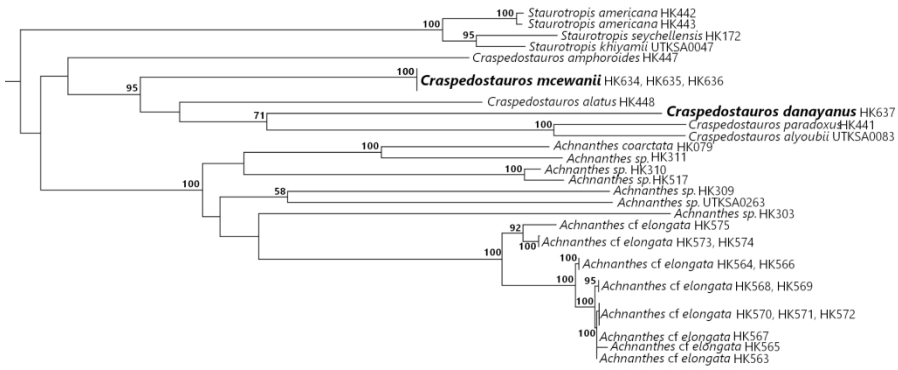

Maximum likelihood (ML) phylogram based on the 3-gene dataset (nuclear-encoded ribosomal SSU, chloroplast encoded rbcL, psbC markers). For clarity, only the clade of raphid diatoms containing Staurotropis, Craspedostauros, and Achnanthes is presented in the figure. The ML tree presenting the complete taxon sampling can be viewed in the Supplementary Figure S1.

170x66mm (300 x 300 DPI)

Table 1

Comparison of *Craspedostauros alatus*, *C. danayanus, C. legouvelloanus*, and *C. macewanii* with several morphologically similar *Craspedostauros* taxa (after Cox 1999, Ashworth et al. 2017, and Majewska et al. 2018).

Character	*C. paradoxus*	*C. capensis*	*C. britannicus*	*C. australis*	*C. alyoubii*	***C. alatus***	***C. danayanus***	***C. legouvelloanus***	***C. macewanii***
Valve outline	linear, slightly constricted	lanceolate, constricted	linear to narrow lanceolate	linear	linear, slightly constricted	linear to linear-lanceolate, slightly constricted	linear, very slightly constricted	linear to linear-lanceolate, slightly constricted	linear to linear-lanceolate, slightly constricted
Reference	Ashworth et al. 2017	Cox 1999	Cox 1999	Cox 1999	Ashworth et al. 2017	Majewska et al. 2018	this article	this article	this article
Valve length(µm)	80-85	25-35	14-60	35-78	83-105	20-37 (26-34)*	28-61	18-34 (23-39)*	26-51
Valve width (µm)	6.5-9	4.5-5.5	5-6	4-6	6-10	3-5 (3-5)*	2-2.5	3-5 (4-6)*	4.5-5.5
Stria density (in 10 µm)	36-40	19	~24	35	~40	26-28 (24-27)*	49-51	46-49 (40-44)*	28-31
Areola size (valve)	largely similar	variable	similar	similar	similar	variable	similar	similar	similar
Number of pores per cribrum (valve)	4-5	5-13	5(+)	4	4-5	highly variable	6-8	4	highly variable
Internal central structure	knob	knob	helictoglossae	knob	knob	rectelevatum	rectelevatum	knob with central cavity	knob
Valve-face mantle junction	indistinct	indistinct	indistinct	indistinct	indistinct	distinct	indistinct	indistinct	distinct
Central lip-like silica flaps	prominent	rudimentary	rudimentary	rudimentary	prominent	rudimentary	absent	well-developed	rudimentary
Valve margin at centre	straight	straight	slightly expanded	straight	straight	very slightly expanded	straight	clearly expanded	straight
Central area	roundish, irregular	bow tie-shaped fascia	bow tie-shaped fascia	bow tie-shaped fascia	rectangular fascia	rectangular fascia	almond-shaped	rectangular fascia	bow tie-shaped fascia
Stauros	strongly reduced/absent	present	present	present	somewhat reduced	present	absent	present	present

* values and descriptions given in brackets refer to the Adriatic populations

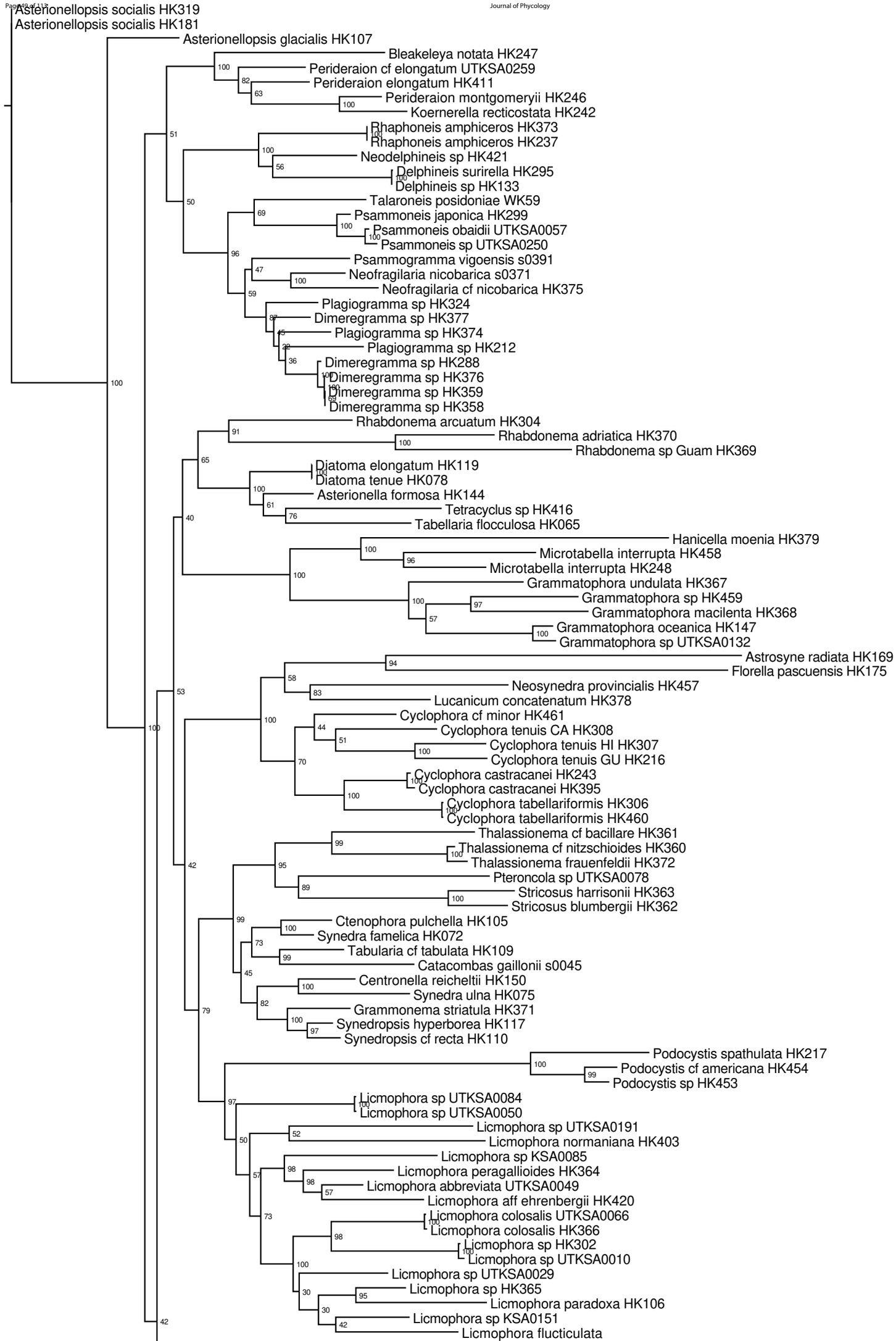
Asterionellopsis socialis HK319
Asterionellopsis socialis HK181
Asterionellopsis glacialis HK107
Bleakeleya notata HK247
Perideraion cf elongatum UTKSA0259
Perideraion elongatum HK411
Perideraion montgomeryii HK246
Koernerella recticostata HK242
Rhaphoneis amphiceros HK373
Rhaphoneis amphiceros HK237
Neodelphineis sp HK421
Delphineis surirella HK295
Delphineis sp HK133
Talaroneis posidoniae WK59
Psammoneis japonica HK299
Psammoneis obaidii UTKSA0057
Psammoneis sp UTKSA0250
Psammogramma vigoensis s0391
Neofragilaria nicobarica s0371
Neofragilaria cf nicobarica HK375
Plagiogramma sp HK324
Dimeregramma sp HK377
Plagiogramma sp HK374
Plagiogramma sp HK212
Dimeregramma sp HK288
Dimeregramma sp HK376
Dimeregramma sp HK359
Dimeregramma sp HK358
Rhabdonema arcuatum HK304
Rhabdonema adriatica HK370
Rhabdonema sp Guam HK369
Diatoma elongatum HK119
Diatoma tenue HK078
Asterionella formosa HK144
Tetracyclus sp HK416
Tabellaria flocculosa HK065
Hanicella moenia HK379
Microtabella interrupta HK458
Microtabella interrupta HK248
Grammatophora undulata HK367
Grammatophora sp HK459
Grammatophora macilenta HK368
Grammatophora oceanica HK147
Grammatophora sp UTKSA0132
Astrosyne radiata HK169
Florella pascuensis HK175
Neosynedra provincialis HK457
Lucanicum concatenatum HK378
Cyclophora cf minor HK461
Cyclophora tenuis CA HK308
Cyclophora tenuis HI HK307
Cyclophora tenuis GU HK216
Cyclophora castracanei HK243
Cyclophora castracanei HK395
Cyclophora tabellariformis HK306
Cyclophora tabellariformis HK460
Thalassionema cf bacillare HK361
Thalassionema cf nitzschioides HK360
Thalassionema frauenfeldii HK372
Pteroncola sp UTKSA0078
Stricosus harrisonii HK363
Stricosus blumbergii HK362
Ctenophora pulchella HK105
Synedra famelica HK072
Tabularia cf tabulata HK109
Catacombas gaillonii s0045
Centronella reicheltii HK150
Synedra ulna HK075
Grammonema striatula HK371
Synedropsis hyperborea HK117
Synedropsis cf recta HK110
Podocystis spathulata HK217
Podocystis cf americana HK454
Podocystis sp HK453
Licmophora sp UTKSA0084
Licmophora sp UTKSA0050
Licmophora sp UTKSA0191
Licmophora normaniana HK403
Licmophora sp KSA0085
Licmophora peragallioides HK364
Licmophora abbreviata UTKSA0049
Licmophora aff ehrenbergii HK420
Licmophora colosalis UTKSA0066
Licmophora colosalis HK366
Licmophora sp HK302
Licmophora sp UTKSA0010
Licmophora sp UTKSA0029
Licmophora sp HK365
Licmophora paradoxa HK106
Licmophora sp KSA0151
Licmophora flucticulata


Pseudostriatella oceanica s0384
Striatella unipunctata FL HK318
Striatella unipunctata Guam HK177
Fragilariforma virescens HK132
Plagiostriata goreensis s0388
Castoridens hyalina HK444
Castoridens striata HK385
Opephora pacifica HK296
Psammotaenia lanceolata HK316
Hendeyella lineata HK325
Hendeyella dimeregrammopsis HK391
Pseudostaurosira construens HK071
Serratifera varisterna HK315
Serratifera varisterna HK424
Opephora guentergrassi s0263
Nanofrustulum cf shiloi HK056
Staurosirella pinnata HK116
Amphora sp UTKSA0275
Amphora obtusa v crassa 6951 AMPH070
Amphora vixvisibilis SZCZCH967
Amphora sp HK502
Bacillaria sp UTKSA0009
cf Bacillaria sp UTKSA0129
cf Bacillaria sp UTKSA0130
Bacillaria paxillifer HK130
Bacillaria sp HK475
Nitzschia sp UTKSA0106
Nitzschia sp UTKSA0173
Nitzschia volvendirostrata KSA0039
Nitzschia martiana HK405
Nitzschia celaenoae KSA0035
Nitzschia sp UTKSA0107
Staurotropis americana HK442
Staurotropis americana HK443
Staurotropis seychellensis HK172
Staurotropis khiyamii UTKSA0047
Craspedostauros amphoroides HK447
Craspedostauros mcewanii HK634
Craspedostauros mcewanii HK635
Craspedostauros mcewanii HK636
Craspedostauros alatus HK448
Craspedostauros danayanus HK637
Craspedostauros paradoxus HK441
Craspedostauros alyoubii UTKSA0083
Achnanthes coarctata HK079
Achnanthes sp HK311
Achnanthes sp HK310
Achnanthes sp HK517
Achnanthes sp HK309
Achnanthes sp UTKSA0263
Achnanthes sp HK303
Achnanthes sp HK575
Achnanthes sp HK574
Achnanthes sp HK573
Achnanthes sp HK564
Achnanthes sp HK566
Achnanthes sp HK569
Achnanthes sp HK568
Achnanthes sp HK572
Achnanthes sp HK570
Achnanthes sp HK571
Achnanthes sp HK567
Achnanthes sp HK565
Achnanthes sp HK563
Nitzschia lorenziana GB
Hantzschia amphioxys v major GB
Nitzschia cf frigida HK468
Nitzschia sp KSA0120
Nitzschia filiformis HK073
Nitzschia sp UTKSA0102
Nitzschia sp HK562
Nitzschia draveillensis GB
Nitzschia longissima GB
Nitzschia sp MX HK472
Nitzschia sp HK469
Nitzschia sp UTKSA0182
Nitzschia sp UTKSA0053
Tryblionella apiculata HK087
Tryblionella gaoana SZCZCH97
Nitzschia sp UTKSA0021
Nitzschia cf longissima HK176
Nitzschia cf longissima UTKSA0124
Cylindrotheca sp UTKSA0082
Cylindrotheca closterium HK180
Cylindrotheca sp UTKSA0079
Nitzschia acidoclinata GB
Nitzschia aurariae SZCZCH966
Nitzschia frustulum GB
Nitzschia sp UTKSA0171
Nitzschia incospicua GB
Denticula kuetzingii HK104
Nitzschia sp SZCZCH658
Psammodictyon pustulum UTKSA0298
Psammodictyon sp UTKSA0280
Psammodictyon sp UTKSA0151
Psammodictyon sp UTKSA117
Psammodictyon constrictum HK471
Psammodictyon constrictum HK440

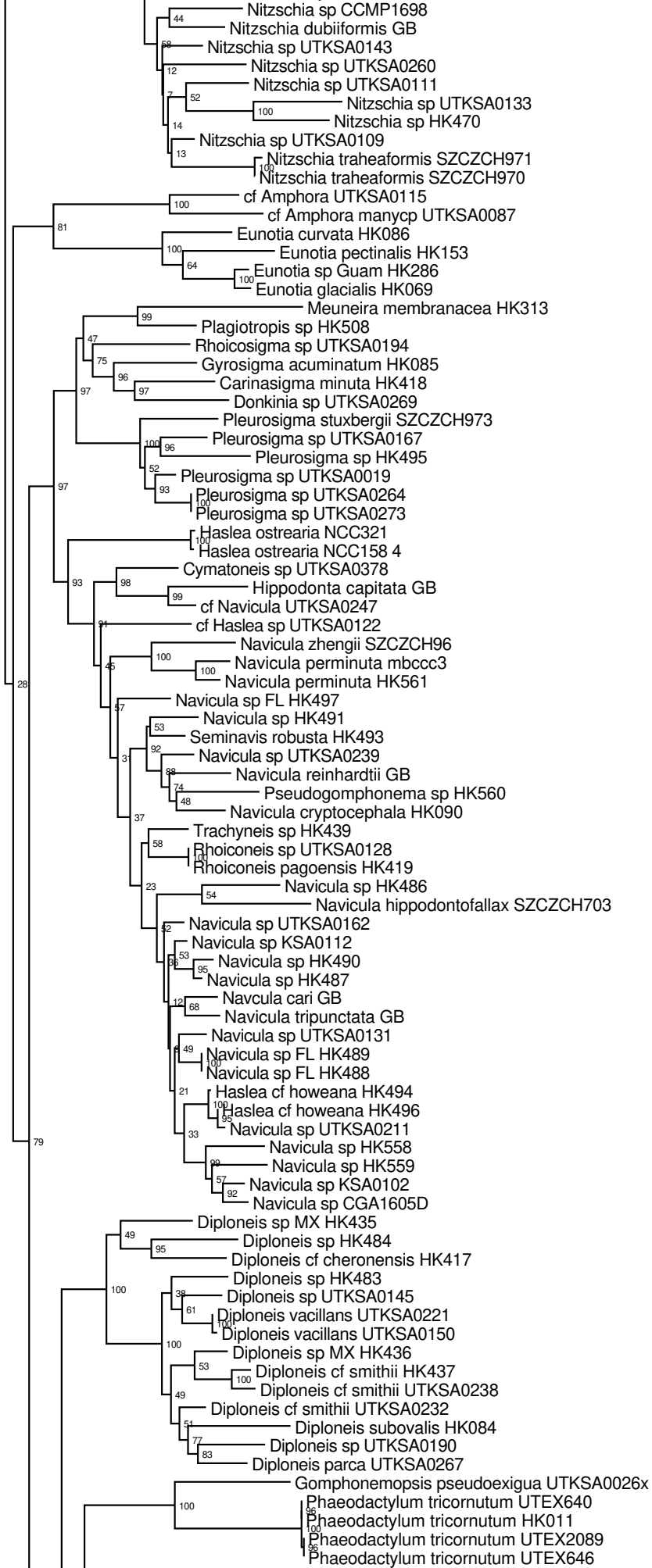
Nitzschia sp CCMP1698
Nitzschia dubiiformis GB
Nitzschia sp UTKSA0143
Nitzschia sp UTKSA0260
Nitzschia sp UTKSA0111
Nitzschia sp UTKSA0133
Nitzschia sp HK470
Nitzschia sp UTKSA0109
Nitzschia traheaformis SZCZCH971
Nitzschia traheaformis SZCZCH970
cf Amphora UTKSA0115
cf Amphora manycp UTKSA0087
Eunotia curvata HK086
Eunotia pectinalis HK153
Eunotia sp Guam HK286
Eunotia glacialis HK069
Meuneira membranacea HK313
Plagiotropis sp HK508
Rhoicosigma sp UTKSA0194
Gyrosigma acuminatum HK085
Carinasigma minuta HK418
Donkinia sp UTKSA0269
Pleurosigma stuxbergii SZCZCH973
Pleurosigma sp UTKSA0167
Pleurosigma sp HK495
Pleurosigma sp UTKSA0019
Pleurosigma sp UTKSA0264
Pleurosigma sp UTKSA0273
Haslea ostrearia NCC321
Haslea ostrearia NCC158 4
Cymatoneis sp UTKSA0378
Hippodonta capitata GB
cf Navicula UTKSA0247
cf Haslea sp UTKSA0122
Navicula zhengii SZCZCH96
Navicula perminuta mbccc3
Navicula perminuta HK561
Navicula sp FL HK497
Navicula sp HK491
Seminavis robusta HK493
Navicula sp UTKSA0239
Navicula reinhardtii GB
Pseudogomphonema sp HK560
Navicula cryptocephala HK090
Trachyneis sp HK439
Rhoiconeis sp UTKSA0128
Rhoiconeis pagoensis HK419
Navicula sp HK486
Navicula hippodontofallax SZCZCH703
Navicula sp UTKSA0162
Navicula sp KSA0112
Navicula sp HK490
Navicula sp HK487
Navcula cari GB
Navicula tripunctata GB
Navicula sp UTKSA0131
Navicula sp FL HK489
Navicula sp FL HK488
Haslea cf howeana HK494
Haslea cf howeana HK496
Navicula sp UTKSA0211
Navicula sp HK558
Navicula sp HK559
Navicula sp KSA0102
Navicula sp CGA1605D
Diploneis sp MX HK435
Diploneis sp HK484
Diploneis cf cheronensis HK417
Diploneis sp HK483
Diploneis sp UTKSA0145
Diploneis vacillans UTKSA0221
Diploneis vacillans UTKSA0150
Diploneis sp MX HK436
Diploneis cf smithii HK437
Diploneis cf smithii UTKSA0238
Diploneis cf smithii UTKSA0232
Diploneis subovalis HK084
Diploneis sp UTKSA0190
Diploneis parca UTKSA0267
Gomphonemopsis pseudoexigua UTKSA0026x
Phaeodactylum tricornutum UTEX640
Phaeodactylum tricornutum HK011
Phaeodactylum tricornutum UTEX2089
Phaeodactylum tricornutum UTEX646

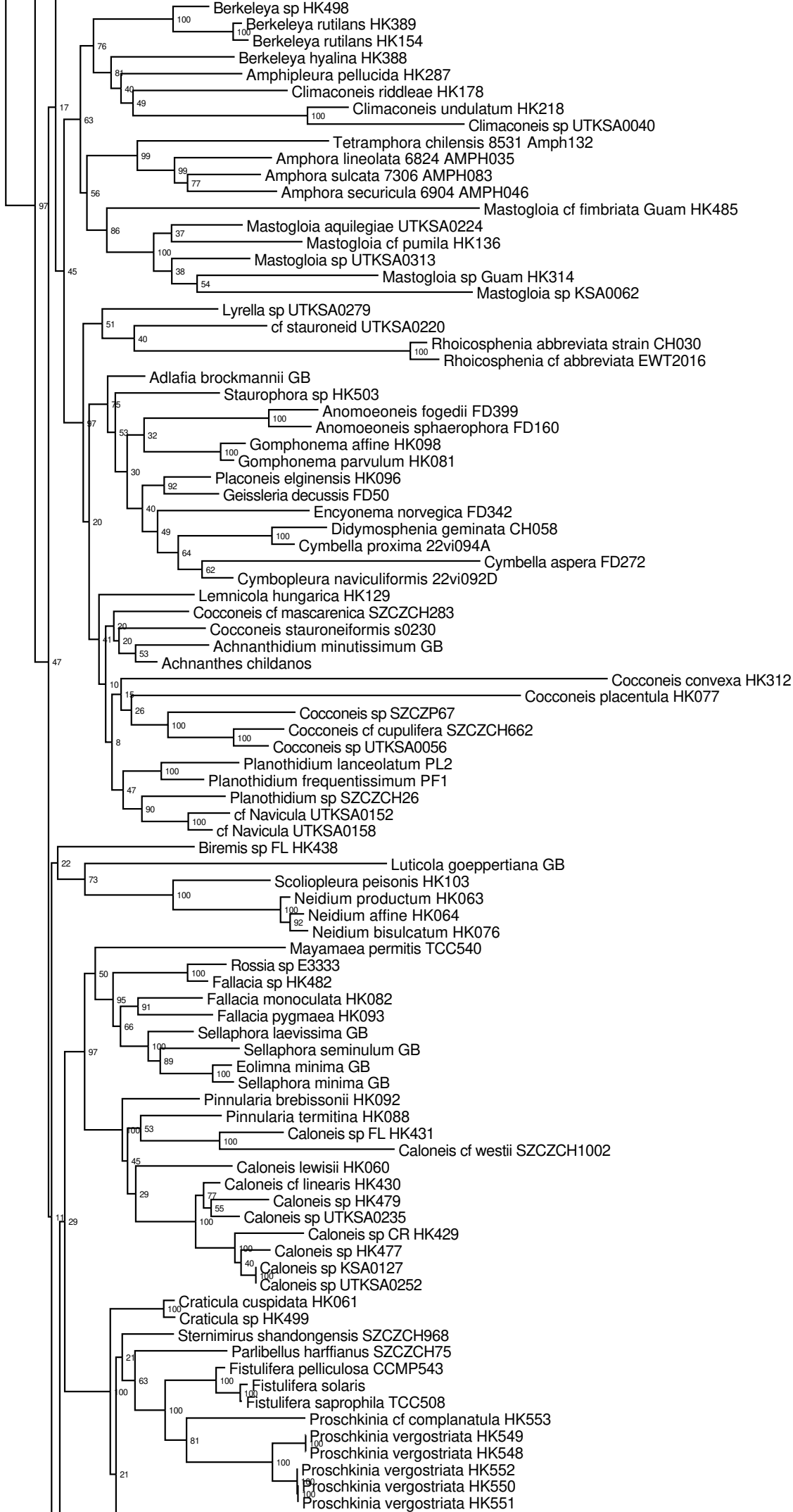
Berkeleya sp HK498
Berkeleya rutilans HK389
Berkeleya rutilans HK154
Berkeleya hyalina HK388
Amphipleura pellucida HK287
Climaconeis riddleae HK178
Climaconeis undulatum HK218
Climaconeis sp UTKSA0040
Tetramphora chilensis 8531 Amph132
Amphora lineolata 6824 AMPH035
Amphora sulcata 7306 AMPH083
Amphora securicula 6904 AMPH046
Mastogloia cf fimbriata Guam HK485
Mastogloia aquilegiae UTKSA0224
Mastogloia cf pumila HK136
Mastogloia sp UTKSA0313
Mastogloia sp Guam HK314
Mastogloia sp KSA0062
Lyrella sp UTKSA0279
cf stauroneid UTKSA0220
Rhoicosphenia abbreviata strain CH030
Rhoicosphenia cf abbreviata EWT2016
Adlafia brockmannii GB
Staurophora sp HK503
Anomoeoneis fogedii FD399
Anomoeoneis sphaerophora FD160
Gomphonema affine HK098
Gomphonema parvulum HK081
Placoneis elginensis HK096
Geissleria decussis FD50
Encyonema norvegica FD342
Didymosphenia geminata CH058
Cymbella proxima 22vi094A
Cymbella aspera FD272
Cymbopleura naviculiformis 22vi092D
Lemnicola hungarica HK129
Cocconeis cf mascarenica SZCZCH283
Cocconeis stauroneiformis s0230
Achnanthidium minutissimum GB
Achnanthes childanos
Cocconeis convexa HK312
Cocconeis placentula HK077
Cocconeis sp SZCZP67
Cocconeis cf cupulifera SZCZCH662
Cocconeis sp UTKSA0056
Planothidium lanceolatum PL2
Planothidium frequentissimum PF1
Planothidium sp SZCZCH26
cf Navicula UTKSA0152
cf Navicula UTKSA0158
Biremis sp FL HK438
Luticola goeppertiana GB
Scoliopleura peisonis HK103
Neidium productum HK063
Neidium affine HK064
Neidium bisulcatum HK076
Mayamaea permitis TCC540
Rossia sp E3333
Fallacia sp HK482
Fallacia monoculata HK082
Fallacia pygmaea HK093
Sellaphora laevissima GB
Sellaphora seminulum GB
Eolimna minima GB
Sellaphora minima GB
Pinnularia brebissonii HK092
Pinnularia termitina HK088
Caloneis sp FL HK431
Caloneis cf westii SZCZCH1002
Caloneis lewisii HK060
Caloneis cf linearis HK430
Caloneis sp HK479
Caloneis sp UTKSA0235
Caloneis sp CR HK429
Caloneis sp HK477
Caloneis sp KSA0127
Caloneis sp UTKSA0252
Craticula cuspidata HK061
Craticula sp HK499
Sternimirus shandongensis SZCZCH968
Parlibellus harffianus SZCZCH75
Fistulifera pelliculosa CCMP543
Fistulifera solaris
Fistulifera saprophila TCC508
Proschkinia cf complanatula HK553
Proschkinia vergostriata HK549
Proschkinia vergostriata HK548
Proschkinia vergostriata HK552
Proschkinia vergostriata HK550
Proschkinia vergostriata HK551

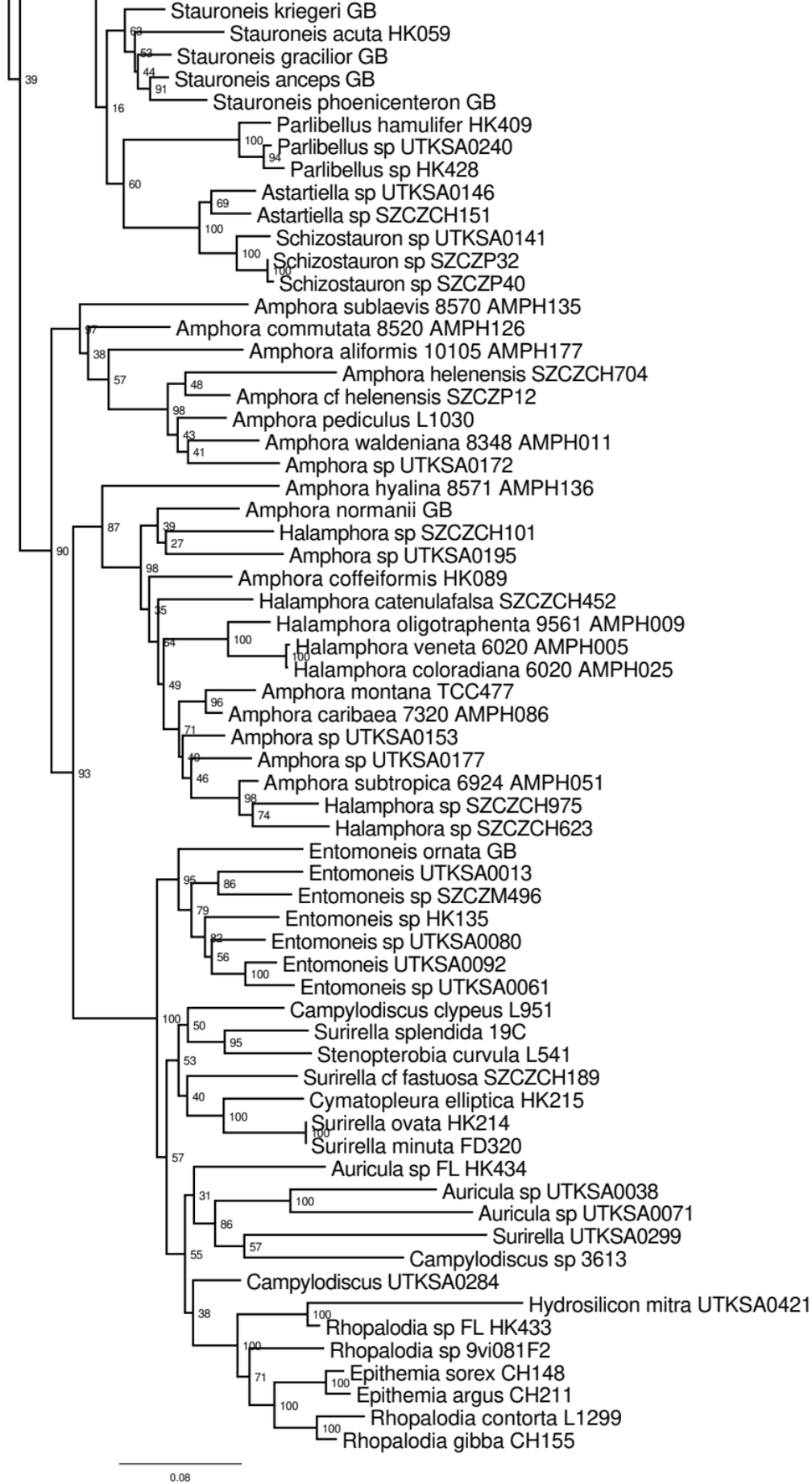
Stauroneis kriegeri GB
Stauroneis acuta HK059
Stauroneis gracilior GB
Stauroneis anceps GB
Stauroneis phoenicenteron GB
Parlibellus hamulifer HK409
Parlibellus sp UTKSA0240
Parlibellus sp HK428
Astartiella sp UTKSA0146
Astartiella sp SZCZCH151
Schizostauron sp UTKSA0141
Schizostauron sp SZCZP32
Schizostauron sp SZCZP40
Amphora sublaevis 8570 AMPH135
Amphora commutata 8520 AMPH126
Amphora aliformis 10105 AMPH177
Amphora helenensis SZCZCH704
Amphora cf helenensis SZCZP12
Amphora pediculus L1030
Amphora waldeniana 8348 AMPH011
Amphora sp UTKSA0172
Amphora hyalina 8571 AMPH136
Amphora normanii GB
Halamphora sp SZCZCH101
Amphora sp UTKSA0195
Amphora coffeiformis HK089
Halamphora catenulafalsa SZCZCH452
Halamphora oligotraphenta 9561 AMPH009
Halamphora veneta 6020 AMPH005
Halamphora coloradiana 6020 AMPH025
Amphora montana TCC477
Amphora caribaea 7320 AMPH086
Amphora sp UTKSA0153
Amphora sp UTKSA0177
Amphora subtropica 6924 AMPH051
Halamphora sp SZCZCH975
Halamphora sp SZCZCH623
Entomoneis ornata GB
Entomoneis UTKSA0013
Entomoneis sp SZCZM496
Entomoneis sp HK135
Entomoneis sp UTKSA0080
Entomoneis UTKSA0092
Entomoneis sp UTKSA0061
Campylodiscus clypeus L951
Surirella splendida 19C
Stenopterobia curvula L541
Surirella cf fastuosa SZCZCH189
Cymatopleura elliptica HK215
Surirella ovata HK214
Surirella minuta FD320
Auricula sp FL HK434
Auricula sp UTKSA0038
Auricula sp UTKSA0071
Surirella UTKSA0299
Campylodiscus sp 3613
Campylodiscus UTKSA0284
Hydrosilicon mitra UTKSA0421
Rhopalodia sp FL HK433
Rhopalodia sp 9vi081F2
Epithemia sorex CH148
Epithemia argus CH211
Rhopalodia contorta L1299
Rhopalodia gibba CH155
0.08

Table S1. Taxa, strain voucher ID and GenBank accession numbers for strains used in the DNA sequence data phylogenetic analysis. Collection site for sample of original strain isolation is also included (where known); in the case of cultures from public collections, the culture ID is provided in this column (UTEX = UTEX Culture Collection of Algae; NCMA = National Center for Marine Algae and Microbiota; CSIRO = Australian National Algae Culture Collection; MCC-NIES = Microbial Culture Collection at National Institute for Environmental Studies). Ingroup taxa (raphid pennates) provided first in the table; outgroup taxa ("araphid pennates") follow after table break. Taxa are listed alphabetically. If species unknown, authority for genus is listed.

Taxon	Strain Voucher	Collection Site (Locality in paretheses)	GenBank Accession (SSU, *rbc*L, *psb*C)
Achnanthes chlidanos M.H.Hohn & Hellerman			KJ658412, KJ658394, N/A
Achnanthes coarctata (Brébisson ex W. Smith) Grunow in Cleve & Grunow	HK079	FD185 (UTEX)	HQ912594, HQ912458, HQ912287
Achnanthes sp Bory	HK303	SanNicholas1 (San Nicholas, Canary Islands)	KC309473, KC309545, KC309617
Achnanthes sp Bory	HK309	ECT3883 (Rainbow Harbor, Long Beach, California)	KC309474, KC309546, KC309618
Achnanthes sp Bory	HK310	ECT3911 (Long Beach, California)	KC309475, KC309547, KC309619
Achnanthes sp Bory	HK311	ECT3684 (Achang Reef, Guam)	KC309476, KC309548, KC309620
Achnanthes sp Bory	HK517	Azo42 (Azores)	MH063437, MH064054, MH063967
Achnanthes sp Bory	HK563	ChelMyC 26V16 (Green Sea Turtle, Turtle Hospital, Marathon, Florida)	N/A, MT432475, MT432494
Achnanthes sp Bory	HK564	ChelMyC 26V16 (Green Sea Turtle, Turtle Hospital,	MT441506, MT432476, MT432495

		Marathon, Florida)	
Achnanthes sp Bory	HK565	ChelMyC 26V16 (Green Sea Turtle, Turtle Hospital, Marathon, Florida)	MT441507, MT432477, MT432496
Achnanthes sp Bory	HK566	ChelMyC 26V16 (Green Sea Turtle, Turtle Hospital, Marathon, Florida)	MT441504, MT432473, MT432492
Achnanthes sp Bory	HK567	ChelMyC 26V16 (Green Sea Turtle, Turtle Hospital, Marathon, Florida)	MT441505, MT432474, MT432493
Achnanthes sp Bory	HK568	FLLoggerheadA2 (Loggerhead Turtle, Florida Bay, Florida)	MT441510, MT432481, MT432500
Achnanthes sp Bory	HK569	FLLoggerheadA2 (Loggerhead Turtle, Florida Bay, Florida)	MT441511, MT432482, MT432501
Achnanthes sp Bory	HK570	GAKempZ6 (Kemp's Ridley Turtle, Georgia)	MT441508, MT432478, MT432497
Achnanthes sp Bory	HK571	GAKempZ6 (Kemp's Ridley Turtle, Georgia)	MT441509, MT432479, MT432498
Achnanthes sp Bory	HK572	GAKempZ6 (Kemp's Ridley Turtle, Georgia)	N/A, MT432480, MT432499

Achnanthes sp Bory	HK573	FLMan45 (Manatee, Ft. Lauderdale, Florida)	MT441502, MT432471, MT432490
Achnanthes sp Bory	HK574	FLMan40 (Manatee, Ft. Lauderdale, Florida)	MT441501, MT432470, MT432489
Achnanthes sp Bory	HK575	CGA1605-D (Manatee, Georgia)	MT441503, MT432472, MT432491
Achnanthes sp Bory	UTKSA0263	KSA2015-16 (Al-Nawras, Jeddah, Saudi Arabia)	MH063438, MH064055, N/A
Achnanthidium minutissimum (Kützing) Czarnecki			AM502032, AM710499, N/A
Adlafia brockmannii (Hustedt) Bruder & Hinz			AM502020, AM710487, N/A
Amphipleura pellucida Kützing	HK287	ECT3568 (Lake Travis, Texas)	KC309477, KC309549, KC309621
Amphora aliformis	AMPH177		KP229525, KP229546, KP229548
Amphora caribaea	AMPH086		KJ463428, KJ463458, KJ463488
Amphora commutata	AMPH126		KP229526, KP229547, KP229549
Amphora cf immarginata Nagumo	UTKSA0172	KSA2015-37 (Rabigh, Saudi Arabia)	MH063439, MH064056, MH063968
Amphora helenensis	SZCZCH704		KT943649, KT943672, KT943709
Amphora cf helenensis	SZCZP12		KU179126, KU179113, KU179140
Amphora hyalina	AMPH136		KJ463432, KJ463462, KJ463492
Amphora lineolata	AMPH035		KJ463435, KJ463465, KJ463495
Amphora obtusa Gregory	UTKSA0275	KSA2015-37 (Rabigh, Saudi Arabia)	MH063440, MH064057, N/A

Amphora obtusa v crassa	AMPH070		KJ463436, KJ463466, KJ463496
Amphora pediculus (Kützing) Grunow		L1030 (UTEX)	HQ912417, HQ912403, HQ912389
Amphora securicula	AMPH046		KJ463440, KJ463470, KJ463500
Amphora sp. Ehrenberg ex Kützing	HK502	PackaryChannelSediment (Mustang Island, Texas)	MH017634, MH064058, MH063969
Amphora sp. Ehrenberg ex Kützing	UTKSA0087	SA12 (Markaz Al Shoaibah, Saudi Arabia)	MH063441, MH064059, MH063970
Amphora sp. Ehrenberg ex Kützing	UTKSA0115	KSA2015-27 (Markaz Al Shoaibah, Saudi Arabia)	MH063442, MH064060, N/A
Amphora sp. Ehrenberg ex Kützing	UTKSA0153	KSA2015-37 (Rabigh, Saudi Arabia)	MH063443, MH064061, MH063971
Amphora sp. Ehrenberg ex Kützing	UTKSA0177	KSA2015-41 (Rabigh, Saudi Arabia)	MH063444, MH064062, MH063972
Amphora sublaevis	AMPH135		KJ463444, KJ463474, KJ463504
Amphora subtropica	AMPH051		KJ463445, KJ463475, KJ463505
Amphora sulcata	AMPH083		KJ463446, KJ463476, KJ463506
Amphora vixvisibilis Li & Witkowski	SZCZCH967		KT943648, KT943670, KT943706
Amphora waldeniana	AMPH011		KJ463447, KJ463477, KJ463507
Anomoeoneis fogedii Reimer		FD399 (UTEX)	KJ011610, KJ011793, N/A
Anomoeoneis sphaerophora Pfitzer		FD160 (UTEX)	KJ011612, KJ011795, N/A
Astartiella sp. A.Witkowski, Lange-Bertalot & Metzeltin	UTKSA0146	KSA2015-11 (Bhadur Resort, Saudi Arabia)	MH063445, MH064063, MH063973
Astartiella sp. A.Witkowski, Lange-Bertalot & Metzeltin	SZCZCH151		N/A, KT943613, KT943624
Auricula sp. Castracane	HK434	21IV14-4D (Rabbit Key Basin, Florida)	KX981842, KX981810, KX981789

Auricula cf complexa (Gregory) Cleve	UTKSA0038	SA12 (Markaz Al Shoaibah, Saudi Arabia)	MH063446, MH064064, MH063974
Auricula cf flabelliformis M. Voigt	UTKSA0071	SA12 (Markaz Al Shoaibah, Saudi Arabia)	MH063447, MH064065, MH063975
Bacillaria paxillifer (O. F. Müller) T. Marsson	HK130	FD468 (UTEX)	HQ912627, HQ912491, HQ912320
Bacillaria sp. J.F.Gmelin	HK475	GU44BK-1 (Gab Gab Beach, Guam)	MH063448, MH064066, MH063976
Bacillaria sp. J.F.Gmelin	UTKSA0009	SA27 (Jeddah, Saudi Arabia)	MH063449, MH064067, MH063977
Bacillaria sp. J.F.Gmelin	UTKSA0129	KSA2015-9 (Bhadur Resort, Saudi Arabia)	MH063450, MH064068, MH063978
Bacillaria sp. J.F.Gmelin	UTKSA0130	KSA2015-9 (Bhadur Resort, Saudi Arabia)	MH063451, MH064069, MH063979
Berkeleya hyalina (F.E.Round & M.E.Brooks) E.J.Cox	HK388	ECT3614 (La Jolla, California)	KJ577847, KJ577882, KJ577917
Berkeleya rutilans (Trentepohl ex Roth) Grunow	HK154	ECT3616 (Laguna Beach, California)	HQ912637, HQ912501, HQ912330
Berkeleya rutilans (Trentepohl ex Roth) Grunow	HK389	ECT3602 (Bolinas, California)	KJ577848, KJ577883, KJ577918
Biremis sp. D.G. Mann & E.J. Cox	HK438	21IV14-2A (Duck Key, Florida)	KX981835, KX981811, N/A
Caloneis lewisii Patrick	HK060	FD54 (UTEX)	HQ912580, HQ912444, HQ912273
Caloneis sp. P.T. Cleve	KSA0127	SA12 (Markaz Al Shoaibah, Saudi Arabia)	KU179135, KU179125, N/A
Caloneis sp. P.T. Cleve	HK429	SantaRosa cor.green (Costa Rica)	KU179134, KU179123, N/A
Caloneis cf linearis (Cleve) Boyer	HK430	21IV14-3A (Captain's Key, Florida)	KU179132, KU179119, KU179146
Caloneis cf excentrica (Grunow) Boyer	HK431	21IV14-2A (Duck Key, Florida)	KU179130, KU179117, KU179144
Caloneis sp. P.T. Cleve	HK477	GU7Y-4 (University of Guam	MH063453, MH064071,

		Marine Laboratories, Guam)	MH063981
Caloneis sp. P.T. Cleve	HK479	GU52V-2 (Outhouse Beach, Guam)	N/A, MH064072, MH063982
Caloneis sp. P.T. Cleve	UTKSA0235	KSA2015-37 (Rabigh, Saudi Arabia)	MH063454, MH064073, MH063983
Caloneis sp. P.T. Cleve	UTKSA0252	KSA2015-42 (Rabigh, Saudi Arabia)	MH063455, MH064074, MH063984
Caloneis cf westii (W. Smith) Hendey	SZCZCH1002		KT943628, KT943654, KT943687
Campylodiscus clypeus (Ehrenberg) Kützing		L951 (UTEX)	HQ912412, HQ912398, HQ912384
Campylodiscus sp. Ehrenberg ex Kützing		ECT3613 (Tomales Bay, California)	HQ912413, HQ912399, HQ912385
Campylodiscus sp. Ehrenberg ex Kützing	UTKSA0284	KSA2015-29 (Markaz Al Shoaibah, Saudi Arabia)	MH063456, MH064075, N/A
Carinasigma minuta (Donkin) G. Reid	HK418	GU7X-6 (University of Guam Marine Lab, Guam)	KX981841, KX981812, KX981790
Climaconeis riddleae Prasad	HK178	ECT3724 (Umatac Bay, Guam)	HQ912644, HQ912508, HQ912337
Climaconeis sp. Grunow	UTKSA0040	SA26 (Jeddah, Saudi Arabia)	KX981836, KX981813, N/A
Climaconeis undulata (Meister) Lobban et al	HK218	ECT3743 (Talofofo Bay, Guam)	KC309478, KC309550, N/A
Cocconeis cf cupulifera Riaux-Gobin, Romero, Compère & Al-Handal	SZCZCH662		N/A, KT943680, KT943718
Cocconeis cf mascarenica Riaux-Gobin & Compère	SZCZCH283		N/A, KT943679, KT943717
Cocconeis placentula Ehrenberg	HK077	FD23 (UTEX)	HQ912592, HQ912456, HQ912285
Cocconeis stauroneiformis (W. Smith) H. Okuna	s0230		AB430614, AB430694, N/A
Cocconeis sp Ehrenberg	UTKSA0056	SA28 (Jeddah, Saudi Arabia)	KU179133, KU179120, KU179147
Cocconeis sp Ehrenberg	HK312	ECT3901 (Channel #5, US-1, Florida)	KC309479, KC309551, KC309622
Cocconeis sp Ehrenberg	SZCZP67		KT943600, KT943614,

			KT943625
Craspedostauros alatus Majewska & Ashworth	HK448	CCMP1120 (NCMA)	KX981860, KX981817, KX981793
Craspedostauros alyoubii J. Sabir & Ashworth	UTKSA0083	SA18 (Duba, Saudi Arabia)	KX981857, KX981814, KX981791
Craspedostauros amphoroides (Grunow) Cox	HK447	CCMP797 (NCMA)	KX981859, KX981815, N/A
Craspedostauros danayanus Majewska & Ashworth	HK637	Mabibi Beach, South Africa (Leatherback Turtle)	N/A, MT432485, MT432505
Craspedostauros mcewanii Majewska & Ashworth	HK634	RM July19 Calypso (Green Sea Turtle, Durban, South Africa)	N/A, MT432486, MT432505
Craspedostauros mcewanii Majewska & Ashworth	HK635	RM July19 Calypso (Green Sea Turtle, Durban, South Africa)	N/A, MT432487, N/A
Craspedostauros mcewanii Majewska & Ashworth	HK636	RM July19 Calypso (Green Sea Turtle, Durban, South Africa)	N/A, MT432488, N/A
Craspedostauros paradoxus Ashworth & Lobban	HK441	GU44BK-1 (Gab Gab Beach, Guam, USA)	KX981858, KX981816, KX981792
Craticula cuspidata (Kützing) Mann	HK061	FD35 (UTEX)	HQ912581, HQ912445, HQ912274
Cylindrotheca closterium (Ehrenberg) Reimann & Lewin	HK180	CCMP1855 (NCMA)	HQ912645, HQ912509, HQ912338
Cylindrotheca sp. Rabenhorst	UTKSA0079	SA12 (Markaz Al Shoaibah, Saudi Arabia)	KX981848, KX981826, KX981801
Cylindrotheca sp. Rabenhorst	UTKSA0082	SA18 (Duba, Saudi Arabia)	KX981847, KX981827, KX981802
Cymatoneis sp. Cleve	UTKSA0378	KSA2016-3 (Bhadur Resort, Saudi Arabia)	MH063457, MH064076, MH063985
Cymatopleura elliptica (Brebisson ex Kutzing) W. Smith	HK215	L1333 (UTEX)	HQ912659, HQ912523,

			HQ912352
Cymbella aspera (Ehrenberg) Cleve		FD272 (UTEX)	KJ011615, KJ011797, N/A
Cymbella proxima Reimer			AM502017, AM710484, N/A
Cymbopleura naviculiformis (Auerswald ex Heiberg) Krammer			AM502004, AM710471, N/A
Denticula kuetzingii Grunow	HK104	FD135 (UTEX)	HQ912610, HQ912474, HQ912303
Didymosphenia geminata (Lyngbye) M. Schmidt	CH058		KJ011636, KJ011819, N/A
Diploneis cf cheronensis (Grunow) Cleve	HK417	GU44AY-6 (Gab Gab Beach, Guam)	MH017637, MH064077, MH063986
Diploneis cf *smithii* (Brébisson in W. Smith) P.T. Cleve	HK437	GU44AY-6 (Gab Gab Beach, Guam)	KX981837, KX981818, KX981794
Diploneis parca (Schmidt in Schmidt et al.) Boyer	UTKSA0267	KSA2015-49 (Duba, Saudi Arabia)	MH063458, MH064078, MH063987
Diploneis cf smithii (Brébisson in W. Smith) P.T. Cleve	UTKSA0232	KSA0215-30 (Markaz Al Shoaibah, Saudi Arabia)	MH063459, MH064079, N/A
Diploneis cf smithii (Brébisson in W. Smith) P.T. Cleve	UTKSA0238	KSA2015-37 (Rabigh, Saudi Arabia)	MH063460, MH064080, MH063988
Diploneis sp. (Ehrenberg) P.T. Cleve	HK435	Coz-4 (Cozumel, Mexico)	KX981839, KX981819, KX981795
Diploneis sp. (Ehrenberg) P.T. Cleve	HK436	Coz-4 (Cozumel, Mexico)	KX981838, KX981820, KX981796
Diploneis sp. (Ehrenberg) P.T. Cleve	HK483	21IV14-2A (Duck Key, Florida)	MH017638, MH064081, MH063989
Diploneis sp. (Ehrenberg) P.T. Cleve	HK484	PackaryChannelPlank (Mustang Island, Texas)	MH017639, MH064082, MH063990
Diploneis sp. (Ehrenberg) P.T. Cleve	UTKSA0190	KSA2015-14 (Bhadur Resort, Saudi Arabia)	MH063461, MH064083, MH063991
Diploneis subovalis Cleve	HK084	FD282 (UTEX)	HQ912597, HQ912461, HQ912290
Diploneis vacillans (A.W.F. Schmidt) Cleve	UTKSA0145	KSA2015-11 (Bhadur Resort, Saudi Arabia)	MH063462, MH064084, MH063992

Diploneis vacillans (A.W.F. Schmidt) Cleve	UTKSA0150	KSA2015-37 (Rabigh, Saudi Arabia)	N/A, MH064085, MH063993
Diploneis vacillans (A.W.F. Schmidt) Cleve	UTKSA0221	KSA2015-7 (Bhadur Resort, Saudi Arabia)	N/A, MH064086, MH063994
Donkinia sp. Ralfs	UTKSA0269	KSA2015-37 (Rabigh, Saudi Arabia)	MH063463, MH064087, MH063995
Encyonema norvegica (Grunow) Mayer		FD342 (UTEX)	KJ011643, KJ011826, N/A
Entomoneis ornata (Bailey) Reimer			HQ912411, HQ912397, HQ912383
Entomoneis sp. Ehrenberg	HK 135	CS782 (CSIRO)	HQ912631, HQ912495, HQ912324
Entomoneis sp. Ehrenberg	SZCZM496		KT943630, KT943656, KT943689
Entomoneis sp. Ehrenberg	UTKSA0013	SA12 (Markaz Al Shoaibah, Saudi Arabia)	N/A, MH064088, MH063996
Entomoneis sp. Ehrenberg	UTKSA0061	SA18 (Duba, Saudi Arabia)	MH063464, MH064089, MH063997
Entomoneis sp. Ehrenberg	UTKSA0080	SA12 (Markaz Al Shoaibah, Saudi Arabia)	MH063465, MH064090, MH063998
Entomoneis sp. Ehrenberg	UTKSA0092	SA18 (Duba, Saudi Arabia)	MH063466, MH064091, MH063999
Eolimna minima (Grunow in Van Heurck) H. Lange-Bertalot			AM501962, AM710427, N/A
Epithemia argus (Ehrenberg) Kützing	CH211		HQ912408, HQ912394, HQ912380
Epithemia sorex Kützing	CH148		HQ912409, HQ912395, HQ912381
Eunotia curvata Lagerstedt	HK086	FD412 (UTEX)	HQ912599, HQ912463, HQ912292
Eunotia glacialis Meister	HK069	FD46 (UTEX)	HQ912586, HQ912450, HQ912279
Eunotia pectinalis (Kützing) Rabenhorst	HK153	NIES461 (MCC-NIES)	HQ912636, HQ912500, HQ912329

Eunotia sp. Ehrenberg	HK286	ECT3676 (Tinago River, Guam)	KC309480, KC309552, KC309623
Fallacia monoculata (Hustedt) Mann	HK082	FD254 (UTEX)	HQ912596, HQ912460, HQ912289
Fallacia pygmaea (Kützing) Stickle & Mann	HK093	FD294 (UTEX)	HQ912605, HQ912469, HQ912298
Fallacia sp. Stickle & D.G. Mann	HK482	GU52X-3 (Outhouse Beach, Guam)	MH063467, MH064092, MH064000
Fistulifera pelliculosa (Brebisson) Lange-Bertalot			AY485454, HQ337547, N/A
Fistulifera saprophila (Lange-Bertalot & Bonik) Lange-Bertalot			KC736618, KC736593, N/A
Geissleria decussis (Østrup) Lange-Bertalot & Metzeltin		FD050 (UTEX)	KJ011647, KJ011830, N/A
Gomphonema affine Kützing	HK098	FD173 (UTEX)	HQ912608, HQ912472, HQ912301
Gomphonema parvulum (Kützing) Kützing	HK081	FD241 (UTEX)	HQ912595, HQ912459, HQ912288
Gomphonemopsis cf pseudoexigua (Simonsen) Medlin	UTKSA0026x	SA18 (Duba, Saudi Arabia)	MH063471, MH064098, MH064005
Gyrosigma acuminatum (Kützing) Rabenhorst	HK085	FD317 (UTEX)	HQ912598, HQ912462, HQ912291
Halamphora catenulafalsa Witkowski & Ch. Li	SZCZCH452		KT943646, KT943669, KT943704
Halamphora coffeaeformis (Agardh) Levkov	HK089	FD75 (UTEX)	HQ912602, HQ912466, HQ912295
Halamphora cf costata (Smith) Levkov	UTKSA0195	KSA2015-22 (Markaz Al Shoaibah, Saudi Arabia)	MH063468, MH064093, MH064001
Halamphora coloradiana J.G. Stepanek & J.P. Kociolek	AMPH025		KJ463450, KJ463480, KJ463510
Halamphora montana (Krasske) Levkov	TCC477		KC736615, KC736590, N/A
Halamphora normanii (Rabenhorst) Levkov			AM501958, AM710424, N/A
Halamphora oligotraphenta (Lange-Bertalot) Levkov	AMPH009		KJ463451, KJ463481, KJ463511
Halamphora sp. (Cleve) Levkov	SZCZCH101		KT943645, KT943682,

			KT943703
Halamphora sp. (Cleve) Levkov	SZCZCH623		KT943647, KT943684, KT943705
Halamphora sp. (Cleve) Levkov	SZCZCH975		KT943650, KT943673, KT943710
Halamphora veneta (Kützing) Levkov	AMPH005		KJ463452, KJ463482, KJ463512
Hantzschia amphioxys v. major Grunow in Van Heurck			HQ912404, HQ912390, HQ912376
Haslea cf *howeana* (Hagelstein) Giffen	HK494	GU7Y-4 (University of Guam Marine Labs, Guam)	N/A, MH040268, MH040241
Haslea cf *howeana* (Hagelstein) Giffen	HK496	PR6 (San Juan, Puerto Rico)	MH017640, MH040269, MH040242
Haslea ostrearia (Gaillon) Simonsen	NCC158.4		N/A, HF563525, HF558667
Haslea ostrearia (Gaillon) Simonsen	NCC321		N/A, HF563527, HF558669
cf *Haslea sp.* Simonsen	UTKSA0122	KSA2015-30 (Markaz Al Shoaibah, Saudi Arabia)	N/A, MH064096, MH064004
Hippodonta capitata (Ehrenberg) Lange-Bertalot, Metzeltin & Witkowski			AM501966, AM710432, N/A
Hydrosilicon mitra Brun	UTKSA0421	KSA2015-37 (Rabigh, Saudi Arabia)	MH063470, MH064097, N/A
Lemnicola hungarica (Grunow) Round	HK129	FD456 (UTEX)	HQ912626, HQ912490, HQ912319
Luticola goeppertiana (Bleisch) D.G.Mann ex J.Rarick, S.Wu, S.S.Lee & Edlund			AM501967, AM710433, N/A
Lyrella hennedyi (W. Smith) Stickle & Mann	UTKSA0279	KSA2015-5 (Bhadur Resort, Saudi Arabia)	MH063472, MH064099,
Mastogloia aquilegiae Grunow in Moller	UTKSA0224	KSA2015-49 (Duba, Saudi Arabia)	N/A, MH064100, MH064007
Mastogloia fimbriata (T. Brightwell) Grunow	HK485	GU52X-1 (Outhouse Beach, Guam)	MH040321, MH040270, MH040243
Mastogloia cf pumila (Grunow) Cleve	HK136	29X07-6B (Mustang Island, Texas)	HQ912632, HQ912496, HQ912325

Mastogloia sp. Thwaites in W. Smith	HK314	ECT3762 (Taeleyag Beach, Guam)	KC309481, KC309553, N/A
Mastogloia sp. Thwaites in W. Smith	KSA0062	SA17 (Duba, Saudi Arabia)	MH063473, MH064101, MH064008
Mastogloia sp. Thwaites in W. Smith	UTKSA0313	KSA0216-44 (Markaz Al Shoaibah, Saudi Arabia)	MH063474, MH064102, MH064009
Mayamea perimitis (Hustedt) K. Bruder & L.K. Medlin	TCC540		KC736630, KC736600, N/A
Meuniera membranacea (Cleve) P. C. Silva	HK313	ECT3896 (Port Aransas Jetty, Texas)	KC309482, KC309554, KC309624
Navicula avium (Tiffany, Herwig et Sterrenburg) Yuhang Li et Kuidong Xu	MBM285981		KY937692, KY937695, N/A
Navicula cari Ehrenberg			AM501991, AM710457, N/A
Navicula cryptocephala Kützing	HK090	FD109 (UTEX)	HQ912603, HQ912467, HQ912296
Navicula hippodontofallax Witkowski & Ch. Li	SZCZCH703		KT943636, KT943661, KT943695
Navicula perminuta Østrup	HK561	FLMan10 (Manatee, Crystal River, Florida)	, MT432484, MT432502
Navicula perminuta Østrup	mbccc3		JQ045340, JQ432375, N/A
Navicula sp. Bory	HK486	Coz4 (Cozumel, Mexico)	MH040322, MH040271, MH040244
Navicula sp. Bory	HK487	Coz4 (Cozumel, Mexico)	N/A, MH064103, MH064010
Navicula sp. Bory	HK488	24IV14-2A (Conch Reef, Florida)	MH063475, MH064104, MH064011
Navicula sp. Bory	HK489	24IV14-3A (Pickles Reef, Florida)	MH063476, MH064105, MH064012
Navicula sp. Bory	HK490	GU7Y-4 (University of Guam Marine Laboratories, Guam)	N/A, MH040272, MH040245
Navicula sp. Bory	HK491	17VIII13-2 (Belfast, Maine)	MT441512, MT432483, MT432503
Navicula sp. Bory	HK493	GU52X-1 (Outhouse Beach, Guam)	N/A, MH064095, MH064003
Navicula sp. Bory	HK500	CGA1605-D (Manatee,	MH017641, MN977810,

		Georgia)	MN977815
Navicula sp. Bory	HK558	FLMan1 (Manatee, Crystal River, Florida)	N/A, MN977809, MN977814
Navicula sp. Bory	HK559	FLMan1 (Manatee, Crystal River, Florida)	MN977831, MN977808, MN977813
Navicula sp. Bory	KSA0102	SA4 (Durrah, Saudi Arabia)	KX981844, KX981821, KX981797
Navicula sp. Bory	KSA0112	SA23 (Al-Wajh, Saudi Arabia)	N/A, MH064106, MH064013
Navicula sp. Bory	UTKSA0131	KSA2015-19 (Al-Nawras, Jeddah, Saudi Arabia)	MH063477, MH064107, MH064014
Navicula sp. Bory	UTKSA0162	KSA2015-14 (Bhadur Resort, Saudi Arabia)	MH063478, MH064108, MH064015
Navicula sp. Bory	UTKSA0211	KSA2015-54 (Duba, Saudi Arabia)	MH063469, MH064094, MH064002
Navicula sp. Bory	UTKSA0239	KSA2015-41 (Rabigh, Saudi Arabia)	MH063479, MH064109, MH064016
Navicula reinhardtii Grunow in Cleve & Möller			AM501976, AM710442, N/A
Navicula tripunctata (O.F. Müller) Bory			AM502028, AM710495, N/A
Navicula zhengii Witkowski & Li	SZCZCH96		KT943632, KT943681, KT943691
Neidium affine (Ehrenberg) Pfitzer	HK064	FD127 (UTEX)	HQ912583, HQ912447, HQ912276
Neidium bisulcatum (Lagerstedt) Cleve	HK076	FD417 (UTEX)	HQ912591, HQ912455, HQ912284
Neidium productum (W. Smith) Cleve	HK063	FD116 (UTEX)	HQ912582, HQ912446, HQ912275
Nitzschia acidoclinata Lange-Bertalot			KC736632, KC736602, N/A
Nitzschia aurariae Cholnoky	SZCZCH966		KT943639, KT943663, KT943698
Nitzschia celaenoae Lobban, Ashworth, Calaor & Theriot	KSA0035	SA4 (Durrah, Saudi Arabia)	KU179128, KU179116, KU179143
Nitzschia draveillensis Coste & Ricard			KC736635, KC736605, N/A

Nitzschia dubiformis Hustedt			AB430616, AB430696, N/A
Nitzschia inconspicua Grunow			KC736636, KC736607, N/A
Nitzschia filiformis (W. Smith) Van Heurck	HK073	FD267 (UTEX)	HQ912589, HQ912453, HQ912282
Nitzschia cf frigida Grunow	HK468	AKIce (Barrow, Alaska)	N/A, MH064110, MH064017
Nitzschia frustulum (Kützing) Grunow	TCC545		KT072974, KT072922, N/A
Nitzschia cf longissima (Brébisson in Kützing) Grunow	HK176	ECT3689 (Sala Glula, Guam)	KX981850, KX981829, KX981804
Nitzschia longissima (Brébisson in Kützing) Grunow	GenBank		AY881968, AY881967, N/A
Nitzschia longissima (Brébisson in Kützing) Grunow	UTKSA0021	SA29 (Jeddah, Saudi Arabia)	MH063480, MH064111, MH064018
Nitzschia longissima (Brébisson in Kützing) Grunow	UTKSA0124	KSA2015-9 (Bhadur Resort, Saudi Arabia)	MH063481, MH064112, MH064019
Nitzschia lorenziana Grunow			KC736637, KC736608, N/A
Nitzschia martiana (C. Agardh) Van Heurck	HK405	3VIII07 (Talofofo Bay, Guam)	N/A, KJ577899, KJ577933
Nitzschia sp. Hassall	KSA0120	SA27 (Jeddah, Saudi Arabia)	KX981849, KX981828, KX981803
Nitzschia sp. Hassall	HK469	Rincon Mangrove (Costa Rica)	MH040323, MH040273, MH040246
Nitzschia sp. Hassall	HK470	Nate Site 1 (Kona, Hawaii)	MH040324, MH040274, MH040247
Nitzschia sp. Hassall	HK472	Coz4 (Cozumel, Mexico)	MH040325, N/A, MH040248
Nitzschia sp. Hassall	HK473	GU52X-4 (Outhouse Beach, Guam)	MH040326, MH040275, MH040249
Nitzschia sp. Hassall	HK474	CCMP1698 (NCMA)	MH040327, MH040276, MH040250
Nitzschia sp. Hassall	UTKSA0053	SA19 (Al-Wajh, Saudi Arabia)	N/A, MH064113, MH064020
Nitzschia sp. Hassall	UTKSA0102	KSA2015-14 (Bhadur Resort, Saudi Arabia)	MH063482, MH064114, MH064021
Nitzschia sp. Hassall	UTKSA0106	KSA2015-49 (Duba, Saudi Arabia)	MH063483, MH064115, MH064022

Nitzschia sp. Hassall	UTKSA0107	KSA2015-49 (Duba, Saudi Arabia)	MH063484, MH064116, MH064023
Nitzschia sp. Hassall	UTKSA0109	KSA2015-16 (Al-Nawras, Jeddah, Saudi Arabia)	MH063485, MH064117, N/A
Nitzschia sp. Hassall	UTKSA0111	KSA2015-23 (Markaz Al Shoaibah, Saudi Arabia)	MH063486, MH064118, MH064024
Nitzschia sp. Hassall	UTKSA0171	KSA2015-11 (Bhadur Resort, Saudi Arabia)	MH063487, MH064119, MH064025
Nitzschia sp. Hassall	UTKSA0173	KSA2015-37 (Rabigh, Saudi Arabia)	MH063488, MH064120, MH064026
Nitzschia sp. Hassall	UTKSA0182	KSA2015-38 (Rabigh, Saudi Arabia)	MH063489, MH064121, MH064027
Nitzschia sp. Hassall	UTKSA0260	KSA2015-11 (Bhadur Resort, Saudi Arabia)	MH063490, MH064122, MH064028
Nitzschia traheaformis Ch. Li, Witkowski & Yu Sh.	SZCZCH970		KT943642, KT943666, KT943701
Nitzschia traheaformis Ch. Li, Witkowski & Yu Sh.	SZCZCH971		KT943643, KT943667, KT943702
Nitzschia volvendirostrata Ashworth, Dabek & Witkowski	KSA0039	SA12 (Markaz Al Shoaibah, Saudi Arabia)	N/A, KU179112, KU179139
Parlibellus hamulifer (Grunow) Cox	HK409	GU44AK-4 (Gab Gab Beach, Guam)	KJ577866, KJ577903, KJ577937
Parlibellus cf *hamulifer* (Grunow) Cox	HK428	SantaRosaCor.green (Costa Rica)	KU179137, KU179122, KU179149
Parlibellus harffianus Witkowski, Ch. Li & S.-X.Yu	SZCZCH75		KT943652, KT943686, KT943715
Phaeodactylum tricornutum Bohlin	HK011	CCMP2561 (NCMA)	HQ912556, HQ912420, HQ912250
Phaeodactylum tricornutum Bohlin	HK538	UTEX640 (UTEX)	MH063492, MH064125, MH064031
Phaeodactylum tricornutum Bohlin	HK539	UTEX646 (UTEX)	MH063493, MH064126, MH064032
Phaeodactylum tricornutum Bohlin	HK540	UTEX2089 (UTEX)	MH063494, MH064127,

			MH064033
Pinnularia brebissonii (Kützing) Rabenhorst	HK092	FD274 (UTEX)	HQ912604, HQ912468, HQ912297
Pinnularia termitina (Ehrenberg) Patrick	HK088	FD484 (UTEX)	HQ912601, HQ912465, HQ912294
Placoneis elginensis (Gregory) Cox	HK096	FD416 (UTEX)	HQ912607, HQ912471, HQ912300
Plagiotropis sp. Pfitzer	HK508	PR5 (Condado Lagoon, Puerto Rico)	MH063495, MH064128, MH064034
Planothidium frequentissimum (Lange-Bertalot) Lange-Bertalot	PF1		KJ658409, KJ658392, N/A
Planothidium lanceolatum (Brébisson ex Kützing) Lange-Bertalot	PL2		KJ658410, KJ658393, N/A
Planothidium sp. Round & Bukhtiyarova	SZCZCH26		KT943653, KT943678, KT943716
Pleurosigma sp. W. Smith	HK495	GU52X-1 (Outhouse Beach, Guam)	MH040327, MH040276, MH040250
Pleurosigma sp. W. Smith	UTKSA0019	SA18 (Duba, Saudi Arabia)	KX981840, KX981822, KX981798
Pleurosigma sp. W. Smith	UTKSA0167	KSA2015-49 (Duba, Saudi Arabia)	MH063496, MH064129, MH064035
Pleurosigma sp. W. Smith	UTKSA0264	KSA2015-16 (Al-Nawras, Jeddah, Saudi Arabia)	MH063497, N/A, MH064036
Pleurosigma sp. W. Smith	UTKSA0273	KSA2015-16 (Al-Nawras, Jeddah, Saudi Arabia)	MH063498, MH064130, MH064037
Pleurosigma stuxbergii Cleve & Grunow	SZCZCH973		N/A, KT943674, KT943711
Proschkinia cf complanatula (Hustedt ex Simonsen) D.G. Mann	HK553	24II18-1G (Half Moon Bay, California)	MK736943, MK757575, MK757579
Proschkinia vergostriata Frankovich, Ashworth & M.J. Sullivan	HK548	CC032217a (Loggerhead turtle, Florida)	N/A, MK757570, N/A
Proschkinia vergostriata Frankovich, Ashworth & M.J. Sullivan	HK549	CC032217a (Loggerhead turtle, Florida)	MK736939, MK757571, N/A
Proschkinia vergostriata Frankovich, Ashworth & M.J.	HK550	ChelMyN 26V16 (Green Sea	MK736940, MK757572,

Sullivan		Turtle, Turtle Hospital, Marathon, Florida)	MK757576
Proschkinia vergostriata Frankovich, Ashworth & M.J. Sullivan	HK551	ChelMyN 26V16 (Green Sea Turtle, Turtle Hospital, Marathon, Florida)	MK736941, MK757573, MK757577
Proschkinia vergostriata Frankovich, Ashworth & M.J. Sullivan	HK552	ChelMyN 26V16 (Green Sea Turtle, Turtle Hospital, Marathon, Florida)	MK736942, MK757574, MK757578
Psammodictyon constrictum (Gregory) Mann in Round, Crawford & Mann	HK440	GU7X-7 (University of Guam Marine Lab, Guam)	KX981851, KX981830, KX981805
Psammodictyon constrictum (Gregory) Mann in Round, Crawford & Mann	HK471	Nate Site 1 (Kona, Hawaii)	MH040329, MH040278, MH040252
Psammodictyon sp. D.G. Mann	UTKSA0117	KSA2015-30 (Markaz Al Shoaibah, Saudi Arabia)	MH063499, MH064131, MH064038
Psammodictyon sp. D.G. Mann	UTKSA0151	KSA2015-37 (Rabigh, Saudi Arabia)	MH063500, MH064132, MH064039
Psammodictyon sp. D.G. Mann	UTKSA0280	KSA2015-2 (Bhadur Resort, Saudi Arabia)	MH063501, MH064133, MH064040
Psammodictyon pustulatum (Voigt ex Meister) Lobban	UTKSA0298	KSA2015-38 (Rabigh, Saudi Arabia)	MH063502, MH064134, MH064041
Rhoiconeis pagoensis C.S. Lobban	HK419	GU7X-7 (University of Guam Marine Lab, Guam)	KX981846, KX981825, KX981800
Rhoiconeis sp. Grunow	UTKSA0128	KSA2015-16 (Al-Nawras, Jeddah, Saudi Arabia)	MH063503, MH064135, N/A
Rhoicosigma sp. Grunow	UTKSA0194	KSA2015-22 (Markaz Al Shoaibah, Saudi Arabia)	MH063504, MH064136, MH064042
Rhoicosphenia abbreviata (C.Agardh) Lange-Bertalot	CH030		KJ011672, KJ011854, N/A
Rhoicosphenia cf abbreviata (C.Agardh) Lange-Bertalot	EWT2016.80		KU965569, KU965580, N/A
Rhopalodia contorta Hustedt		L1299 (UTEX)	HQ912406, HQ912392, HQ912378

Rhopalodia gibba (Ehrenberg) O. Müller			HQ912407, HQ912393, HQ912379
Rhopalodia sp. O. Müller	HK433	21IV14-4D (Rabbit Key Basin, Florida)	KX981843, KX981823, KX981799
Rhopalodia sp. O. Müller		ECT3678 (Tinago River, Guam)	HQ912405, HQ912391, HQ912377
Rossia sp. Voigt			EF151968, EF143281, N/A
Schizostauron sp. Grunow	UTKSA0141	KSA2015-11 (Bhadur Resort, Saudi Arabia)	MH063505, MH064137, MH064043
Schizostauron sp. Grunow	SZCZP32		KT943595, KT943606, KT943619
Schizostauron sp. Grunow	SZCZP40		KT943596, KT943607, KT943620
Scoliopleura peisonis Grunow	HK103	FD13 (UTEX)	HQ912609, HQ912473, HQ912302
Sellaphora laevissima (Kützing) D.G.Mann	THR4		EF151981, EF143309, N/A
Sellaphora minima Grunow	TCC524		KF959656, KF959642, N/A
Sellaphora seminulum (Grunow) D.G. Mann	TCC461		KF959642, KC736613, N/A
Seminavis robusta D.B.Danielidis & D.G.Mann	HK492	GU7X-7 (University of Guam Marine Laboratories, Guam)	MH040330, MH040279, MH040253
Stauroneis acuta W. Smith	HK059	FD51 (UTEX)	HQ912579, HQ912443, HQ912272
Stauroneis anceps Ehrenberg			AM502008, AM710475, N/A
Stauroneis gracilior Reichardt			AM501988, AM710454, N/A
Stauroneis kriegeri Patrick			AM501990, AM710456, N/A
Stauroneis phoenicentron (Nitzsch) Ehrenberg			AM502031, AM710498, N/A
Stauroneis sp. Ehrenberg	UTKSA0410	KSA2016-9 (Bhadur Resort, Saudi Arabia)	MH063506, MH064138, MH064044
Sternimirus shandongensis Witkowski & Li	SZCZCH968		KT943637, KT943662, KT943696
Staurotropis americana Ashworth	HK442	FishPassMangrove (Mustang Island, Texas)	KX981855, KX981834, KX981808
Staurotropis americana Ashworth	HK443	Coz4 (Cozumel, Mexico)	KX981854, KX981833,

			KX981807
Staurotropis khiyamii J. Sabir & Ashworth	UTKSA0047	SA18 (Duba, Saudi Arabia)	KX981853, KX981832, KX981806
Staurotropis seychellensis (Giffen) Paddock	HK172	ECT3721 (University of Guam Marine Lab, Guam)	KX981856, N/A, KX981809
Stenopterobia curvula (W. Smith) Krammer		L541 (UTEX)	HQ912416, HQ912402, HQ912388
Surirella cf fastuosa (Ehrenberg) Ehrenberg		SZCZCH189	KT943629, KT943655, KT943688
Surirella minuta Van Heurck		FD320 (UTEX)	HQ912658, HQ912522, HQ912351
Surirella ovata Kützing	HK214	L1241 (UTEX)	HQ912658, HQ912522, HQ912351
Surirella splendida (Ehrenberg) Kützing			HQ912415, HQ912401, HQ912387
Surirella sp. Turpin	UTKSA0299	KSA2015-2 (Bhadur Resort, Saudi Arabia)	MH063507, MH064139, MH064045
Tetramphora chilensis (Hustedt) Stepanek & Kociolek		AMPH132	KU665638, KU665639, KU665640
Trachyneis sp. P.T. Cleve	HK439	SantaRosaCor.green (Costa Rica)	KX981845, KX981824, N/A
Tryblionella apiculata Gregory	HK087	FD465 (UTEX)	HQ912600, HQ912464, HQ912293
Tryblionella gaoana Witkowski & Ch. Li	SZCZCH97		KT943638, KT943683, KT943697
unidentified diploneid	UTKSA0368	KSA0216-36 (Duba, Saudi Arabia)	MH063508, MH064140, MH064046
unidentified monoraphid	HK380	ECT3899 (Pacific Grove, California)	KJ577839, KJ577874, KJ577911
unidentified monoraphid	HK427	BallenaEstRock (Costa Rica)	KU179136, KU179121, KU179148
unidentified monoraphid	UTKSA0152	KSA2015-37 (Rabigh, Saudi Arabia)	MH063509, MH064141, MH064047

unidentified monoraphid	UTKSA0158	KSA2015-37 (Rabigh, Saudi Arabia)	MH063510, MH064142, N/A
unidentified naviculoid	HK497	23X15-5B (Harbor Branch Oceanographic Institute boat launch)	MH063511, MH064143, MH064048
unidentified naviculoid	UTKSA0247	KSA2015-5 (Bhadur Resort, Saudi Arabia)	MH063512, MH064144, MH064049
unidentified stauroneid	UTKSA0220	KSA2015-7 (Bhadur Resort, Saudi Arabia)	MH063513, MH064145, MH064050
Araphid Outgroups			
Asterionella formosa Hassall	HK144	UTCC605	HQ912633, HQ912497, HQ912326
Asterionellopsis glacialis (Castracane) Round	HK107	CCMP134 (NCMA)	HQ912613, HQ912477, HQ912306
Asterionellopsis socialis (Lewin & Norris) Crawford & Gardner	HK181	CCMP1717 (NCMA)	HQ912646, HQ912510, HQ912339
Asterionellopsis socialis (Lewin & Norris) Crawford & Gardner	HK319	ECT3920 (Ft. Stevens State Park, Oregon)	JX413545, JX413562, JX413579
Astrosyne radiata Ashworth & Lobban	HK169	ECT3697 (Gab Gab Beach, Guam)	JN975238, JN975252, JN975267
Bleakeleya notata (Grunow in Van Heurck) F.E. Round	HK247	ECT3733 (Pago Bay, Guam)	HM627330, HM627327, HM627324
Castoridens hyalina Ashworth, Witkowski & Li	HK444	C1 12-7-13 (Destin-Choctawhatchee Bay, Florida)	N/A, KU851892, KU851907
Castoridens striata Ashworth, Li & Witkowski	HK385	15VI11-2A (Baffin Bay, Texas)	KJ577844, KJ577879, KJ577915
Catacombas gaillonii (Bory de Saint-Vincent) Williams & Round	s0045		KR048195, KR048217, KR048229
Centronella reicheltii Voigt	HK150	CCAP1011/1	HQ912635, HQ912499, HQ912328
Ctenophora pulchella (Ralfs ex Kützing) Williams & Round	HK105	FD150 (UTEX)	HQ912611, HQ912475, HQ912304
Cyclophora castracanei Ashworth & Lobban	HK243	GU44AB-6 (Gab Gab Beach,	JN975242, JN975256,

		Guam)	JN975271
Cyclophora castracanei Ashworth & Lobban	HK395	GU44AN-7 (Gab Gab Beach, Guam)	KJ577854, KJ577889, N/A
Cyclophora cf minor Ashworth & Lobban	HK461	24IV14-3A (Pickles Reef, Florida)	MH040308, MH040254, MH040230
Cyclophora tabellariformis Ashworth & Lobban	HK306	ECT3892 (Carrabelle, Florida)	JN975243, JN975257, JN975272
Cyclophora tabellariformis Ashworth & Lobban	HK460	GU44AY-6 (Gab Gab Beach, Guam)	MH040309, MH040255, N/A
Cyclophora tenuis Castracane	HK216	ECT3723 (Umatac Bay, Guam)	HQ912660, HQ912524, HQ912353
Cyclophora tenuis Castracane	HK307	ECT3854 (Kahana Beach Park, Oahu, Hawaii)	JN975240, JN975254, JN975269
Cyclophora tenuis Castracane	HK308	ECT3838 (Long Beach, California)	JN975241, JN975255, JN975270
Delphineis surirella (Ehrenberg) G.W. Andrews	HK133	CCMP1095	HQ912629, HQ912493, HQ912322
Delphineis surirella (Ehrenberg) G.W. Andrews	HK295	ECT3886 (Bald Head Island, North Carolina)	JX413544, JX413561, JX413578
Diatoma elongata (Lyngbye) C.Agardh	HK119	UTCC62	HQ912622, HQ912486, HQ912315
Diatoma tenue Agardh	HK078	FD106 (UTEX)	HQ912593, HQ912457, HQ912286
Dimeregramma sp. J. Ralfs in A. Pritchard	HK288	ECT3864 (MSI, Port Aransas, Texas)	JN975244, JN975258, JN975273
Dimeregramma sp. J. Ralfs in A. Pritchard	HK358	15VI11-2A (Baffin Bay, Texas)	JX401231, JX401249, JX401267
Dimeregramma sp. J. Ralfs in A. Pritchard	HK359	ECT3891 (St. George Island, Florida)	JX401232, JX401250, JX401268
Dimeregramma sp. J. Ralfs in A. Pritchard	HK376	25VI12-1C (Hunting Island, South Carolina)	KF701596, KF701605, KF701614
Dimeregramma sp. J. Ralfs in A. Pritchard	HK377	AtlanticPlankton#8 (Florida)	KF701597, KF701606, KF701615

Florella pascuensis Navarro	HK175	ECT3756 (Guam)	JN975246, JN975260, JN975275
Fragilariforma virescens (Ralfs) Williams & Round	HK132	FD291 (UTEX)	HQ912628, HQ912492, HQ912321
Glyphodesmis sp. Greville	HK357	ECT3891 (St. George Island, Florida)	N/A, JX401248, JX401266
Grammatophora macilenta W. Smith	HK368	GU44AK-4 (Gab Gab Beach, Guam)	JX401241, JX401259, JX401276
Grammatophora oceanica Ehrenberg	HK147	CCMP410	HQ912634, HQ912498, HQ912327
Grammatophora sp. Ehrenberg	HK459	Nate Site 1 (Hawaii)	MG684352, MG684323, MG684295
Grammatophora sp. Ehrenberg	UTKSA0132	KSA2015-16 (Al-Nawras, Jeddah, Saudi Arabia)	MH063514, MH064146, MH064051
Grammatophora undulata Ehrenberg	HK367	Coz-3 (Cozumel, Mexico)	JX401240, JX401258, JX401275
Grammonema striatula (Lyngbye) Agardh	HK371	ECT3897 (Pebble Beach, California)	KF701591, KF701600, KF701609
Hanicella moenia Lobban & Ashworth	HK379	GU44AK-6 (Gab Gab Beach, Guam)	KF701599, KF701608, KF701617
Hendeyella dimeregrammopsis Ashworth	HK391	Coz-1 (Cozumel, Mexico)	KJ577850, KJ577885, KJ577920
Hendeyella lineata Ashworth & Lobban	HK325	GU44AI-3 (Gab Gab Beach, Guam)	JX413547, JX413564, JX413581
Koernerella recticostata (Körner) Ashworth, Lobban & Theriot	HK242	GU44AB-8 (Gab Gab Beach, Guam)	HM627331, HM627328, HM627325
Licmophora abbreviata Agardh	UTKSA0049	SA29 (Jeddah, Saudi Arabia)	KP125882, KP125883, KP125884
Licmophora colosalis Belando, Aboal & Jiménez	HK366	ECT3907 (Rabbit Key Basin, Florida)	JX401239, JX401257, JX401274
Licmophora colosalis Belando, Aboal & Jiménez	UTKSA0066	SA29 (Jeddah, Saudi Arabia)	MG684358, MG684329, MG684299
Licmophora aff ehrenbergii (Kützing) Grunow	HK420	GU7X-6 (University of Guam	KP125876, KP125879,

		Marine Lab, Guam)	KP125881
Licmophora flucticulata Lobban, Schefter & Ruck		GU56-A (Cocos Wall, Guam)	HQ997923, JN975262, JN975277
Licmophora normaniana (Greville) Wahrer in Wahrer, Fryxell & Cox	HK403	26II12-1 (Mustang Island, Texas)	KJ577860, KJ577897. KJ577931
Licmophora paradoxa (Lyngbye) Agardh	HK106	CCMP2313	HQ912612, HQ912476, HQ912305
Licmophora peragallioides (Lobban) Lobban & Ashworth	HK364	GU44AL-3 (Gab Gab Beach, Guam)	JX401237, JX401255, JX401273
Licmophora cf remulus Grunow	HK302	GU52-O (Outhouse Beach, Guam)	JN975248, JN975263, N/A
Licmophora sp. Agardh	HK365	Coz-2 (Cozumel, Mexico)	JX401238, JX401256, N/A
Licmophora sp. Agardh	KSA0085	SA4 (Durrah, Saudi Arabia)	MG684353, MG684324, N/A
Licmophora sp. Agardh	KSA0151	SA1 (Durrah, Saudi Arabia)	MG684354, MG684325, N/A
Licmophora sp. Agardh	UTKSA0010	SA29 (Jeddah, Saudi Arabia)	MG684355, MG684326, MG684296
Licmophora sp. Agardh	UTKSA0029	SA18 (Duba, Saudi Arabia)	MG684356, MG684327, MG684297
Licmophora sp. Agardh	UTKSA0050	SA18 (Duba, Saudi Arabia)	MG684357, MG684328, MG684298
Licmophora sp. Agardh	UTKSA0084	SA18 (Duba, Saudi Arabia)	MG684359, MG684330, MG684300
Licmophora sp. Agardh	UTKSA0191	KSA2015-14 (Bhadur Resort, Saudi Arabia)	MH063515, MH064147, MH064052
Lucanicum concatenatum Lobban & Ashworth	HK378	GU44AI-3 (Gab Gab Beach, Guam)	KF701598, KF701607, KF701616
Microtabella interrupta (Ehrenberg) Round	HK248	ECT3700 (Gab Gab Beach, Guam)	JN975247, JN975261, JN975276
Microtabella interrupta (Ehrenberg) Round	HK458	20X15-1 (Boca Chica Channel, Florida)	MH040319, MH040265, MH040238
Nanofrustulum cf shiloi (J.J. Lee, C.W. Reimer, & M.E. McEnery) F.E. Round, H. Hallsteinsen, & E. Paasche	HK056	CCMP2649	HQ912578, HQ912442, HQ912271
Neodelphineis sp. Takano	HK421	FijiBottleNY (New York)	KP125875, KP125878, N/A

Neofragilaria nicobarica Desikachary, Prasad & Prema	s0371		AB433340, KR048216 KR048228
Neofragilaria cf nicobarica Desikachary, Prasad & Prema	HK375	Coz-1 (Cozumel, Mexico)	KF701595, KF701604, KF701613
Neosynedra provincialis (Grunow) Williams & Round	HK457	24IV14-3A (Pickles Reef, Florida)	N/A, MH040266, MH040239
Opephora guenter-grassi (Witkowski & Lange-Bertalot) Sabbe & Vyverman		s0263	AB436781, KR048218, N/A
Opephora pacifica (Grunow) Petit	HK296	ECT3831 (Ward Island, Texas)	JN975249, JN975264, JN975278
Perideraion elongatum Jordan, Arai & Lobban	HK411	GU44AK-6 (Gab Gab Beach, Guam)	KJ577868, KJ577905, KJ577939
Perideraion cf elongatum Jordan, Arai & Lobban	UTKSA0259	KSA2015-49 (Duba, Saudi Arabia)	MH063516, MH064148, MH064053
Perideraion montgomeryii Lobban, Jordan & Ashworth	HK246	GU7 (University of Guam Marine Lab, Guam)	HM627332, HM627329, HM627326
Plagiogramma sp. Greville	HK212	ECT3776 (Taeleyag Beach, Guam)	HQ912656, HQ912520, HQ912349
Plagiogramma sp. Greville	HK324	ECT3924 (Potlatch State Park, Washington)	JX413546, JX413563, JX413580
Plagiogramma sp. Greville	HK374	25VI12-1C (Hunting Island, South Carolina)	KF701594, KF701603, KF701612
Plagiostriata goreensis Sato & Medlin	s0388		KR048198, KR048220, KR048232
Psammogramma vigoensis Sato & Medlin	s0391		KR048194, KR048215, KR048227
Psammoneis japonica Sato, Kooistra & Medlin	HK299	GU52-O (Outhouse Beach, Guam)	JN975250, JN975265, JN975279
Psammoneis obaidii Ashworth & Sabir	UTKSA0057	SA12 (Markaz Al Shoaibah, Saudi Arabia)	KR059023, KR059022, KR059024
Psammoneis sp. Sato, Kooistra & Medlin	UTKSA0250	KSA2015-42 (Rabigh, Saudi Arabia)	MH063517, MH064149, N/A
Psammotaenia lanceolata Ashworth, Li & Witkowski	HK316	10X10-2 (St. George Island,	JX413543, JX413560,

		Florida)	JX413577
Pseudostriatella oceanica Sato, Mann & Medlin	s0384		KR048197, KR048219, KR048231
*Pteroncola sp.*R.W. Holmes & D.A. Croll	UTKSA0078	SA29 (Jeddah, Saudi Arabia)	MG684376, N/A, MG684316
Podocystis cf americana Bailey	HK453	19X15-1A (Channel #5, Florida)	MH040320, MH040267, MH040240
Podocystis cf americana Bailey	HK454	19X15-1B (Channel #5, Florida)	MG684360, MG684331, MG684301
Podocystis spathulata (Shadbolt) Van Heurck	HK217	ECT3733 (Pago Bay, Guam)	HQ912661, HQ912525, HQ912354
Rhabdonema adriaticum Kützing	HK370	Coz-3 (Cozumel, Mexico)	JX401243, JX401261, JX401278
Rhabdonema arcuatum (Lyngbye) Kützing	HK304	ECT3898 (Pebble Beach, California)	JN975251, JN975266, JN975280
Rhabdonema sp. Kützing	HK369	GU44AI-1 (Gab Gab Beach, Guam)	JX401242, JX401260, JX401277
Rhaphoneis amphiceros (Ehrenberg) Ehrenberg	HK237	ECT3828 (Redfish Bay, Texas)	HQ912673, HQ912537, KC309625
Rhaphoneis amphiceros (Ehrenberg) Ehrenberg	HK373	25VI12-1A (Hunting Island, South Carolina)	KF701593, KF701602, KF701611
Serratifera varisterna Li, Ashworth & Witkowski	HK315	9X10-2 (Florida State University Marine Lab, Florida)	JX413542, JX413559, JX413576
Serratifera varisterna Li, Ashworth & Witkowski	HK424	PackaryChannelPlankton (Mustang Island, Texas)	KU851868, KU851879, KU851894
Staurosira construens Ehrenberg	HK071	FD232 (UTEX)	HQ912587, HQ912451, HQ912280
Staurosirella pinnata (Ehrenberg) Williams & Round	HK116	CCMP330 (NCMA)	HQ912620, HQ912484, HQ912313
Striatella unipunctata (Lyngbye) Agardh	HK177	ECT3648 (Asan Beach, Guam)	HQ912643, HQ912507, HQ912336
Striatella unipunctata (Lyngbye) Agardh	HK318	ECT3874 (Channel #5, Florida)	JX419383, JX419384, JX419385

Stricosus blumbergii Theriot & Ashworth	HK362	15VI11-2A (Baffin Bay, Texas)	JX401235, JX401253, JX401271
Stricosus harrisonii Lobban & Theriot	HK363	GU44AI (Gab Gab Beach, Guam)	JX401236, JX401254, JX401272
Synedra famelica Kützing	HK072	FD255 (UTEX)	HQ912588, HQ912452, HQ912281
Synedra ulna (Nitzsch) Ehrenberg	HK075	FD404 (UTEX)	HQ912590, HQ912454, HQ912283
Synedropsis hyperborea (Grunow) Hasle, Medlin & Syvertsen	HK117	CCMP1423 (NCMA)	HQ912621, HQ912485, HQ912314
Synedropsis cf recta Hasle, Medlin & Syvertsen	HK110	CCMP1620 (NCMA)	HQ912616, HQ912480, HQ912309
Tabellaria flocculosa (Roth) Kützing	HK065	FD133 (UTEX)	HQ912584, HQ912448, HQ912277
Tabularia cf tabulata (Agardh) Snoeijs	HK109	CCMP846 (NCMA)	HQ912615, HQ912479, HQ912308
Talaroneis posidoniae Kooistra & De Stefano	WK59		AY216905, KR048214, KR048226
Tetracyclus sp. Ralfs	HK416	B12 (Lake Baikal, Russia)	KJ577873, KJ577910, KJ577944
Thalassionema cf bacillare (Heiden) Kolbe	HK361	ECT3929 (Gulf of Mexico, Texas)	JX401234, JX401252, JX401270
Thalassionema frauenfeldii (Grunow) Tempère & Peragallo	HK372	25VI12-1A (Hunting Island, South Carolina)	KF701592, KF701601, KF701610
Thalassionema cf nitzschioides (Grunow) Mereschkowsky	HK360	ECT3929 (Gulf of Mexico, Texas)	JX401233, JX401251, JX401269

On sea turtle-associated *Craspedostauros* (Bacillariophyta), with description of three novel species

*Roksana Majewska**

Unit for Environmental Sciences and Management, School of Biological Sciences, North-West University, Potchefstroom 2520, South Africa

South African Institute for Aquatic Biodiversity (SAIAB), Grahamstown 6140, South Africa

*author for correspondence: roksana.majewska@nwu.ac.za

ORCID: https://orcid.org/0000-0003-2681-4304

Matt P. Ashworth

Department of Molecular Biosciences, The University of Texas at Austin, Austin, TX. 78712, USA

ORCID: https://orcid.org/0000-0002-4162-2004

Sunčica Bosak

Department of Biology, Faculty of Science, University of Zagreb, 10000 Zagreb, Croatia

ORCID: https://orcid.org/0000-0002-4604-2324

William E. Goosen

Centre for High Resolution Transmission Electron Microscopy, Faculty of Science, Nelson Mandela University, 6031 Port Elizabeth, South Africa

ORCID: https://orcid.org/0000-0002-8877-6086

Christopher Nolte

Department of Zoology, Institute for Coastal and Marine Research, Nelson Mandela University, 6031 Port Elizabeth, South Africa

ORCID: https://orcid.org/0000-0002-1429-587X

Klara Filek

Department of Biology, Faculty of Science, University of Zagreb, 10000 Zagreb, Croatia

ORCID: https://orcid.org/0000-0003-2518-4494

Bart Van de Vijver

Research Department, Botanic Garden Meise, B-1860 Meise, Belgium

Department of Biology, University of Antwerp, ECOBE, 2020 Antwerpen, Belgium

ORCID: https://orcid.org/0000-0002-6244-1886

Jonathan C. Taylor

Unit for Environmental Sciences and Management, School of Biological Sciences, North-West University, Potchefstroom 2520, South Africa

South African Institute for Aquatic Biodiversity (SAIAB), Grahamstown 6140, South Africa

ORCID: https://orcid.org/0000-0003-2717-3246

Schonna R. Manning

Department of Molecular Biosciences, The University of Texas at Austin, Austin, TX. 78712, USA

ORCID: https://orcid.org/0000-0002-7705-2111

and Ronel Nel

Department of Zoology, Institute for Coastal and Marine Research, Nelson Mandela University, 6031 Port Elizabeth, South Africa

ORCID: https://orcid.org/0000-0003-2551-6428

43

44 Running title: Sea turtle-associated *Craspedostauros*

ABSTRACT

Despite recent advances in the research on sea turtle-associated diatoms, some of the key aspects of the diatom-sea turtle relationship, including compositional and functional features of the epizoic diatom community, remain understudied and poorly understood. The current paper focuses on four species belonging to the primarily marine diatom genus *Craspedostauros* that were observed growing attached to numerous sea turtles and sea turtle-associated barnacles from Croatia and South Africa. Three of the examined taxa, *C. danayanus* sp. nov., *C. legouvelloanus* sp. nov., and *C. macewanii* sp. nov. represent novel species and are described based on morphological and, whenever possible, molecular characteristics. The new taxa exhibit characters not yet observed in other members of the genus, such as the presence of more than two rows of cribrate areolae on the girdle bands, shallow perforated septa, and a complete reduction of the stauros. In addition, *C. alatus*, recently described from museum sea turtle specimens, is reported for the first time from loggerheads rescued in Europe. A 3-gene phylogenetic analysis including DNA sequence data for three sea turtle-associated *Craspedostauros* species and other marine and epizoic diatom taxa indicated that *Craspedostauros* is monophyletic and sister to *Achnanthes*. This study, being based on a large number of samples and animal specimens analysed and using different preservation and processing methods, provides some new insights into the genus ecology and biogeography and sheds more light on the level of intimacy and permanency in the host-epibiont interaction within the epizoic *Craspedostauros* species.

Key index words: *Craspedostauros*, barnacle, *Chelonibia*, epizoic diatom, leatherback, loggerhead, phylogeny, *Platylepas*, sea turtle

Abbreviations: BS, bootstrap support; CRW, Comparative RNA Web; LM, light microscopy; ML, maximum likelihood; SEM, scanning electron microscopy; SSU, small subunit

INTRODUCTION

As indicated by several studies, diatom communities inhabiting both the skin and the carapace of marine turtles are composed largely of species not observed on other biotic or abiotic substrata (Frankovich et al. 2015, 2016, Majewska et al. 2015a, 2015b, 2017a, 2017b, Robinson et al. 2016, Azari et al. 2020). These observations further suggest a certain level of host-specific evolutionary adaptations used by diatoms. Although intimate relationships between animals and microbes are common and extensively studied, reports of truly epizoic microalgae are generally rare (Ezenwa et al. 2012, Redford et al. 2012, Apprill 2017). Perhaps due to the fact that ubiquitous photosynthetic organisms, such as diatoms, are not immediately perceived as an essential element of any vertebrate microbiome, these new findings are particularly noteworthy. Based on their high frequency of occurrence and high relative abundances recorded from various sea turtle species and geographical regions, as well as lack of records from other types of substrata, several of the newly described sea turtle-associated diatom taxa are currently believed to be strictly epizoic or even sea turtle-specific. While this may be true, many other diatoms present in the sea turtle samples are likely opportunistic species that attached to biofilm in the later stages of its development (Majewska et al. 2015b, 2017b, 2019a,b). Although opportunistic taxa often dominate specific epizoic habitats in terms of the species number, they rarely reach high relative abundance, which may suggest their lack of some key functional adaptations to the epizoic lifestyle.

The present study focuses on the sea turtle-associated species belonging to the diatom genus *Craspedostauros* E.J.Cox. At present, the genus comprises ten validly described species including one, *C. alatus* Majewska et Ashworth, described from museum specimens of sea turtles (Cox 1999, Sabbe et al. 2003, Van de Vijver et al. 2012, Ashworth et al. 2017, Majewska et al. 2018). *Craspedostauros* is a predominantly marine genus, although *C. laevissimus* (W. et G.S. West) Sabbe is described as “a widespread endemic species restricted to the Antarctic Continent” and may

be of brackish or freshwater origin (Sabbe et al. 2003, Van de Vijver et al. 2012). Most of the *Craspedostauros* members share the typical of the genus morphological characters such as cribrate areolae, numerous doubly-perforated girdle bands, two fore and aft chloroplasts, and a usually narrow stauros. Nevertheless, the latter is reduced or strongly reduced in two species: *C. alyoubii* J.Sabir et Ashworth and *C. paradoxus** Ashworth et Lobban. Molecular phylogenetic analysis indicated that the genus is closely related to *Achnanthes* Bory and *Staurotropis* Paddock (Ashworth et al. 2017). Both taxa, as well as another marine genus *Druehlago* Lobban et Ashworth, which has yet to be characterized molecularly, share several morphological similarities with *Craspedostauros* (Cox 1999, Ashworth et al. 2017). For example, all the above-mentioned taxa possess valves and girdle bands perforated by cribrate areolae. Moreover, *Craspedostauros* and *Druehlago* share the general frustule morphology, including frustules with central constriction (Ashworth et al. 2017), whereas the fore and aft arrangement of chloroplasts, typical of *Craspedostauros,* can be observed in several *Achnanthes* species (Cox 1999).Three novel species, *C. danayanus* Majewska et Ashworth sp. nov., *C. legouvelloanus* Majewska et Bosak sp. nov., and *C. macewanii* Majewska et Ashworth sp. nov., were found in the course of the ongoing survey on sea turtle-associated diatoms and are described in the current paper. Moreover, a small population of *C. alatus* is for the first time reported from Europe. A large number of samples analysed and different preservation and processing techniques applied allowed us to document the ultrastructure of the frustule and, whenever possible, the morphology of the plastids as well as the colony type and attachment mode of the cells. These observations were supplemented by a 3-gene phylogenetic analysis including DNA sequence data for three sea turtle-associated *Craspedostauros* species and other marine and epizoic diatom taxa.

* the specific epithet in *Craspedostauros paradoxa* should be changed to '*paradoxus*' following the recommendations of the International Code of Nomenclature for algae, fungi, and plants (Articles 23.5 & 62; Turland et al. 2018).

MATERIALS AND METHODS

Material collection and preservation

Diatom samples were collected from captive and wild sea turtles from Croatia and South Africa. All biofilm samples from carapace and skin were taken using single-use sterile toothbrushes according to the sampling protocols suitable for diatom culturing and standard morphology-based diatom analysis proposed by Pinou et al. (2019). In Croatia, 76 (skin and carapace) samples were collected from 38 loggerhead sea turtles *Caretta caretta* L. rescued and rehabilitated at the Marine Turtle Rescue Centre in Aquarium Pula between 2016 and 2019, on the day of or shortly after their arrival at the facility. In South Africa, 196 (skin and carapace) biofilm samples were collected from 78 loggerheads and 20 leatherbacks *Dermochelys coriacea* Vandelli nesting in Kosi Bay (Indian Ocean) over two nesting seasons, in 2017/2018 and 2018/2019. In addition, 6-mm skin biopsy punches were taken from either front or rear flippers of 30 loggerheads and six leatherbacks and preserved in 4 % formaldehyde solution in seawater immediately after collection. Samples of sea turtle-associated barnacles *Chelonibia testudinaria* L. from 100+ loggerheads and *Platylepas coriacea* Monroe et Limpus from 15 leatherbacks were taken using a plastic paint scraper or a blunt knife during four nesting seasons, in 2015/2016, 2016/2017, 2017/2018, and 2018/2019. Barnacle samples comprised of more than one specimen, were divided into two parts and either frozen (-20°C) or fixed with 4 % formaldehyde solution in seawater. Single-specimen barnacle samples were frozen (-20°C). Furthermore, skin and carapace samples were collected from seven sea turtles (three loggerheads, three green turtles *Chelonia mydas* L., and one hawksbill *Eretmochelys imbricata* L.) resident at the uShaka Sea World in Durban on 28 June 2019.

Material collection was performed by, or under close supervision of, qualified field researchers, and the applied techniques and procedures respected ethical principles of the Declaration of Helsinki (World Medical Association 2013) as well as all applicable national laws.

Material processing and microscopy

Diatoms were detached from the frozen barnacles using a Transsonic T310 (Elma, Singen, Germany) ultrasound bath as described in Majewska et al. (2019b). Diatom biofilm from the sea turtle skin, carapace, and barnacles was cleaned from organic matter using either a rapid digestion with a mixture of concentrated HNO_3 and H_2SO_4 (at a ratio of 2:1) according to the method proposed by von Stosch (South African and Croatian samples; Hasle and Syvertsen 1997) or heated 37% H_2O_2 with addition of $KMnO_4$ (Croatian culture strain; van der Werff 1953). Cleaned material was mounted on slides using Naphrax (Brunel Microscopes Ltd, Chippenham, UK; Croatian samples) and Pleurax prepared according to the method proposed by von Stosch (1974; South African samples). The slides were examined using a Nikon Eclipse 80i light microscope with Differential Interference Contrast (DIC) and a Nikon DS-Fi1 5MP digital camera (Nikon Instruments Inc., Melville, NY; South African samples) as well as a Zeiss Axio Imager A2 with DIC and an Axiocam 305 digital camera (Carl Zeiss, Jena, Germany; Croatian samples). In addition, fresh material containing living diatoms attached to the sea turtle scutes and skin flakes was stained with blue writing ink (Scheaffer ®) to reveal the colonies of the diatom-associated bacteria.

For scanning electron microscopy (SEM), the oxidized suspension was filtered through 1-µm or 1.2-µm Isopore™ (Merck Millipore, Darmstadt, Germany) or 3-µm Nucleopore (Nucleopore, Pleasanton, CA, USA) polycarbonate membrane filters. Formalin-preserved skin and barnacle samples were dehydrated in an alcohol series (30%, 50%, 60%, 70%, 80%, 90%, 95%, 99.9%) followed by critical point-drying in an E3100 Critical Point Dryer (Microscience Division, Watford,

UK). Subsequently, the samples were mounted on aluminium stubs with carbon tape and sputter-coated with either gold-palladium using Cressington 108Auto and Cressington 208HR sputter-coaters (Cressington Scientific Instruments Ltd., Watford, UK), palladium using a Precision Etching and Coating System, PECS II (Gatan Inc., CA, USA), or iridium using Emitech K575X (Emitech Ltd., Ashford, Kent, UK) and Cressington 208 Bench Top sputter-coaters. Diatom specimens were analysed with JEOL JSM-7800F, JEOL JSM-7001F (JEOL, Tokyo, Japan), FEI Quanta Feg 250 (FEI Corporate, Hillsboro, OR, USA), Zeiss Ultra Plus (Carl Zeiss, Oberkochen, Germany), and Zeiss SUPRA 40 VP (Carl Zeiss Microscopy, Thornwood, NY, USA) scanning electron microscopes at 3−10 kV. To determine the relative abundance of the new species, 400 diatom valves were counted and identified in each sample along arbitrarily chosen transects using SEM. The morphology and frustule ultrastructure of the new taxa was compared with those of all known *Craspedostauros* species worldwide (Cox 1999, Sabbe et al. 2003, Van de Vijver et al. 2012, Ashworth et al. 2017, Majewska et al. 2018).

Culturing

Living diatoms from the fresh material (unpreserved samples containing sea turtle biofilm and filtered seawater; Pinou et al. 2019) were isolated using a glass pipette with a tip pulled and thinned over a flame into 16x100 mm glass culture tubes (South African strains) or plastic culture flasks (Croatian strains) filled with 34 PSU (South African strains) or 38 PSU (Croatian strains) f/2 growth medium (Guillard 1975). Strains were lit by natural light from a south-facing window (South African strains) or white fluorescent light with a photoperiod of 12h (Croatian strains) and maintained at a temperature of 20–24°C. The well-growing cultures were divided into two parts, one of which was used for DNA extraction. The remaining part was cleaned with a mixture of 30% H_2O_2 and 70% HNO_3 and rinsed with distilled water until the near-neutral pH of the fluid phase was reached. Croatian strain (PMFTB0003) was cleaned using saturated $KMnO_4$ solution and ca. 30%

192 HCl following a slightly modified protocol proposed by Simonsen (1974). Permanent microscopy
193 slides and SEM stubs were prepared as described above.

194

195 *DNA preparation and phylogenetic analysis*

196 The cultures were harvested as cell pellets using an Eppendorf 5415C centrifuge (Eppendorf North
197 America, Hauppauge, NY, USA) for 10 minutes at 8000 rpm. The QIAGEN DNeasy Plant Mini Kit
198 (QIAGEN Sciences, Valencia, California, USA) was used for DNA extraction following the
199 manufacturer's protocol, with the addition of an initial cell disruption by 1.0 mm glass beads in a
200 Mini-Beadbeater (Biospec Products, Inc, Bartlesville, OK, USA) for 45 sec. PCR-based DNA
201 amplification and di-deoxy Sanger sequencing of small-subunit nuclear rRNA and the chloroplast-
202 encoded rbcL and psbC markers followed Theriot et al. (2010).

203 Phylogenetic analysis of the DNA sequence data was conducted using a three-gene dataset: nuclear-
204 encoded small subunit (SSU) rRNA, and plastid-encoded *rbc*L and *psb*C. Alignment of the SSU
205 sequences, accounting for secondary structure, was done using the SSUalign program (Nawrocki et
206 al. 2009), with the covariance model based on the 10 diatoms included with the program download,
207 plus 23 additional diatoms from the CRW website (Cannone et al. 2002). Post alignment, SSU
208 sequences were concatenated to the chloroplast sequences into a single matrix (Supplementary
209 Table S1). Eight separate partitions were created for the data (SSU paired and unpaired sites, plus
210 the first, second and third codon positions of each of *rbc*L and *psb*C). This dataset and partitioning
211 scheme were run under maximum likelihood (ML) using RAxML ver. 8.2.7 (Stamatakis 2014)
212 compiled as the pthread-AVX version on an Intel i7 based processor, using the GTR+G model.
213 Twenty-five replicates, each with 500 rapid BS replicates, were run with ML optimizations.
214 Bootstrap support was assessed using the BS replicates from the run with the optimal ML score.

215

RESULTS

Morphological observations

Craspedostauros danayanus Majewska & Ashworth sp. nov. (Figs 2–24)

Cells with two fore and aft H-shaped chloroplasts (Figs 2–5). Frustules extremely delicate and very lightly silicified (Figs 6–16). In girdle view, frustules rectangular, moderately constricted at the centre (Figs 5, 7 & 11). Valves narrow, linear, very slightly constricted in the valve middle, with bluntly rounded apices (Figs 4, 12–16).

Light microscopy (Figs 12–16):

Valve dimensions (n = 30): length 28–61 μm, width 2–2.5 μm, length/width ratio: 14–30.5. In cleaned (acid-digested) material, partially dissolved valve margins barely noticeable (Figs 14 & 15, arrows), intact frustules absent. Striae indiscernible (Figs 12–16). Raphe-sternum thickened, clearly visible (Figs 12–16). Thickenings at both central and terminal raphe endings (Figs 12–16).

Scanning electron microscopy (Figs 17–24):

Externally: In cleaned material, valve face appearing flat, with very shallow mantle and straight margin (Figs 17 & 18). Striae uniseriate, 49–51 in 10 μm, parallel, becoming radiate towards the apices, alternate or opposite, composed of up to eight areolae (Figs 17 & 18). Areolae largely similar in size, becoming somewhat smaller around the central area, squarish to roundish, externally occluded by cribra (Figs 17–19). Each cribrum perforated by 2–8 pores (Fig. 17). Axial area narrow (Figs 17 & 18). Raphe-sternum not raised (Figs 17–19). Raphe branches straight (Fig. 18). Central area large, symmetrical, amygdaliform (Figs 18 & 19). Central raphe endings straight, elongated, slightly expanded (Figs 18 & 19). Terminal raphe endings disappearing under somewhat triangular

239 silica flaps extending from the raphe-sternum, giving the impression of unilaterally bent terminal
240 raphe fissures (Figs 17 & 18). A large, irregular depression present at the apical flap fold (Figs 17 &
241 18, arrowheads). Shortened striae composed of cribrate areolae radiating around the apices beyond
242 the apical silica flaps (Fig. 17). Asymmetrical pore-free area present beyond the terminal raphe
243 endings in the immediate vicinity of the apical flap fold (Fig. 17).

244 Internally: Raphe slit opening laterally onto the more or less uniformly thickened and distinctly
245 raised raphe-sternum (Fig. 20). Stauros absent (Figs 20 & 21). Central area mirroring the external
246 structure in size and shape (Figs 20 & 21). Central raphe endings elongated, very slightly
247 unilaterally bent, terminating onto weakly constricted rectelevatum (Figs 20 & 21). Terminal raphe
248 endings positioned somewhat laterally on a large and rounded apical part of the raphe-sternum,
249 terminating in helictoglossae (Figs 20 & 23). Asymmetrical thickening extending from the apical
250 part of the raphe-sternum towards the valve margin, corresponding to the external apical silica flaps
251 (Fig. 23, arrowheads). Areolae externally occluded with cribra (Figs 21–23).

252 Cingulum composed of numerous (14+) open copulae, bearing two rows of typically squarish,
253 roundish or elongated areolae, ca. 50–60 in 10 μm (Figs 18, 23 & 24). Areolae occluded externally
254 by cribra (Figs 23 & 24).

255

256 **Taxonomic remarks**

257 *Craspedostauros danayanus* is most similar to *C. paradoxus*, sharing the general valve outline and
258 lacking the stauros. However, *C. danayanus* differs from the latter in being distinctly smaller (28–
259 61 μm vs 80–85 μm) and more slender (2–2.5 μm vs 6.5–9 μm), possessing a higher stria density
260 (49–51 vs 36–40), and lacking the lip-like silica flaps (externally) and the central knob (internally)
261 present in *C. paradoxus* (Table 1).

262

HOLOTYPE: Permanent slide SANDC-ST012 (prepared from sample ZA0019A/ZA1824E) deposited in the South African Diatom Collection housed by North-West University, Potchefstroom, South Africa.

TYPE LOCALITY: Mabibi Beach, Elephant Coast, South Africa (27° 21′ 30″ S, 32° 44′ 20″ E). Collected from the barnacle *Platylepas coriacea* growing on the egg-lying leatherback sea turtle (tag numbers: ZA0019A, ZA1824E) by R. Majewska, 7 December 2018.

ETYMOLOGY: The epithet honours Danay A. Stoppel (North-West University, Potchefstroom, South Africa), who made the first observations of the new taxon, in recognition of her contribution to the sea turtle diatom project in South Africa.

ECOLOGY: Epizoic on carapaces of adult leatherback sea turtles and on leatherback-associated barnacles *Platylepas coriacea* growing on adult leatherbacks from Kosi Bay (South Africa). Attaching to the animal surface through one end of the valve, motile in culture.

The taxon was found in twelve leatherback skin samples (out of 20 examined) and in all *P. coriacea* samples examined (n = 15) reaching relative abundances of 35% (skin samples) and 79% (barnacle samples). It was found in neither loggerhead nor loggerhead-associated barnacle samples from the same location (Kosi Bay, South Africa). Leatherback skin samples containing *C. danayanus* were dominated by *Navicula* spp., *Tursiocola* sp., and *Poulinea* spp. The new taxon was dominant in most of the *P. coriacea* samples along with *Cylindrotheca* sp. Both taxa colonised various anatomical parts of the barnacle showing preference for rough surfaces and cavities. The extremely lightly silicified frustules may be an adaptation to the pelagic lifestyle of the host, as the open ocean waters contain significantly lower concentrations of dissolved silica than coastal habitats (Tréguer et al. 1995).

Craspedostauros legouvelloanus **Majewska & Bosak sp. nov. (Figs 25–47)**

Light microscopy (Figs 25–30):

Intact frustules lying almost always in girdle view (due to large cell depth/valve width ratio), slightly constricted in the middle (Figs 25, 26, 28–30), with several girdle bands (Figs 26, 28 & 30). Valve margin expanded at the centre (Figs 25, 28 & 30). Frustules lightly silicified and delicate. Valves narrow, linear to linear-lanceolate, slightly constricted at the central area, with bluntly rounded apices (Fig. 27). Valve dimensions (n = 30): length 18–34 μm, width 3–5 μm, length/width ratio: 5.6–9.4. Striae indiscernible (Figs 25–30). Stauros narrow (Figs 25, 27–30), widening towards the biarcuate valve margins (Fig. 30, arrows). Raphe-sternum clearly visible (Figs 25–30). Raphe straight, biarcuate in girdle view (Figs 25, 26, 28 & 30).

Scanning electron microscopy (Figs 31–40):

Externally: Valves somewhat convex, with no clear valve face-mantle junction (Figs 31–33). Valve margin clearly expanded at the centre beyond the stauros (Fig. 33). Striae uniseriate, 46–49 in 10 μm, parallel throughout the valve centre, becoming convergent near the apices, alternate or opposite, composed of up to 13 areolae (Figs 31, 32 & 38). Areolae similar in size throughout the entire valve, squarish, externally occluded by cribra (Figs 31–33 & 38). Each cribrum perforated by 4 pores (Figs 31–33 & 38). Axial area very narrow (Figs 31 & 32). Raphe-sternum very slightly raised (Figs 31–33). Raphe branches more or less straight (Fig. 31). Central area forming a narrow rectangular fascia (Figs 31 & 38). Central raphe endings covered entirely by rimmed lip-like silica flaps extending from one side of the axial area (Figs 31 & 38). At the apices, axial area expanding into somewhat triangular silica flaps covering the terminal raphe endings giving the impression of unilaterally bent terminal raphe fissures (Figs 31–33). An oval or irregular depression present at the apical flap fold (Fig. 31, arrows). Shortened stria composed of regular areolae and simple puncta radiating around the apices beyond the terminal raphe endings (Figs 31–33).

Internally: Raphe slit opening laterally onto the uniformly thick and clearly raised raphe-sternum (Figs 35 & 36). Stauros raised, very narrow, broadening abruptly at the mantle expansion and merging with the pore-free area at the valve margin (Figs 36 & 39), slightly more expanded on the side corresponding to the external lip-like silica flaps (Figs 36, arrowheads, 39 & 40). Central raphe endings straight or slightly unilaterally bent, terminating onto weakly developed, elongated and flattened helictoglossae (Figs 35, 36, 39 & 40). A blunt cylindrical knob with a small central cavity present between the raphe endings (Figs 35, 36, 39 & 40). Areolae externally occluded by cribra, appearing sunken, especially close to the stauros (Figs 39 & 40). Stauros-adjacent virgae appearing hollow, suggesting a more complex valve structure in that area (Fig. 39, arrowheads). Terminal raphe endings positioned somewhat laterally on the raphe-sternum, terminating onto prominent helictoglossae. At the apices, raphe-sternum expanded laterally towards the valve margin, merged with pore-free area corresponding to the external apical silica flaps (Figs 36 & 37).

Cingulum composed of numerous (12+) open copulae, bearing two rows of typically squarish or elongated areolae, ca. 50–60 in 10 μm (Figs 32–35). Areolae occluded externally by cribra with 4–12 pores per cribrum (Figs 32–35). Valvocopula curved, distinctly narrower and pore-free beside the stauros (Fig. 33, arrowheads). An internal ridge perforated by puncta, resembling a reduced septum, present in each copula except for valvocopula (Figs 33–35, arrowheads).

Adriatic population (Figs 41–47)

Specimens resembling *C. leguovelloanus* were found on the carapace of six loggerhead sea turtles sampled on the Croatian coast of the Adriatic Sea. Most of the morphological features observed in the Adriatic population (Figs 41–47) agreed well with those found in *C. legouvelloanus*. The cells possessed two fore and aft H-shaped chloroplasts (Fig. 41, arrows) observed previously in other *Craspedostauros* species (Cox 1999, Ashworth et al. 2017, Majewska et al. 2018). The specimens were slightly longer (23–39 μm) and wider (3.5–6 μm, length/width ratio: 5.2–7.8, $n = 25$) than

those from the South African population and their stria density was lower (40–44 in 10 μm vs. 46–49 in 10 μm; Table 1). In general, the frustules showed a relatively high degree of irregularity in the areolae structure and the size and shape of stauros, axial area, and facia (Figs 42–45).

Taxonomic remarks

Currently, *C. legouvelloanus* is the only *Craspedostauros* species with septate girdle bands. Valves of this species differ from those of all known stauros-bearing *Craspedostauros* species in possessing a very high stria density (above 40 in 10 μm). Although a similarly high or higher stria density was observed in *C. alyoubii* (~40 in 10 μm) and *C. danayanus* (49–51 in 10 μm), the two species are larger (83–105 μm and 28–61 μm) than *C. legouvelloanus* (18–34 [39] μm) and their general morphology differs remarkably from that of the new taxon in, for example, possessing a reduced or strongly reduced stauros (Table 1). Several of the characters of *C. legouvelloanus*, such as largely uniform valve areolae with four pores per cribrum and internal central knob, agree with the description of *C. australis* E.J.Cox (Cox 1999). However, the new species can be easily distinguished from the latter by its clearly centrally expanded valve margin and well-developed lip-like silica flaps externally covering the central raphe endings absent in *C. australis* (Table 1).

Although wild specimens belonging to the Adriatic population of *C. legouvelloanus* exhibited numerous irregularities in the shape and size of taxonomically important characters such as areolae, striae, stauros, and central area, we were unable to indicate and unambiguously describe features that would distinguish them from the type population. High morphological plasticity and polymorphy in diatoms have been reported from both epizoic and non-epizoic habitats (Cox 2011, De Martino et al. 2011, Urbánková et al. 2016, Riaux-Gobin et al. 2014, 2017, Edlund and Burge 2019), and it is conceivable that the morphological differences observed between the two populations could be induced by environmental triggers, such as differences in salinity or nutrient concentrations (Schultz 1971, Czarnecki 1987, 1994, De Martino et al. 2011). Unfortunately, the

Croatian strain PMFTB0003 (Figs 41, 43, 45 & 46) isolated from the sample TB13 did not survive and the DNA material could not be obtained at the time of this study. Therefore, in the light of the current lack of any additional information about the phylogenetic relationships between the two populations, they should be considered conspecific until otherwise proven.

HOLOTYPE: Permanent slide SANDC-ST003 and unmounted material (prepared from sample ZA0762D/ZA0763D) deposited in the South African Diatom Collection housed by North-West University, Potchefstroom, South Africa.

PARATYPE: Permanent slide HRNDC000150 and unmounted material (TB13) deposited in the Croatian National Diatom Collection housed by Faculty of Science, University of Zagreb, Croatia.

ISOTYPES: Permanent slides BR-XXXX and BR-XXXX deposited in the BR-collection housed by Meise Botanic Garden, Meise, Belgium.

TYPE LOCALITY: Kosi Bay, South Africa (26° 59′ 39″ S, 32° 51′ 60″ E). Collected from the carapace of the egg-lying loggerhead sea turtle (tag numbers: ZA0762D, ZA0763D) by R. Majewska, 15 December 2017 (holotype).

Marine Turtle Rescue Centre, Pula, Croatia (44°50′ 07″ N, 13°49 ′ 58″ E). Collected from a semi-adult female loggerhead *Caretta caretta* named ‘Mimi’ by K. Gobić Medica, 28 May 2019 (paratype).

ETYMOLOGY: The epithet honours Dr Diane Z. M. Le Gouvello du Timat (Nelson Mandela University, Port Elizabeth, South Africa), who assisted during the type material collection, in recognition of her invaluable help and on-going support to the sea turtle diatom project and sea turtle research in South Africa.

ECOLOGY: Epizoic on carapaces and skin of adult loggerhead sea turtles and on loggerhead-associated barnacles *Chelonibia testudinaria* growing on adult loggerheads from Kosi Bay (South

Africa) and the Adriatic Sea (Croatia). Attaching to the animal surface through one end of the valve, motile in culture.

Although the taxon was present in numerous samples, its relative abundance rarely exceeded 4% of the total diatom number. Samples with *C. legouvelloanus* from both locations were each time dominated by *Poulinea* spp., *Berkeleya* spp., *Halamphora* spp., and *Nitzschia* spp., with addition of *Achnanthes elongata* Majewska et Van de Vijver, *Cyclophora tenuis* Castracane, *Proschkinia* spp., *Navicula* spp., *Licmophora* spp., and *Haslea* spp.

***Craspedostauros macewanii* Majewska & Ashworth sp. nov. (Figs 48–62)**

Light microscopy (Figs 48–54):

Cells with two fore and aft H-shaped chloroplasts (Figs 48 & 51). Frustules delicate and lightly silicified (Figs 48–54). In girdle view, frustules rectangular, moderately to strongly constricted at the centre (Figs 48–50). Cingulum composed of several girdle bands (Figs 49–50). Valves narrow, linear to linear-lanceolate, slightly constricted at the central area, with bluntly rounded apices (Figs 51–54). Valve margin straight (Fig. 49, arrow). Valve dimensions (n = 20): length 26–51 μm (up to 65 μm in culture), width 4.5–5.5 μm (up to 6 μm in culture), length/width ratio: 5.4–11.3. Valve face-mantle junction visible on each side of the raphe (Figs 52–54, arrows). Striae barely discernible, 28–31 in 10 μm (Figs 52–54). Central area narrow, bow tie-shaped (Figs 52–54). Raphe-sternum thickened (Figs 52–54). Raphe straight (Fig. 54) with thickenings at the terminal raphe endings (Figs 52–54).

Scanning electron microscopy (Figs 55–62):

Externally: Valves slightly concave at the centre, with distinct valve face-mantle junction marked by a narrow pore-free area (Figs 55 & 57). Valve face flat (Fig. 55). Mantle very deep (Fig. 55).

Valve margin straight, with narrow pore-free area at the mantle edge (Figs 56 & 57). Striae uniseriate, parallel through most of the valve, becoming convergent near the apices, alternate or opposite, composed of up to 21 areolae (2–8 on the valve face and up to 13 on the mantle; Figs 55–58). Areolae similar in size, squarish, externally occluded by cribra (Figs 56–58). Areolae bordering the narrow axial area usually only slightly larger and somewhat irregular in shape (Figs 56–58). Each cribrum perforated by highly variable number of pores (up to 13+; Figs 56–58). Raphe branches more or less straight (Fig. 55). Central area in the form of a narrow bow tie-shaped fascia (Figs 55 & 57). Central raphe endings covered by small lip-like silica flaps extending from one side of the axial area (Figs 55 & 57). Apices pore-free (Figs 55, 56 & 58). Terminal raphe endings covered by triangular silica flaps giving the impression of unilaterally bent terminal raphe fissures (Figs 55, 56 & 58). An oval or irregular depression (Figs 55, arrowhead, 56 & 58) with several small areolae (Figs 56 & 58, arrowheads) present at the apical flap fold. Shortened striae composed of a single areola (occasionally with additional puncta) radiating around the apices beyond the terminal raphe endings (Figs 56 & 58).

Internally: Raphe slit opening more or less centrally onto the uniformly thick raphe-sternum (59–61). Stauros raised, narrow, tapering towards the valve face-mantle junction and widening significantly on the valve mantle towards the mantle edge (Figs 59 & 61). Central raphe endings straight, elongated, terminating onto weakly developed, elongated and flattened helictoglossae (Figs 59 & 61). A flatly ended cylindrical knob present at the central nodule (Figs 59 & 61). Areolae externally occluded by cribra, appearing sunken, especially close to the raphe-sternum (Figs 60 & 61). Terminal raphe endings terminating onto prominent helictoglossae within an expanded and thickened pore-free area corresponding to the curvature of the external silica flaps (Fig. 60). Several small areolae present at the end of the curved thickening (Fig. 60, arrowheads).

Cingulum composed of numerous open copulae bearing up to five rows of cribrate squarish or elongated areolae, ca. 38–45 in 10 μm (Figs 55, 59 & 62). Advalvar part of valvocopula pore-free beside the stauros (Fig. 59).

Taxonomic remarks

The morphological character pattern in *Craspedostauros macewanii* is most similar to *C. australis* and *C. capensis* Cox. The three species share several features such as the presence of a bow tie-shaped fascia, rudimentary lip-like silica flaps extending from the raphe-sternum and partially covering the external central raphe endings, valve margin straight at the centre, and internally, a single knob at the central nodule (Table 1). Moreover, valve dimensions of *C. macewanii* (26–51 μm long, 4.5–5.5 μm wide) overlap with those reported for *C. australis* (35–78 μm long, 4–6 μm wide) and *C. capensis* (25–35 μm long, 4.5–5.5 μm wide). In *C. macewanii*, however, the stria density (28–31 in 10 μm) is significantly higher than in *C. capensis* (~19 in 10 μm) and lower than in *C. australis* (35 in 10 μm). In addition, *C. macewanii* can be distinguished from both *C. australis* and *C. capensis* by the presence of a distinct valve face-mantle junction running as a narrow, though clearly visible, pore-free ridge from apex to apex. *Craspedostauros macewanii* differs further from *C. capensis* in possessing areolae of a similar size throughout the entire valve (variable in *C. capensis*), and from *C. australis* in having convergent stria at the apices (parallel in *C. australis*) and extended apical hyaline zone (Cox 1999). The new taxon is also the only *Craspedostauros* species with girdle bands perforated by up to five rows of squarish areolae instead of two rows of usually transapically elongated areolae observed in other species.

HOLOTYPE: Permanent slide SANDC-ST242 (prepared from sample ST242) deposited in the South African Diatom Collection housed by North-West University, Potchefstroom, South Africa.

TYPE LOCALITY: uShaka Sea World, Durban, South Africa (29° 52′ 02.79″ S, 31° 02′ 45.29″ E). Collected from the carapace of a captive juvenile loggerhead named "Bubbles" by R. Majewska, 28 June 2019.

ETYMOLOGY: The epithet honours Tony McEwan, the uShaka Sea World director, whose scientific enthusiasm and support to the sea turtle diatom project are highly appreciated and acknowledged.

ECOLOGY: Epizoic on skin and carapaces of captive loggerheads and green turtles. Attaching to the animal surface through one end of the valve, motile in culture.

The taxon was found on two captive loggerheads (a juvenile named "Bubbles" and an adult female named "DJ") and two captive green turtles (a subadult named "Calypso" and an adult male named "Napoleon") each time reaching relative abundance of 0.5–1%. All carapace samples containing *C. macewanii* were dominated by the so-called "marine gomphonemoids": *Poulinea* spp. and *Chelonicola* spp., accompanied by *Amphora* spp., *Nitzschia* spp., *Achnanthes elongata* and *A. squaliformis* Majewska et Van de Vijver, whereas the most abundant taxa in the four skin samples were *Tursiocola* spp., *Medlinella* sp., and the two previously mentioned *Achnanthes* species.

Craspedostauros alatus **Majewska & Ashworth (Figs 63–74)**

Craspedostauros alatus was found on the carapaces of several loggerhead sea turtles sampled at the Marine Turtle Rescue Centre in Pula, Croatia. The taxon co-occurred with *C. legouvelloanus*. As in the case of the latter, relative abundance of *C. alatus* was low (ca. 1–3% of the total diatom number). The observed morphological features of the Adriatic population agreed with the original description of the species (Majewska et al. 2018; Figs 63–74, Table 1). The examined specimens were 26–34 μm long and 3–5 μm wide (length/width ratio: 6.3–8.8), with stria density 24–27 in 10 μm (n = 20), and possessed all species-specific features, including a very distinct valve face-mantle

junction and deep mantle (Figs 68, arrows, 69–71), wing-like silica flaps at the apices (Fig. 70), and rectelevatum with central cavity (Figs 73 & 74).

DNA-based phylogeny

The genus *Craspedostauros* is monophyletic based on DNA sequence data generated from cultured material thus far (Fig. 75), though not with strong bootstrap support (bs < 50%). Regarding the taxa described here, *Craspedostauros macewanii* is sister to the rest of the clade (except *C. amphoroides*) with high support (bs = 96%), while *C. danayanus* is sister to *C. alyoubii* and *C. paradoxus* (bs = 71%).

Consistent with other molecular phylogenetic studies which include the genus (Ashworth et al. 2017), the position of the *Craspedostauros* clade can be found in a poorly supported (bs < 50%) assemblage containing the *Staurotropis* clade and a clade of marine *Achnanthes* species. This assemblage can be found within a clade with the Bacillariales (Supplementary Figure S1), though the relationship between the *Staurotropis*+*Achnanthes*+*Craspedostauros* clade and the three Bacillariales clades is poorly resolved. For taxa, strain voucher ID and GenBank accession numbers for strains used in the analysis see Supplementary Table S1.

DISCUSSION

The three new species described in the current study share most of the morphological characters typical of the genus *Craspedostauros*, such as squarish or rectangular areolae occluded by cribra on the valve and girdle bands, multiple copulae with at least two rows of perforations, and two fore and aft chloroplasts. Their linear or linear-lanceolate valve outline and the central constriction of the cell seen in girdle view resemble previously described species. Interestingly, two of the novel species, *C. macewanii* and *C. legouvelloanus*, present features not yet observed in any other member of the

504 genus. The former possesses more than two rows of cribrate areolae on the girdle bands, whereas
505 the latter shows shallow perforated septa. Moreover, the leatherback-associated *C. danayanus*
506 presents a complete reduction of the stauros being the second, after *C. paradoxus*, *Craspedostauros*
507 species lacking this character.

508 It is interesting to note that as the number of character states, such as the reduction/loss of the
509 stauros (*C. paradoxus* and *C. danayanus*) or addition of septate copulae (C. *legouvelloanus*), within
510 *Craspedostauros* changes, the molecular data remain constant in their support (however tenuous) of
511 monophyly for the genus. Cox (1999) ascribed the constricted girdle view to the presence of
512 stauros. Yet the frustules of the two species lacking the latter, still show the central constriction,
513 which may indicate that the lack of stauros is a secondary loss. One of the morphological features of
514 the genus which has been maintained, regardless of newly described diversity, has been the cribrate
515 areolar covering. While the degree of cribrum poration might change among species, the overall
516 gestalt ultrastructure remains unchanged. Even more interesting is that this cribrum ultrastructure is
517 also seen in *Staurotropis* and the *Achnanthes* species, which are commonly found (again, somewhat
518 tenuously) sister to the *Craspedostauros* clade in molecular phylogenies. While there are other
519 morphological similarities between the three genera, such as the stauros (though missing in some
520 species of *Craspedostauros* and *Achnanthes*) and the fore and aft H-shaped or plate-like
521 chloroplasts (missing in *Staurotropis* and some species of *Achnanthes*), so far it is the cribrate
522 areolae ultrastructure that remains constant. In this context, the phylogenetic position of the genus
523 *Druehlago*, which shares the same cribrum ultrastructure and the same chloroplast morphology of
524 *Staurotropis* and *Achnanthes longipes* Agardh, but thus far lacks a stauros-bearing taxon, is all the
525 more intriguing.

526 Microscopical analyses of the fresh and critical-point-dried sea turtle skin pieces and barnacles
527 revealed the mode of attachment and growth form of *C. danayanus* that attaches to the animal
528 substratum through one pole of the cell. A similar mode of attachment to the natural substratum was

observed in several members of the genus (R.Majewska, pers. observ.) suggesting that these taxa can either develop as firmly attached, sessile colonies or remain motile in less favourable conditions (e.g. in culture tubes).

In the course of the on-going surveys on sea turtle-associated diatoms, a recently described taxon, *C. alatus*, was observed growing on the carapaces of several loggerhead sea turtles rescued in Croatia. *Craspedostauros alatus* was originally described from museum specimens of juvenile Kemp's ridleys (*Lepidochelys kempii* Garman) and a juvenile green turtle found cold-stunned and beyond recovery on the New York (USA) beaches during various seasons between 2012 and 2014 (Majewska et al. 2018). Although the relative abundance of *C. alatus* did not exceed 5.5% (current study, Majewska et al. 2018), observations of this taxon on a sea turtle from the Adriatic Sea may indicate that a) *C. alatus* is not an uncommon element of the sea turtle diatom flora; b) being associated with highly migratory animals such as sea turtles its geographical range is likely linked to that of its hosts.

A similar conclusion can be drawn based on the records of *C. legouvelloanus*. The species occurred on several of the Adriatic loggerheads as well as on dozens of sea turtles belonging to the same species and their associated barnacles sampled on the eastern coast of South Africa. Even though the taxon was found in two different ocean basins, it cannot be excluded that the sea turtles acted as vectors that facilitated its dispersal among the various seas and oceans. There is a strong observational and molecular evidence that the Indian Ocean loggerheads interact and mate with the Atlantic members of the species (Bowen et al. 1994, Bowen and Karl 2007, Le Gouvello du Timat et al., in prep.). Thus, it is conceivable that any diatom able to endure the changing conditions during the migrations of their hosts and survive in competition with native flora would inoculate all appropriate and available media and substrata encountered. With the exception of *C. danayanus*, the sea turtle-associated *Craspedostauros* species, although common on the sea turtle carapaces, were never among the dominant taxa, and it is still unclear whether the animal body surface is their

554 preferred or alternative habitat. It is possible that the occurrence of these species in the sea turtle
555 biofilm samples is linked to the presence of some other sea turtle epibionts (e.g. barnacles, sponges,
556 bryozoans). *Craspedostauros danayanus* dominated most of the leatherback skin and barnacle
557 samples that were analysed, and it is likely that this taxon is highly adapted to the conditions
558 provided by the smooth body of the largest among the sea turtles, and, being associated with both
559 the skin and the leatherback-specific barnacle species, *Platylepas coriacea*, its relationship with the
560 host may be obligatory. Leatherbacks, contrary to other extant sea turtles, show the fully oceanic
561 developmental pattern spending most of their lives in highly homogenous open-water environment
562 devoid of refugia (Bolten 2003). They are unique among modern reptiles in being endothermal
563 (Frair et al. 1972). This ability allows them to survive in both tropical and near-freezing waters
564 (James et al. 2006). They are also significantly faster swimmers and deeper divers than other sea
565 turtles (Eckert 2002, Doyle et al. 2008). Therefore, microhabitats provided by these animals, and
566 thus their microbiomes, would differ substantially from those present on other sea turtles. Under
567 such unique conditions, far from the diverse, species-rich shallow-water ecosystems, specific eco-
568 physiological adaptations may be required to survive, and fewer diatom species would manage to
569 thrive on the demanding substratum. An analogous phenomenon is known from marine cetaceans
570 that seem to be colonised by only a few, highly specialized diatom taxa (e.g. Nemoto 1956, Holmes
571 et al. 1993, Ferrario et al. 2018).

572

573 **ACKNOWLEDGEMENTS**

574 We thank Diane Z. M. Le Gouvello du Timat (Nelson Mandela University, South Africa), Franco
575 De Ridder (North-West University, South Africa), and Karin Gobić Medica and Milena Mičić
576 (Aquarium Pula, Croatia) for their help during the material collection. Danay A. Stoppel and Carla
577 Swanepoel (North-West University, South Africa) processed some of the diatom samples collected
578 in South Africa. Tony McEwan, Leanna Botha, and the rest of the uShaka Sea World staff and

members of the South African Association for Marine Biological Research (SAAMBR) are acknowledged for their help in the sea turtle biofilm collection at the uShaka Sea World as well as their great enthusiasm, interest and support to this project. We are further grateful to Jan Neethling and the staff from the Centre for High Resolution Transmission Electron Microscopy, Nelson Mandela University (Port Elizabeth, South Africa) for their generous help during the SEM analyses.

All sampling activities performed in the iSimangaliso Wetland Park (South Africa) were carried out under research permits issued by the South African Department of Environmental Affairs (RES2016/67, RES2017/73, RES 2018/68, and RES 2019/05).

This work was done with partial financial support from The Systematics Association (UK) through the Systematics Research Fund Award granted to R. Majewska (2017) and the Croatian Science Foundation under the project UIP-2017-05-5635 (TurtleBIOME).

591 **References**

592 Apprill, A. 2017. Marine animal microbiomes: toward understanding host–microbiome interactions
593 in a changing ocean. *Front. Mar. Sci.* 4:222. doi: 10.3389/fmars.2017.00222.

594 Ashworth, M. P., Lobban, C. S., Witkowski, A., Theriot, E. C., Sabir, M. J., Baeshen, M. N.,
595 Hajarah, N. H., Baeshen, N. A., Sabir J. S. & Jansen, R. K. 2017. Molecular and morphological
596 investigations of the stauros-bearing, raphid pennate diatoms (Bacillariophyceae): *Craspedostauros*
597 E.J. Cox, and *Staurotropis* T.B.B. Paddock, and their relationship to the rest of the Mastogloiales.
598 *Protist* 168:48–70.

599 Azari, M., Farjad, Y., Nasrolahi, A., De Stefano, M., Ehsanpour, M., Dobretsov, S., Majewska, R.
600 2020. Diatoms on sea turtles and floating debris in the Persian Gulf (Western Asia). *Phycologia,*
601 DOI: 10.1080/00318884.2020.1752533.

602 Bolten, A. B. 2003. Variation in Sea Turtle Life History Patterns: Neritic vs. Oceanic
603 Developmental Stages. *In* Lutz, P. L., Musick, J. A. & Wyneken, J. [Eds.] *The Biology of Sea*
604 *Turtles*, vol. 2. CRC Press, Boca Raton, USA, pp. 234–58.

605 Bowen, B. W., Kamezaki, N., Limpus, C. J., Hughes, G. H., Meylan, A. B. & Avise, J. C. 1994.
606 Global phylogeography of the loggerhead turtle (*Caretta caretta*) as indicated by mitochondrial
607 DNA haplotypes. *Evolution* 48:1820–8.

608 Bowen, B. W. & Karl, S. A. 2007. Population genetics and phylogeography of sea turtles. *Mol.*
609 *Ecol.* 16:4886–907.

610 Cannone, J.J., Subramanian, S., Schnare, M.N., Collett, J.R., D'Souza, L.M., Du, Y., Feng, B., Lin,
611 N., Madabusi, L.V., Müller, K.M., Pande, N., Shang, Z., Yu, N. & Gutell, R.R. 2002. The
612 Comparative RNA Web (CRW) Site: an online database of comparative sequence and structure
613 information for ribosomal, intron, and other RNAs. *BMC Bioinformatics* 3:2.

614 Cox, E. J. 1999. *Craspedostauros* gen. nov., a new diatom genus for some unusual marine raphid
615 species previously placed in *Stauroneis* Ehrenberg and *Stauronella* Mereschkowsky. *Eur. J. Phycol.*
616 34:131–47.

617 Cox E.J. 2011. Morphology, cell wall, cytology, ultrastructure and morphogenetic studies. *In*
618 Seckbach, J. & Kociolek, J. P. [Eds.] *The Diatom World*. Dordrecht, Springer, pp. 21–45.

619 Czarnecki, D. B. 1987. Mastogloia revisited: Laboratory confirmation of Stoermer's observation. *IX*
620 *North American Diatom Symposium, Abstracts No. 7*, Treehaven Field Station, Tomahawk,
621 Wisconsin.

622 Czarnecki, D. B. 1994. The freshwater diatom culture collection at Loras College, Dubuque, Iowa.
623 *In* Kociolek J.P. [Ed.] *Proc. Eleventh Int. Diatom Symp., Mem. Calif. Acad. Sci., Nr. 17*. San
624 Francisco, California Academy of Sciences, pp. 155–73.

625 De Martino, A., Bartual, A., Willis, A., Meichenin, A., Villazán, B., Maheswari, U. & Bowler, C.
626 2011. Physiological and molecular evidence that environmental changes elicit morphological
627 interconversion in the model diatom *Phaeodactylum tricornutum*. *Protist* 162:462–81.

628 Doyle, T. K., Houghton, J. D. R., O'Súilleabháin, P. F., Hobson, V. J., Marnell, F., Davenport, J. &
629 Hays, G. C. 2008. Leatherback turtles satellite-tagged in European waters. Endanger. *Species Res.*
630 4:23–31.

631 Eckert, S. A. 2002. Swim speed and movement patterns of gravid leatherback sea turtles
632 (*Dermochelys coriacea*) at St Croix, US Virgin Islands. *J. Exp. Biol.* 205:3689–97.

633 Edlund, M. B. & Burge, D. R. L. 2019. Polymorphism in *Mastogloia* (Bacillariophyceae) revisited.
634 *Plant Ecol. Evol.* 152:351–7.

635 Ezenwa, V. O., Gerardo, N. M., Inouye, D. W., Medina, M. & Xavier, J. B. 2012. Animal behavior
636 and the microbiome. *Science* 338:198–9.

637 Ferrario, M. E., Cefarelli, A. O., Fazio, A., Bordino, P. & Romero, O. E. 2018. *Bennettella ceticola*
638 (Nelson ex Bennett) Holmes on the skin of Franciscana dolphin (*Pontoporia blainvillei*) of the
639 Argentinean Sea: an emendation of the generic description. *Diatom Res.* 33:485–97.

640 Frair, W., Ackman, R. G. & Mrosovsky, N. 1972. Body temperatures of *Dermochelys coriacea*:
641 warm turtle from cold water. *Science* 177:791–3.

642 Frankovich, T. A., Sullivan, M. J. & Stacy, N. I. 2015. *Tursiocola denysii* sp. nov. (Bacillariophyta)
643 from the neck skin of Loggerhead sea turtles (*Caretta caretta*). *Phytotaxa* 234:227–36.

644 Frankovich, T. A., Ashworth, M. P., Sullivan, M. J., Vesela, J. & Stacy, N. I. 2016. *Medlinella*
645 *amphoroidea* gen. et sp. nov. (Bacillariophyta) from the neck skin of loggerhead sea turtles (*Caretta*
646 *caretta*). *Phytotaxa* 272:101–14.

647 Guillard, R.R.L. 1975. Culture of phytoplankton for feeding marine invertebrates. *In* Smith, W. L.
648 & Chanley, M. H. [Eds.] *Culture of Marine Invertebrate Animals*. Springer, Boston, MA. pp. 26–
649 60.

650 Hasle, G. R. & Syvertsen, E. E. 1997. Marine diatoms. *In* Tomas, C. R. [Ed.]. *Identifying marine*
651 *phytoplankton*. Academic Press, San Diego, pp. 5–385.

652 Holmes, R.W., Nagasawa, S. & Takano, H. 1993. The morphology and geographic distribution of
653 epidermal diatoms of the Dall's porpoise (*Phocoenoides dalli* True) in the Northern Pacific Ocean.
654 *Bull. Nat. Sci. Mus. Tokyo, Ser. B, Bot.* 19:1–18.

655 James, M. C., Davenport, J. & Hays, G. C. 2006. Expanded thermal niche for a diving vertebrate: a
656 leatherback turtle diving into near-freezing water. *J. Exp. Mar. Biol. Ecol.* 335:221–6.

657 Majewska, R., Kociolek, J.P., Thomas, E.W., De Stefano, M., Santoro, M., Bolanos, F. & Van De
658 Vijver, B. 2015a. *Chelonicola* and *Poulinea*, two new gomphonemoid diatom genera
659 (Bacillariophyta) living on marine turtles from Costa Rica. *Phytotaxa* 233:236–50.

660 Majewska, R., Santoro, M., Bolanos, F., Chaves, G. & De Stefano, M. 2015b. Diatoms and other
661 epibionts associated with olive ridley (*Lepidochelys olivacea*) sea turtles from the Pacific coast of
662 Costa Rica. *PLoS ONE*, 10:e0130351. doi: 10.1371/journal.pone.0130351.

663 Majewska, R., Van De Vijver, B., Nasrolahi, A., Ehsanpour, M., Afkhami, M., Bolaños, F.,
664 Iamunno, F., Santoro, M. & De Stefano, M. 2017a. Shared epizoic taxa and differences in diatom
665 community structure between green turtles (*Chelonia mydas*) from distant habitats. *Microb. Ecol*.
666 74:969–78.

667 Majewska, R., De Stefano, M., Ector, L., Bolaños, F., Frankovich, T. A., Sullivan, M. J., Ashworth,
668 M. P. & Van De Vijver, B. 2017b. Two new epizoic *Achnanthes* species (Bacillariophyta) living on
669 marine turtles from Costa Rica. *Botanica Mar.* 60:303–18.

670 Majewska, R., Ashworth, M. P., Lazo-Wasem, E., Robinson, N. J., Rojas, L., Van de Vijver, B. &
671 Pinou, T. 2018. *Craspedostauros alatus* sp. nov., a new diatom (Bacillariophyta) species found on
672 museum sea turtle specimens. *Diatom Res.* 33:229–40.

673 Majewska, R., Bosak, S., Frankovich, T. A., Ashworth, M. P., Sullivan, M. J., Robinson, N. J.,
674 Lazo-Wasem, E. A., Pinou, T., Nel, R., Manning, S. R. & Van de Vijver, B. 2019a. Six new
675 epibiotic *Proschkinia* (Bacillariophyta) species and new insights into the genus phylogeny. *Eur. J.*
676 *Phycol.* 54:609–31.

677 Majewska, R., Robert, K., Van de Vijver, B. & Nel, R. 2019b. A new species of *Lucanicum*
678 (Cyclophorales, Bacillariophyta) associated with loggerhead sea turtles from South Africa. *Bot.*
679 *Letters.* DOI: https://doi.org/10.1080/23818107.2019.1691648

680 Nawrocki, E.P., Kolbe, D.L. & Eddy, S.R. 2009. Infernal 1.0: inference of RNA alignments.
681 *Bioinformatics* 25:1335–1337.

682 Nemoto, T. 1956. On the diatoms of the skin film of whales in the Northern Pacific. *Sci. Rep.*
683 *Whales Res. Inst., Tokyo* 11:99–132.

684 Pinou, T., Domenech, F., Lazo-Wasem, E. A., Majewska, R., Pfaller, J. B., Zardus, J. D. &
685 Robinson, N. J. 2019. Standardizing sea turtle epibiont sampling: outcomes of the epibiont
686 workshop at the 37th International Sea Turtle Symposium. *Mar. Turtle Newsl.* 157:22–32.

687 Redford, K. H., Segre, J. A., Salafsky, N., Martinez del Rio, C. & McAloose, D. 2012.
688 Conservation and the microbiome. *Conserv. Biol.* 26:195–7.

689 Riaux-Gobin, C., Coste, M., Jordan, R. W., Romero, O. E. & Le Cohu, R. 2014. *Xenococconeis*
690 *opunohusiensis* gen. et sp. nov. and *Xenococconeis neocaledonica* comb. nov. (Bacillariophyta)
691 from the tropical South Pacific. *Phycol. Res.* 62:153–69.

692 Riaux-Gobin, C., Witkowski, A., Kociolek, J. P., Ector, L., Chevallier, D. & Compère, P. 2017.
693 New epizoic diatom (Bacillariophyta) species from sea turtles in the Eastern Caribbean and South
694 Pacific. *Diatom Res.* 32:109–25.

695 Robinson, N. J., Majewska, R., Lazo-Wasem, E., Nel, R., Paladino, F. V., Rojas, L., Zardus, J. D. &
696 Pinou, T. 2016. Epibiotic diatoms are universally present on all sea turtle species. *PLoS ONE* 11:
697 e0157011. doi: 10.1371/journal.pone.0157011.

698 Sabbe, K., Verleyen, E., Hodgson, D. A., Vanhoutte, K. & Vyverman, W. 2003. Benthic diatom
699 flora of freshwater and saline lakes in the Larsemann Hills and Rauer Islands, East Antarctica. *Ant.*
700 *Sci.* 15:227–48.

701 Simonsen, R. 1974. The diatom plankton of the Indian Ocean Expedition of R/V" Meteor" 1964-
702 1965. *Meteor Forsch. Ergebnisse. Reihe D*. 19:1–107.

703 Schultz M. E. 1971. Salinity-related polymorphism in the brackish-water diatom *Cyclotella*
704 *cryptica*. *Can. J. Bot.* 49:1285–9.

705 Stamatakis, A. 2014. RAxML version 8: A tool for phylogenetic analysis and post analysis of large
706 phylogenies. *Bioinformatics* 30:1312–3.

707 Theriot, E.C., Ashworth, M., Ruck, E., Nakov, T. & Jansen, R.K. 2010. A preliminary multigene
708 phylogeny of the diatoms (Bacillariophyta): challenges for future research. *Plant Ecol. Evol.*
709 143:278–96.

710 Tréguer, P., Nelson, D. M., Van Bennekom, A. J., DeMaster, D. J., Leynaert, A. & Quéguiner, B.
711 1995. The silica balance in the world ocean: a reestimate. *Science* 268:375–9.

712 Turland, N. J., Wiersema, J. H., Barrie, F. R., Greuter, W., Hawksworth, D. L., Herendeen, P. S.,
713 Knapp, S., Kusber, W.-H., Li, D.-Z., Marhold, K., May, T. W., McNeill, J., Monro, A. M., Prado,
714 J., Price, M. J. & Smith, G. F. 2018. *International Code of Nomenclature for algae, fungi, and*
715 *plants (Shenzhen Code) adopted by the Nineteenth International Botanical Congress Shenzhen,*
716 *China, July 2017*. Regnum Vegetabile 159. Glashütten: Koeltz Botanical Books.

717 Urbánková, P., Scharfen, V. & Kulichová, J. 2016. Molecular and automated identification of the
718 diatom genus Frustulia in northern Europe. *Diatom Res.* 31:217–29.

719 van der Werff, A. 1953. A new method of concentrating and cleaning diatoms and other organisms.
720 *Int. Ver. Theor. Angew. Limnol. Verh.* 12:276–7.

721 Van De Vijver, B., Tavernier, I., Kellogg, T. B., Gibson, J. A., Verleyen, E., Vyverman, W. &
722 Sabbe, K. 2012. Revision of type materials of Antarctic diatom species (Bacillariophyta) described
723 by West &West (1911), with the description of two new species. *Fottea* 12:149–69.

724 von Stosch, H.A. (1974) Pleurax, seine Synthese und seine Verwendung zur Einbettung und
725 Darstellung der Zellwände von Diatomeen, Peridineen und anderen Algen, sowie für eine neue
726 Methode zur Elektivfärbung von Dinoflagellaten-Panzern. *Arch. Protistenk.* 116: 132–141.

727 World Medical Association. 2013. World Medical Association Declaration of Helsinki, Ethical
728 principles for medical research involving human subjects. *J. Am. Med. Assoc.* 310:2191–4.
729 doi:10.1001/jama.2013.281053

730 **Figures legends**

731 **Fig. 1**. Sampling locations where *Craspedostauros danayanus* (1), *C. legouvelloanus* (2), *C.*
732 *macewanii* (3), and *C. alatus* (4) were found.

733

734 **Figures 2–11.** *Craspedostauros danayanus*. **Fig. 2.** Living cells of *C. danayanus* and *Cylindrotheca*
735 sp. attached to the leatherback skin scutes (light microscopy). **Fig. 3.** Stained colony of *C.*
736 *danayanus* and associated bacteria on the leatherback skin scutes. **Fig. 4.** Valve view of a living cell
737 (cultured strain). **Fig. 5.** Girdle view of a living cell (cultured strain). **Figs 6–11.** Scanning electron
738 micrographs of *C. danayanus* attached to its original substratum. **Fig. 6.** Monospecific colony
739 growing among the flaking skin of leatherback (dorsal side of the hind flipper). **Fig. 7.** Extremely
740 delicate and fragile cells of *C. danayanus* attached to the leatherback skin (dorsal side of the hind
741 flipper). **Fig. 8.** An overview of the leatherback-associated barnacle, *Platylepas coriacea*, colonized
742 by *C. danayanus*. **Fig. 9.** A detail of the external part of the barnacle with a sheath of host sea turtle
743 tissue overgrown with *C. danayanus*. Arrows indicate some of the monospecific clumps of *C.*
744 *danayanus* colonies. **Fig. 10.** A detail of the moveable plates of the barnacle overgrown with *C.*
745 *danayanus*. **Fig. 11.** A single cell of *C. danayanus* among dense colony of *Cylindrotheca* sp.
746 attached to the folds in the moveable plates of *P. coriacea*. Scale bars: 10 μm = **Figs 3–5, 7, 11**; 50
747 μm = **Fig. 2**; 100 μm = **Figs 6, 9 & 10**; 1mm = **Fig. 8**

748

749 **Figures 12–24.** *Craspedostauros danayanus*. **Figs 12–16.** Valve view (light micrographs). Arrows
750 indicate the barely noticeable valve margins. **Figs 17–24.** Scanning electron micrographs. **Fig. 17.**
751 Detail of the apical part of the valve (external view). Arrowheads indicate the large irregular
752 depression at the fold of the apical silica flap. **Fig. 18.** Frustule with partially detached girdle bands
753 (external view). Arrowheads indicate the large irregular depression at the fold of the apical silica

754 flap. **Fig. 19.** Detail of the central part of the valve (external view). **Fig. 20.** Internal valve view.
755 **Fig. 21.** Detail of the central part of the valve (internal view). **Fig. 22.** Cribrate areolae (internal
756 view). **Fig. 23.** Detail of the apical part of the valve (internal view). Arrowheads indicate the
757 asymmetrical thickening extending from the apical part of the raphe-sternum towards the valve
758 margin. **Fig. 24.** Detail of the girdle bands. Scale bars: 10 μm = **Figs 12–16, 18, 20**; 1 μm = **Figs**
759 **17, 19, 21–24**

760

761 **Figures 25–40.** *Craspedostauros legouvelloanus*. **Figs 25–30.** Light micrographs. **Figs 25, 26, 28–**
762 **30.** Girdle view. **Fig. 25.** Valve with two girdle bands attached. **Figs 28 & 29.** Frustules with
763 detached valves. **Figs 26 & 30.** Complete frustules. Arrows indicate the biarcuate valve margin.
764 **Fig. 27.** Valve view. **Figs 31–40.** Scanning electron micrographs. **Fig. 31.** External valve view.
765 Arrows indicate depressions at the apical flap fold. **Fig. 32.** Detail of the apical part of the frustule
766 (external view). **Fig. 33.** Valve with attached girdle bands (girdle view). **Fig. 34.** Detail of the girdle
767 bands (internal view). Arrowheads indicate the internal thickening (septum). **Fig. 35.** Valve with
768 partially detached girdle bands (internal view). **Fig. 36.** Internal valve view. Arrowheads indicate
769 the slight expansion of the stauros on the side corresponding to the external lip-like silica flaps. **Fig.**
770 **37.** Detail of the apical part of the valve (internal view). **Fig. 38.** Detail of the central part of the
771 valve (external view). **Figs 39 & 40.** Detail of the central part of the valve (internal view).
772 Arrowheads indicate the hollows in the stauros-adjacent virgae. Scale bars: 10 μm = **Figs 25–31,**
773 **33, 35 & 36**; 1 μm = **Figs 32, 34 & 37–39**; 500nm = **Fig. 40**

774

775 **Figures 41–47.** *Craspedostauros legouvelloanus*. **Fig. 41.** Living cells in culture (light
776 microscopy). Arrows indicate the H-shaped chloroplasts with one lobe pressed against each valve, a
777 feature characteristic of the genus. **Fig. 42.** External valve view (wild population). **Fig. 43.** External
778 valve view (cultured strain). **Fig. 44.** Internal valve view (wild population). **Fig. 45.** Internal valve

779 view (cultured strain). **Fig. 46.** Detail of a girdle band showing internal thickening (septum) with
780 perforations. **Fig. 47.** A single girdle band (external and internal view). Scale bars: 10 μm = **Figs**
781 **41–45**; 1 μm = **Figs 46 & 47**

782

783 **Figures 48–62.** *Craspedostauros macewanii*. **Figs 48–54.** Light micrographs. **Figs 48–51.** Fresh
784 (unpreserved) material. **Figs 48 & 51.** Living cells. **Fig. 48.** Girdle view. **Fig. 51.** Valve view. **Figs**
785 **49 & 50.** Damaged cells in girdle view with the cell content (including plastids) spilling beyond the
786 cell wall. **Figs 49.** Arrow indicates the straight valve margin. **Figs 52–54.** Cleaned material.
787 Detached valves in valve view. Arrows indicate the distinct valve face-mantle junction. **Figs 55–62.**
788 Scanning electron micrographs. **Fig. 55.** External valve view. **Fig. 56.** Detail of the apical part
789 (external valve view). **Fig. 57.** Detail of the central area (external valve view). **Fig. 58.** Detail of the
790 apical part (external girdle view). **Fig. 59.** Internal valve view and partially detached valvocopula.
791 **Fig. 60.** Detail of the apical part (internal valve view). Arrowheads indicate several small areolae
792 present at the end of the curved thickening. **Fig. 61.** Detail of the central area (internal valve view).
793 **Fig. 62.** Detail of the valvocopula (internal view).

794 Scale bars: 10 μm = **Figs 48–55 & 59**; 1 μm = **Figs 56–58 & 60–62**

795

796 **Figures 63–74.** *Craspedostauros alatus* (Adriatic population). **Figs 63–68.** Light micrographs. **Figs**
797 **63, 66 & 67.** Valve view. **Fig. 63.** Broken frustule with both valves lying in valve view. **Fig. 64.**
798 Single valve with attached girdle bands. **Figs 65 & 68.** Girdle view. Arrows indicate the clear valve
799 face-mantle junction. **Figs 69–74.** Scanning electron micrographs. **Fig. 69.** Frustule with partially
800 detached girdles bands (external view). **Fig. 70.** Detail of the apical part of the frustule with the
801 winged-liked silica flaps, a feature typical of the species (external view). **Fig. 71.** Frustule with
802 partially detached girdles bands (external girdle view). **Fig. 72.** Internal valve view. **Figs 73 & 74.**

Detail of the central part of the valve (internal view). Scale bars: 10 μm = **Figs 63–69, 71 & 72**; 1 μm = **Figs 70 & 73**; 500 nm = **Fig. 74**

Figure 75. Maximum likelihood (ML) phylogram based on the 3-gene dataset (nuclear-encoded ribosomal SSU, chloroplast encoded rbcL, psbC markers). For clarity, only the clade of raphid diatoms containing *Staurotropis*, *Craspedostauros*, and *Achnanthes* is presented in the figure. The ML tree presenting the complete taxon sampling can be viewed in the Supplementary Figure S1.

Supplementary Figure S1

Maximum likelihood tree based on the 3-gene dataset (nuclear-encoded ribosomal SSU, chloroplast-encoded rbcL, psbC markers) with bootstrap values from 1000 pseudoreplicates over the corresponding nodes. The araphid pennate taxon outgroup *Asterionellopsis socialis* was used as the outgroup.

299x198mm (240 x 240 DPI)

368x244mm (240 x 240 DPI)

409x273mm (240 x 240 DPI)